

REGULATION OF LIVER METABOLISM BY
FIBROBLAST GROWTH FACTOR 19

APPROVED BY SUPERVISORY COMMITTEE

David J. Mangelsdorf, Ph.D.

Steven A. Kliewer, Ph.D.

Cheng-Ming Chiang, Ph.D.

Melanie H. Cobb, Ph.D.

Makoto Kuro-o, M.D., Ph.D.

REGULATION OF LIVER METABOLISM BY
FIBROBLAST GROWTH FACTOR 19

by

SERKAN KIR

DISSERTATION

Presented to the Faculty of the Graduate School of Biomedical Sciences

The University of Texas Southwestern Medical Center at Dallas

In Partial Fulfillment of the Requirements

For the Degree of

DOCTOR OF PHILOSOPHY

The University of Texas Southwestern Medical Center at Dallas

Dallas, Texas

November, 2011

Copyright

by

SERKAN KIR, 2011

All Rights Reserved

ACKNOWLEDGEMENTS

First, I would like to thank my mentors David Mangelsdorf and Steven Kliewer for giving me the opportunity to work in their lab. I am very grateful for their limitless support and encouragement. I benefited much from the independence and freedom I was given in the lab, which I think allowed me to develop my courage and self assurance for doing scientific research. Yet, Davo and Steve provided me with invaluable feedback, their precious time and lots of funds and resources. Besides their support on my research, I am also thankful to them for helping me improve my communication and presentation skills that will be very instrumental in my future scientific career as well.

I am grateful to all past and current members of Mangelsdorf/Kliewer lab for their help, suggestions and support. I thank everyone who taught me any one of the many techniques that I have learnt in this lab. I especially thank Yuan Zhang who has taken care of all mouse breeding and generated HNF4 α -LRH-1 double floxed mice for my studies. I also thank Xunshan Ding for sharing his β -Klotho knockout mice.

I sincerely thank my thesis committee members; Melanie Cobb, Cheng-Ming Chiang and Makoto Kuro-o. I appreciate their time, feedback and suggestions. I am especially grateful to Melanie for her advice on the signaling part of my project and for sharing reagents and tools. I performed in vitro kinase assays in the Cobb lab. I thank the Cobb lab members including Steve Stippec and Eric Wauson who generously helped me.

With Davo and Steve's support, I have worked with many collaborators and received a significant amount of help. I want to thank all of our collaborators for their kind support and contributions. Dr. Robert Gerard from UT Southwestern helped me

make adenoviruses and prepared crude and purified viruses for cell culture and animal studies. Kelly Suino-Powell from Dr. Eric Xu's lab at Van Andel Institute prepared FGF19 protein. Dr. Stephen Previs from Merck and Paul Miller from his lab helped me with mass spectrometry analysis of deuterium-labeled protein samples and estimation of protein synthesis rate. Varman Samuel and Sara Beddow from Dr. Gerard Shulman's lab at Yale University performed hyperglycemic clamp studies on rats to measure rate of hepatic glycogen synthesis. It was a great pleasure to work with all these experts from different fields of biologic research.

Finally, I thank my family and friends for their limited but genuine support. I am very thankful to my mother who was my only true supporter but unfortunately she couldn't make it to see my graduation. May she rest in peace.

REGULATION OF LIVER METABOLISM BY
FIBROBLAST GROWTH FACTOR 19

SERKAN KIR, Ph.D.

The University of Texas Southwestern Medical Center at Dallas, 2011

Supervising Professors: David J. Mangelsdorf, Ph.D.,
Steven A. Kliewer, Ph.D.

Fibroblast Growth Factor (FGF) 19 is a postprandial enterokine up-regulated by bile acid receptor FXR upon bile acid uptake into the ileum. FGF19 inhibits hepatic bile acid synthesis through transcriptional repression of cholesterol 7 α -hydroxylase (CYP7A1) via a mechanism involving nuclear receptor Small Heterodimer Partner (SHP). Here, I show that two other nuclear receptors, Hepatocyte Nuclear Factor 4 α (HNF4 α) and Liver Receptor Homolog-1 (LRH-1), enable SHP binding to the *Cyp7a1* promoter and therefore are important for negative feedback regulation of *Cyp7a1*. HNF4 α and LRH-1 are also crucial activators of *Cyp7a1* transcription. They maintain

active transcription histone marks on the *Cyp7a1* promoter, whereas FGF19 down-regulates these marks in a SHP-dependent way.

Secondly, I show that the MEK/ERK signaling pathway is an integral regulator of bile acid metabolism. ERK activity is necessary to maintain hepatic *Shp* and *Cyp7a1* transcription at their physiologic levels. Inhibition of this pathway causes loss of *Shp* transcription by disrupting HNF4 α and LRH-1 binding to the *Shp* promoter. Independent from the effects on *Shp*, MEK/ERK inhibition induces *Cyp7a1* transcription. Unexpectedly, the MEK/ERK pathway is not required for repression of *Cyp7a1* by FGF19. Although this pathway is activated by FGF19 in livers of *Fgf receptor 4 (Fgfr4)*-deficient mice probably via other FGFRs, *Cyp7a1* repression is largely impaired. Thus, I propose that a signaling mechanism uniquely regulated by FGFR4 must be responsible for FGF19-dependent repression of bile acid synthesis.

In addition to its roles in bile acid metabolism, I also show that FGF19 stimulates hepatic protein and glycogen synthesis, but does not induce lipogenesis. The effects of FGF19 are independent of the activity of either insulin or the protein kinase Akt, and instead are mediated through a mitogen-activated protein kinase signaling pathway that activates components of the protein translation machinery and stimulates glycogen synthase activity. Mice lacking FGF15 (the mouse FGF19 ortholog) fail to properly regulate blood glucose and fail to maintain normal postprandial amounts of liver glycogen. FGF19 treatment restored the loss of glycogen in diabetic animals lacking insulin. Thus, FGF19 activates a physiologically important, insulin-independent endocrine pathway that regulates hepatic protein and glycogen metabolism.

TABLE OF CONTENTS

Title Fly	i
Title Page	ii
Copyright	iii
Acknowledgements	iv
Abstract	vi
Table of Contents	viii
Prior Publication	xii
List of Figures and Tables	xiii
List of Abbreviations	xv
CHAPTER 1	1
General Introduction	1
1.1 Nuclear Receptors	1
1.1.1 Farnesoid X Receptor (FXR, NR1H4)	3
1.1.2 Hepatocyte Nuclear Factor 4 Alpha (HNF4 α , NR2A1)	4
1.1.3 Liver Receptor Homolog 1 (LRH-1, NR5A1)	5
1.1.4 Small Heterodimer Partner (SHP, NR0B2)	6
1.2 Fibroblast Growth Factors and Metabolism	7
1.3 FGF19 and Liver Metabolism	11
1.3.1 FGF19 Regulates Bile Acid Metabolism	11
1.3.2 FGF19 Improves Glucose Metabolism in Diabetic Mice	15
CHAPTER 2	17

Nuclear Receptors HNF4 α and LRH-1 Are Essential Regulators of <i>Cyp7a1</i>	
Transcription.....	17
2.1 General Introduction	17
2.2 Results	18
2.2.1 SHP Interacts with Both HNF4 α and LRH-1	18
2.2.2 SHP, HNF4 α and LRH-1 Bind to the Same Location on the <i>Cyp7a1</i>	
Promoter	21
2.2.3 SHP Interacts with Both HNF4 α and LRH-1 on the <i>Cyp7a1</i> Promoter	24
2.2.4 HNF4 α and LRH-1 Are Essential Regulators of the <i>Cyp7a1</i> Promoter	
<i>In Vivo</i>	26
2.2.5 FGF19 Does Not Regulate Nuclear Receptor Binding to the <i>Cyp7a1</i>	
Promoter.....	28
2.2.6 FGF19 Causes Histone Deacetylation and Demethylaton on the <i>Cyp7a1</i>	
Promoter.....	30
2.3 Discussion	33
2.4 Summary	35
CHAPTER 3	37
The MEK-ERK Pathway Is Integral for Regulation of Bile Acid Synthesis But Not	
Crucial for Regulation by FGF19	
3.1 General Introduction	37
3.2 Results	38
3.2.1 MEK Inhibition Has Profound Effects on <i>SHP</i> and <i>CYP7A1</i> mRNA	
Levels.....	38

3.2.2 MEK Inhibition Disrupts <i>Shp</i> and <i>Cyp7a1</i> Promoter Activity	44
3.2.3 HNF4 α and LRH-1 Are Important for Regulation of <i>Shp</i> Transcription...	48
3.2.4 The MEK/ERK Pathway Is Dispensable for Regulation of <i>Shp</i> and <i>Cyp7a1</i> by FGF19	49
3.2.5 FGF19-dependent ERK Activation Is Not Sufficient for <i>Cyp7a1</i> Repression.....	53
3.3 Discussion	55
3.4 Summary	56
CHAPTER 4	58
FGF19 Regulates Hepatic Protein and Glycogen Synthesis	58
4.1 General Introduction	58
4.2 Results	58
4.2.1 FGF19 Induces Phosphorylation of Translation Machinery Components.	58
4.2.2 FGF19 Activates the Ras/ERK/RSK Signaling Pathway	60
4.2.3 FGF19-dependent Phosphorylation of rpS6 and eIF4B Depends on ERK/RSK Activity	60
4.2.4 FGF19 Promotes Protein Synthesis in Liver.....	62
4.2.5 FGF19 Inhibits GSK3 Kinases and Activates Glycogen Synthase.....	63
4.2.6 FGF19 Promotes Glycogen Synthesis in Liver.....	64
4.2.7 FGF19-dependent Phosphorylation of GSK3 and GS Depends on ERK/RSK Activity	66
4.2.8 FGF19 Promotes Glycogen Synthesis in Diabetic Animals Lacking Insulin	67

4.3 Discussion	69
4.3.1 FGF19 and Insulin Work in a Coordinated Temporal Fashion.....	69
4.3.2 FGF19 and Insulin Activate Different Signaling Pathways and Have Both Overlapping and Separate Effects on Liver Metabolism	69
4.3.3 FGF19 as a Therapeutic Agent in the Treatment of Diabetes.....	73
4.4 Summary	74
CHAPTER 5	76
Materials and Methods.....	76
5.1 Cell Culture and Reagents	76
5.2 Mouse Animal Experiments	77
5.3 RT-qPCR.....	78
5.4 Chromatin Immunoprecipitation	79
5.5 Electrophoretic Mobility Shift Assay (EMSA)	81
5.6 Nuclear Lysate Preparation	81
5.7 Western Blotting.....	82
5.8 Mouse Primary Hepatocyte Isolation	83
5.9 ³ H -Labeling of Protein-bound Alanine.....	83
5.10 Protein Synthesis Rate Calculations.....	84
5.11 Glycogen Synthase Activity Assay	85
5.12 Glycogen Content Determination.....	86
5.13 Hyperglycemic-Basal Insulin Clamp Study	86
5.14 Statistical Analysis	87
Bibliography	88

PRIOR PUBLICATIONS

Chan EY, Kir S, Tooze SA. 2007. siRNA screening of the kinome identifies ULK1 as a multidomain modulator of autophagy. *J Biol Chem.* **282**: 25464-25474.

Gur-Dedeoglu B, Konu O, Kir S, Ozturk AR, Bozkurt B, Ergul G, Yulug IG. 2008. A resampling-based meta-analysis for detection of differential gene expression in breast cancer. *BMC Cancer* **8**: 396.

Kir S, Beddow SA, Samuel VT, Miller P, Previs SF, Suino-Powell K, Xu HE, Shulman GI, Kliewer SA, Mangelsdorf DJ. 2011. FGF19 as a postprandial, insulin-independent activator of hepatic protein and glycogen synthesis. *Science* **331**: 1621-1624.

Li T, Holmstrom SR, Kir S, Umetani M, Schmidt DR, Kliewer SA, and Mangelsdorf DJ. 2011. The G Protein-Coupled Bile Acid Receptor, TGR5, Stimulates Gallbladder Filling. *Mol Endocrinol* **25**: 1066-1071.

Kir S, Kliewer SA, Mangelsdorf DJ. 2011. Roles of FGF19 in liver metabolism. *Cold Spring Harb Symp Quant Biol.*

LIST OF FIGURES AND TABLES

Figure 1.1 Nuclear receptors and their ligands	2
Figure 1.2 FGF family	8
Figure 1.3 Nuclear receptor-FGF signaling	10
Figure 1.4 Regulation of bile acid metabolism by CCK and FGF19.....	14
Figure 2.1 SHP interactions with HNF4 α and LRH-1	20
Figure 2.2 SHP, HNF4 α and LRH-1 binding to the <i>Cyp7a1</i> promoter.....	22
Figure 2.3 HNF4 α and LRH-1 co-occupy the <i>Cyp7a1</i> promoter	23
Figure 2.4 Mutagenesis of HNF4 α and LRH-1 binding sites on the <i>Cyp7a1</i> promoter ..	24
Figure 2.5 SHP requires HNF4 α or LRH-1 for binding to the <i>Cyp7a1</i> promoter.	25
Figure 2.6 HNF4 α and LRH-1 maintain <i>Cyp7a1</i> expression and regulate FGF19- dependent repression.....	27
Figure 2.7 FGF19 does not change SHP binding to the <i>Cyp7a1</i> promoter.....	29
Figure 2.8 FGF19 does not change HNF4 α and LRH-1 binding to the <i>Cyp7a1</i> promoter	30
Figure 2.9 FGF19 reduces histone H3 acetylation on the <i>Cyp7a1</i> promoter.....	31
Figure 2.10 FGF19 reduces histone H3K4 trimethylation on the <i>Cyp7a1</i> promoter.....	32
Figure 3.1 PD-0325901 treatment of HepG2 cells	39
Figure 3.2 U0126 treatment of HepG2 cells.....	40
Figure 3.3 Treatment of HepG2 cells with various kinase inhibitors	41
Figure 3.4 Dose response analysis of PD-0325901 treatment in mice	43
Figure 3.5 Time course analysis of PD-0325901 treatment in mice.....	45
Figure 3.6 Effects of PD-0325901 on the <i>Shp</i> promoter activity.....	46

Figure 3.7 Effects of PD-0325901 on the <i>Cyp7a1</i> promoter activity	47
Figure 3.8 PD-0325901 treatments of HNF4 α or LRH-1 liver specific knockout mice..	49
Figure 3.9 FGF19 and PD-0325901 co-treatment in mice.....	50
Figure 3.10 FGF19 and PD-0325901 co-treatment in mouse primary hepatocytes.....	52
Figure 3.11 FGF19 signaling in <i>Fgfr4</i> ^{-/-} mice is intact but <i>Cyp7a1</i> repression is impaired	54
Figure 4.1 Stimulation by FGF19 of the signaling pathways that regulate protein synthesis in liver	59
Figure 4.2 FGF19-induced signaling depends on ERK and RSK kinase activity.....	61
Figure 4.3 Increased rates of protein synthesis in mice liver after FGF19 treatment	63
Figure 4.4 FGF19 inhibits GSK3 signaling to induce liver glycogen synthase in mice..	64
Figure 4.5 Liver glycogen synthesis is regulated by FGF15/19	65
Figure 4.6 FGF19-induced signaling depends on RSK kinase activity	66
Figure 4.7 FGF19-induced glycogen synthesis is independent of insulin	68
Figure 4.8 Insulin and FGF19 act through different signaling pathways to coordinate overlapping but distinct postprandial responses in liver	71
Table 4.1 Metabolic effects of FGF19 and insulin in liver	72
Figure 4.9 FGF19 activates STAT1 and STAT3 in liver.....	73

LIST OF ABBREVIATIONS

- AF-1 – Activation Function 1
- AF-2 – Activation Function 2
- Akt – Protein Kinase B (PKB)
- BAT – Bile Acid CoA:Amino Acid N-Acyltransferase
- BACS – Bile Acid-CoA Synthetase
- BSEP – Bile Salt Export Pump
- cAMP – Cyclic Adenosine MonoPhosphate
- CCK – Cholecystokinin
- ChIP – Chromatin Immunoprecipitation
- CREB – cAMP Response Element-Binding Protein
- CYP7A1 – Cholesterol 7 α -Hydroxylase
- CYP8B1 – Sterol 12 α -Hydroxylase
- CYP27A1 – Sterol 27-Hydroxylase
- DMSO – Dimethyl Sulfoxide
- DR-1 – Direct Repeat 1
- FOXO1 – Forkhead Box O1a
- eIF4 – Eukaryotic Initiation Factor 4
- EMSA – Electrophoretic Mobility Shift Assay
- ER α – Estrogen Receptor α
- ERK – Extracellular Signal-Regulated Kinase
- ERR – Estrogen-Related Receptor

F19 – Fibroblast Growth Factor 19
FGF – Fibroblast Growth Factor
FGFR – Fibroblast Growth Factor Receptor
FXR – Farnesoid X Receptor
G6pase – Glucose-6-Phosphatase
GIP – Gastric Inhibitory Polypeptide
GLP-1 – Glucagon-Like Peptide 1
GR – Glucocorticoid Receptor
GS – Glycogen Synthase
GSK3 α/β – Glycogen Synthase Kinase 3 α/β
H3K4 – Histone H3 Lysine 4
HEK293 – Human Embryonic Kidney 293
HepG2 – Liver Hepatocellular Carcinoma Cell Line
HNF4 α – Hepatocyte Nuclear Factor 4 α
IBABP – Intestinal Bile Acid-Binding Protein
IgG – Immunoglobulin G
i.p. – Intraperitoneal
IRS1/2 – Insulin Receptor Substrate 1/2
IR-1 – Inverted Repeat 1
i.v. – Intravenous
JNK – c-Jun N-terminal Kinase
HBSS – Hank's Buffered Salt Solution
KLB – Klotho β

LRH-1 – Liver Receptor Homolog 1

LXR – Liver X Receptor

MAP kinase/MAPK – Mitogen-activated Protein kinase

MEK – MAPK/Erk Kinase

Mnk1 – MAPK-Interacting Kinase 1

MODY1 – Maturity Onset Diabetes of the Young 1

mRNA – Messenger Ribonucleic Acid

mTOR – mammalian Target Of Rapamycin

MRP2 – Multidrug Resistance-Associated Protein 2

NGFI-B – Nerve Growth Factor IB

NR – Nuclear Receptor

OST α/β – Organic Solute Transporter α/β

PBS – Phosphate Buffered Saline

PD – PD-0325901

Pepck – PhosphoEnolPyruvate Carboxykinase

PGC1 α – PPAR-Gamma Coactivator 1 α

PI3K – Phosphatidylinositol 3-Kinase

PPAR α – Peroxisome Proliferator-Activated Receptor α

Ras – Rat Sarcoma small GTPase

rpS6 – ribosomal protein S6

RSK – Ribosomal S6 Kinase (p90)

RT-qPCR – Reverse Transcription quantitative Polymerase Chain Reaction

RXR – Retinoid X Receptor

S6K – Ribosomal S6 Kinase (p70)

SDS-PAGE – Sodium Dodecyl Sulfate Polyacrylamide Gel Electrophoresis

SEM – Standard Error of Mean

SHP – Small Heterodimer Partner

SREBP-1c – Sterol Regulatory Element-Binding Protein 1c

Stat – Signal Transducer and Activator of Transcription

STZ – Streptozotocin

VDR – Vitamin D Receptor

Veh – Vehicle

CHAPTER 1

General Introduction

1.1 NUCLEAR RECEPTORS

Nuclear Receptors (NRs) form a large family of transcription factors that are regulated by ligands. Ligand binding activates NRs and induces expression of their target genes. Ligand-dependent activation of NRs let them act as transcriptional switches in response to their ligands which include lipophilic hormones, vitamins and dietary lipids (Sonoda et al. 2008). First NRs discovered more than two decades ago were endocrine NRs, such as Glucocorticoid Receptor (GR) and Estrogen Receptor α (ER α) which bind to their lipophilic hormones with high affinity ($K_d = \text{nM}$ range). Sequence comparisons among first discovered NRs led to the understanding that NRs share common domain structure. Search for other proteins sharing similar sequence homology led to the discovery of other NRs, some of which were not shown to have physiologic ligands and so named as orphan NRs (Fig. 1.1).

In the last two decades, some of the orphan NRs were de-orphanized by the discovery of their physiologic ligands, forming the group of so-called adopted orphan NRs. This group of NRs responds to endogenous and dietary lipids with low binding affinity ($K_d = \mu\text{M}$ range). Examples include Liver X Receptor (LXR), which is characterized as an oxysterol receptor, and Farnesoid X Receptor (FXR) that is regulated by bile acids. Some orphan NRs were shown to interact with lipid molecules, however, physiologic regulation of these NRs by the interacting ligands has not been established

(Sonoda et al. 2008). Hepatocyte Nuclear Factor 4 α (HNF4 α) and Liver Receptor Homolog 1 (LRH-1) are examples shown to bind to fatty acids and phospholipids, respectively (Fayard et al. 2004; Forman 2005; Bolotin et al. 2010). However, a number of orphan NRs have not been shown to interact with any ligands and, based on the size of their ligand binding pocket, some of them are unlikely to be regulated by ligands. Nerve Growth Factor IB (NGFI-B) NRs well exemplify this group (Fig. 1.1).

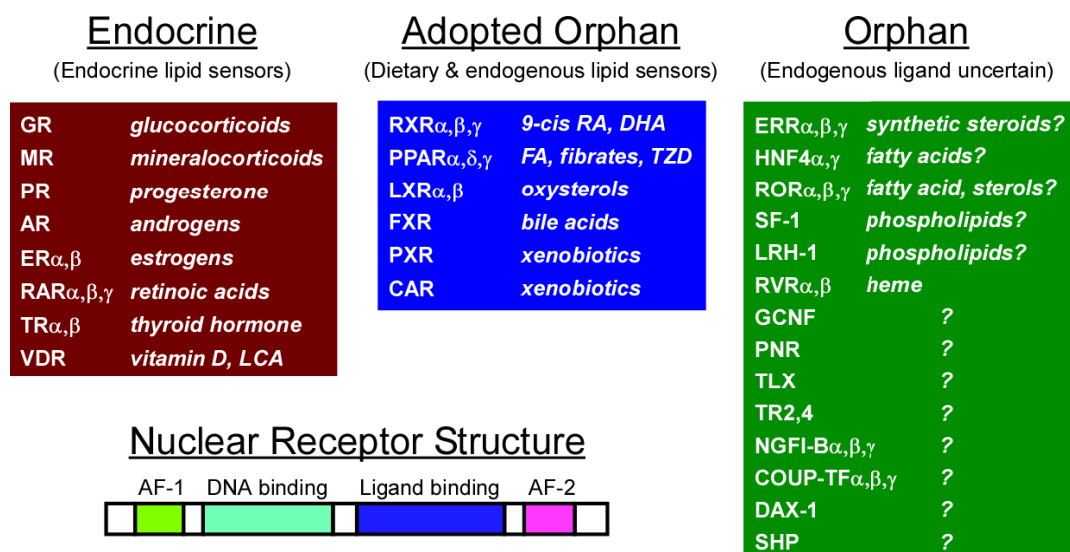


Figure 1.1 Nuclear receptors and their ligands. 48 human nuclear receptors are grouped and their known ligands are shown on the right. General nuclear receptor domain structure is also depicted.

NR common structural motifs include an Activation Function 1 (AF-1) motif, a DNA binding domain at the N-terminus, a ligand binding domain, and an Activation Function 2 (AF-2) motif at the C-terminus. AF-1 motif is a ligand-independent activation domain, whereas AF-2 motif is regulated by ligands. Ligand binding causes conformational changes on AF-2 and induces release of co-repressors and recruitment of

co-activators. The DNA binding domain consists of two highly conserved zinc finger motifs unique to NRs. Most NRs form dimers and bind to two hexanucleotide sequences of AGGTCA or its variants separated by a gap of a certain number of nucleotides. NR binding specificity is determined by the number of nucleotides in the gap and the orientation of the hexonucleotide binding sites (direct, inverted or everted). The ligand binding domain is unique to NRs and is required for receptor dimerization, ligand binding and co-activator interaction (Sonoda et al. 2008).

In the following sections, NRs that were studied in this dissertation will be discussed briefly.

1.1.1 Farnesoid X Receptor (FXR, NR1H4)

FXR was named on the basis of its weak interaction with farnesol. Later, FXR was identified as the bile acid nuclear receptor as certain bile acids were shown to bind to and potently activate it. FXR (also called FXR α) is predominantly expressed in liver, intestine, kidney and adrenal glands. A second *FXR* gene, *Fxr β* , is also present in rodents, rabbits and dogs; however, it is a pseudogene in primates and human. FXR heterodimerizes with Retinoid X Receptor (RXR) and binds to inverted repeat NR binding sites separated by a gap of 1 nucleotide (IR-1) (Lee et al. 2006a).

FXR has been shown to play a central role in regulation of bile acid metabolism in liver and intestine. Bile acids produced in liver are conjugated with taurine or glycine and secreted across the bile canalicular membrane for storage in the gallbladder. Activated by bile acids, FXR induces expression of bile acid conjugation enzymes Bile

Acid CoA:Amino Acid N-Acyltransferase (BAT) and Bile Acid-CoA Synthetase (BACS). FXR also induces expression of bile acid transporters Bile Salt Export Pump (BSEP) and Multidrug Resistance-Associated Protein 2 (MRP2) (Lee et al. 2006a). After each meal, bile acids stored in the gallbladder are released into the intestine where 95% of them are re-absorbed. In the intestine, bile acids activate FXR which then induces expression of Intestinal Bile Acid-Binding Protein (IBABP) and bile acid transporters Organic Solute Transporter α (OST α) and OST β to facilitate bile acid transport into the portal circulation. In the ileum, FXR also up-regulates expression of FGF19 (or FGF15 in rodents) which acts as an endocrine hormone and suppresses bile acid synthesis in liver through transcriptional repression of bile acid synthetic enzymes Cholesterol 7 α -Hydroxylase (CYP7A1) and Sterol 12 α -Hydroxylase (CYP8B1). In liver, FXR also induces expression of nuclear receptor SHP which plays an important role in negative feedback regulation of CYP7A1 and CYP8B1 in response to both bile acids and FGF15/19 (Lee et al. 2006a).

1.1.2 Hepatocyte Nuclear Factor 4 alpha (HNF4 α , NR2A1)

HNF4 α is predominantly expressed in adult liver, kidney, pancreas, intestine and colon as well as visceral endoderm. It is an important transcriptional regulator in both early embryogenesis and adulthood. HNF4 α binds to direct repeat (DR-1) NR binding sites exclusively as homodimers, unlike most NRs that heterodimerize with RXR. HNF4 α activates expression of many genes involved in glucose, fatty acid, cholesterol, bile acid, xenobiotic and drug metabolism. Fatty acids were proposed to be ligands for HNF4 α ,

however, this is highly debatable since physiologic regulation of HNF4 α by ligands has not been shown (Bolotin et al. 2010). Mutations in human *HNF4A* gene are directly linked to maturity onset diabetes of the young 1 (MODY1), a form of type II diabetes. In addition, mutations in HNF4 α binding sites in promoters of blood coagulation factors lead to certain types of hemophilia (Bolotin et al. 2010).

Mice lacking hepatic *Hnf4 α* were shown to accumulate lipids in liver and exhibit greatly reduced serum cholesterol and triglyceride levels. These mice also exhibited elevated serum bile acid levels although expression of bile acid synthetic enzymes *Cyp7a1*, *Cyp8b1* and *Cyp27a1* were reduced. Increased serum bile acid levels in *Hnf4 α* deficient mice were linked to impaired bile acid uptake into liver since expression of hepatic bile acid transporters were down-regulated. These defects caused by loss of hepatic *Hnf4 α* indicate that HNF4 α is a prominent regulator of bile acid and lipid metabolism in liver (Hayhurst et al. 2001; Inoue et al. 2006b).

1.1.3 Liver Receptor Homolog 1 (LRH-1, NR5A1)

LRH-1 expression is largely confined to liver, pancreas and intestine. As germline knockout of *Lrh-1* in mice causes embryonic lethality, LRH-1 is also considered as an important regulator of development. Unlike most NRs which form either homodimers or heterodimers with RXR, LRH-1 binds to DNA as a monomer. The LRH-1 DNA binding sequence also differs from other NR binding sites. The LRH-1 consensus binding sequence is YCAAGGYCR, where Y is a pyrimidine and R is a purine. LRH-1 has been shown to regulate cholesterol and bile acid metabolism as well as exocrine

pancreas secretion (Fayard et al. 2004). Phospholipids have been proposed as LRH-1 ligands; however, physiologic regulation of LRH-1 by ligands has not been established (Forman 2005; Sonoda et al. 2008).

Mice lacking hepatic *Lrh-1* were shown to have altered bile acid composition due to significantly reduced *Cyp8b1* expression levels. Although LRH-1 was implicated to be a positive regulator of *CYP7A1* transcription in vitro, liver *Lrh-1* knockout mice did not display altered *Cyp7a1* expression possibly because of compensatory responses mediated by HNF4 α (Mataki et al. 2007; Lee et al. 2008). In addition, bile acid negative feedback regulation by FXR was not compromised in *Lrh-1*-deficient mice, indicating that LRH-1 is not essential for this process. *Lrh-1* depletion also caused striking decreases in *Shp* mRNA levels showing that LRH-1 is necessary for transcription of this gene (Mataki et al. 2007; Lee et al. 2008).

1.1.4 Small Heterodimer Partner (SHP, NR0B2)

SHP is predominantly expressed in liver. Lower levels of *SHP* mRNA were also detected in other tissues including heart, pancreas and intestine. SHP is an exceptional NR that lacks a DNA binding domain. The presence of a ligand binding domain classifies SHP as a NR; however, no ligands have been described for SHP so far and whether SHP ligand binding pocket can accommodate a ligand is unknown due to the lack of three dimensional structure analysis. SHP acts as a negative regulator of transcription and associates with transcriptional co-repressors. SHP has been proposed to regulate gene expression through its interactions with other NRs, including LXR, LRH-1, HNF4 α , ERs

and ERRs (Bavner et al. 2005). SHP is a crucial regulator of bile acid metabolism as bile acid negative feedback regulation by FXR or FGF15/19 is abolished in *Shp*-deficient mice (Inagaki et al. 2005).

1.2 FIBROBLAST GROWTH FACTORS AND METABOLISM

Fibroblast Growth Factor (FGF) family contains important regulators of a variety of developmental processes such as brain and limb development. These growth factors act as paracrine cytokines that regulate tissue patterning and organogenesis during embryogenesis. FGF19, FGF21 and FGF23 differ from the rest of the FGF family and form the FGF19 subfamily (Fig. 1.2). Unlike other FGFs that have paracrine functions, FGF19 subfamily members have reduced affinity for heparin that permits them to escape the extracellular matrix and circulate as endocrine hormones. Thus, FGF19 subfamily proteins are also referred to as endocrine FGFs (Beenken et al. 2009).

The primary source of endocrine FGF19 is the ileum where FGF19 expression is controlled by the bile acid nuclear receptor FXR (Holt et al. 2003; Inagaki et al. 2005). Bile acids released into the intestine after a meal bind to and activate FXR and thereby induce expression of FGF19. In humans, the postprandial rise in serum bile acids is followed by a synchronous serum FGF19 peak that takes place around 3 hours after a meal (Lundasen et al. 2006). This close relationship between FGF19 and bile acids renders FGF19 a postprandial hormone (Fig. 1.3 and 1.4).

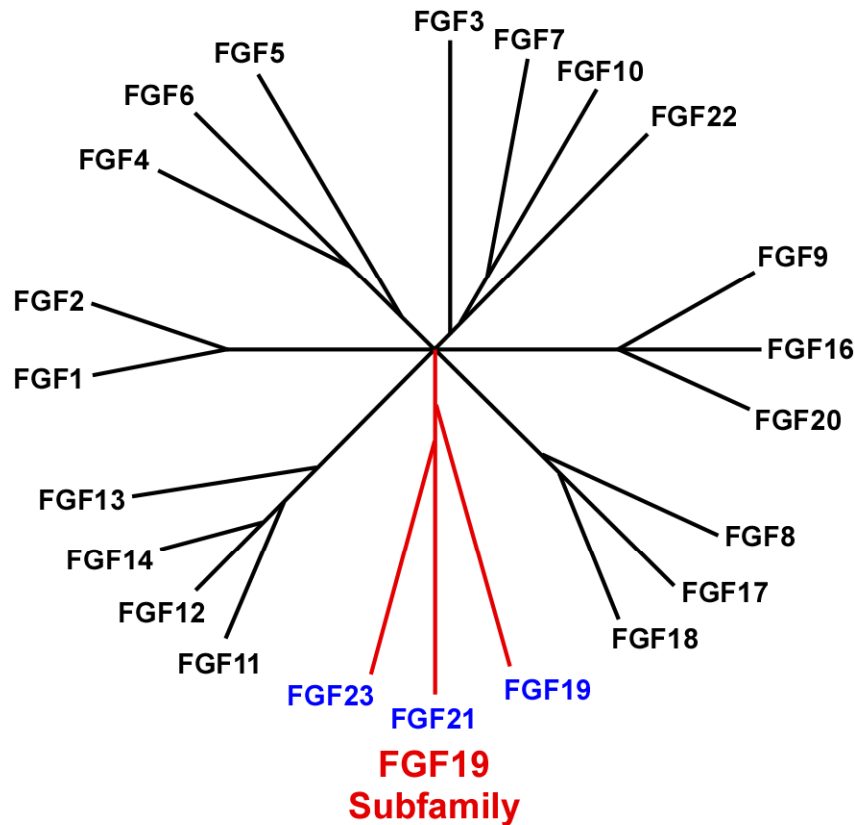


Figure 1.2 FGF family. The FGF19 subfamily contains the endocrine FGFs: FGF19, FGF21 and FGF23.

On its own, FGF19 fails to activate FGF receptors (FGFRs) as a result of its reduced affinity towards extracellular matrix glucosaminoglycans that promote the interaction between FGFs and their receptors. Recent studies have shown that FGF19 requires another transmembrane protein, β -Klotho, which enables FGF19 binding to FGFR4 (its preferred receptor) and acts as the obligatory co-receptor that permits FGF19-FGFR4 signaling (Kurosu et al. 2007; Lin et al. 2007). Thus, to be a target of FGF19, a tissue must express both FGFR4 and β -Klotho. This requirement makes liver the main target of endocrine FGF19 as both FGFR4 and β -Klotho are highly expressed in this

organ. In liver, FGF19 has been shown to regulate bile acid metabolism (Inagaki et al. 2005).

Just like FGF19, FGF21 and FGF23 are also regulated by nuclear receptors. FGF21 expression in liver is controlled by the nuclear receptor PPAR α that is activated by fatty acid metabolites. FGF23 is produced in bones where its expression is regulated by the Vitamin D Receptor (VDR). Like FGF19, FGF21 and FGF23 also fail to activate FGFRs as a result of their reduced affinity for the extracellular matrix. Both FGF21 and FGF23 signal through FGFR1c. FGF21 requires β -Klotho as the co-receptor, whereas FGF23 requires Klotho protein. Restricted expression of Klotho and β -Klotho along with FGFR1c determines primary target tissues. FGF21 regulates carbohydrate and lipid metabolism in the adipose tissue, whereas FGF23 is involved in phosphate and vitamin D metabolism in the kidney (Fig. 1.3).

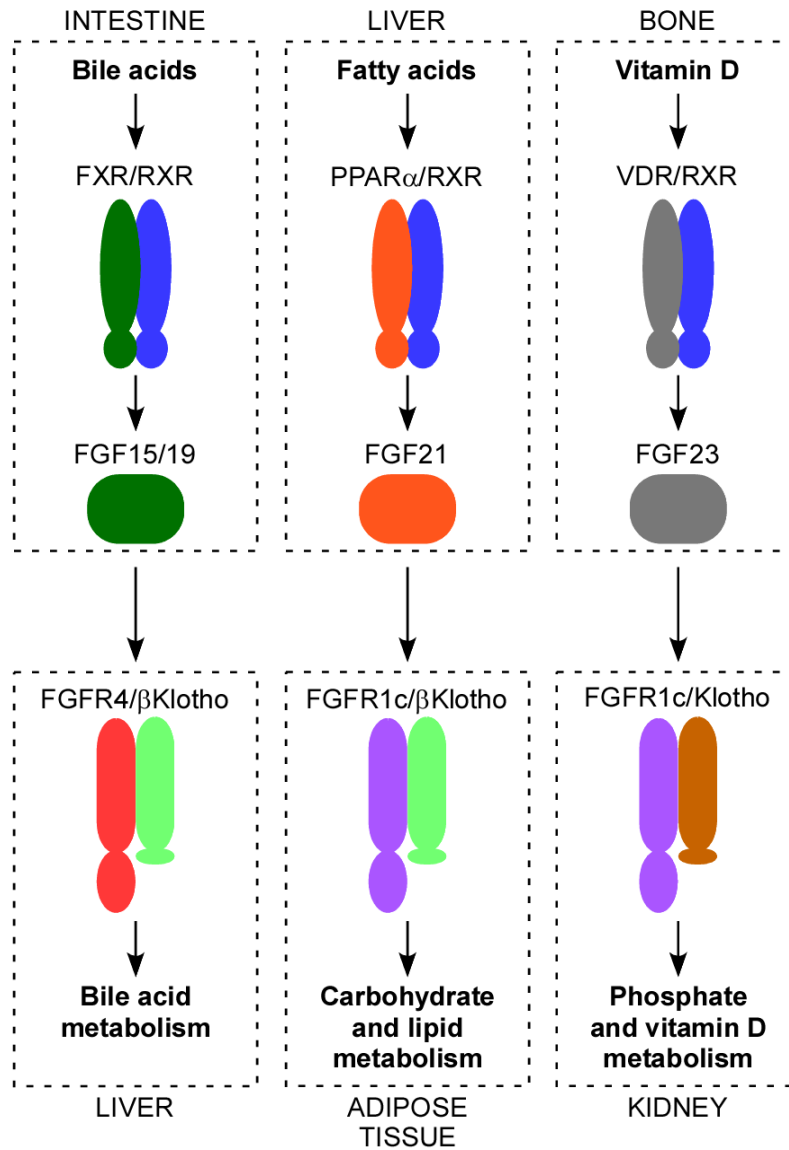


Figure 1.3 Nuclear receptor-FGF signaling. Nuclear receptors regulate expression of the endocrine FGFs in the source tissues. Target tissues of the endocrine FGFs are determined by spatial co-expression of their FGFRs and Klotho/ β -Klotho co-receptors.

1.3 FGF19 AND LIVER METABOLISM

1.3.1 FGF19 Regulates Bile Acid Metabolism

Bile acids are strong detergents produced by catabolism of cholesterol in liver. After a meal, bile acids stored in gallbladder are released into the intestine to facilitate solubilization and absorption of lipids and lipid soluble vitamins. Because of their toxic nature, synthesis of bile acids must be tightly regulated. This regulation takes place at the level of gene expression through a bile acid-dependent negative feedback mechanism. Cholesterol 7 α -hydroxylase (CYP7A1) is the enzyme that catalyzes the first and the rate limiting step in the major bile acid synthesis pathway and it is the main target of the feedback regulation. Bile acids repress transcription of the *CYP7A1* gene and thereby downregulate their own synthesis.

The nuclear receptor FXR has been shown to play a crucial role in regulation of bile acid homeostasis. The negative feedback regulation of bile acid synthesis is abolished in *Fxr*-deficient mice and, thus, *Cyp7a1* expression levels are elevated in these animals (Sinal et al. 2000). Initially, it was assumed that FXR function in liver was solely responsible for *Cyp7a1* repression. However, studies have shown that the negative feedback regulation also requires FXR-dependent synthesis of FGF19 in intestine. As first described by Holt *et al.* (2003), *FGF19* is a direct bile acid-dependent target gene of FXR. The *FGF19* promoter contains a single FXR-response element that is conserved in rodents and human. FGF19 alone is able to repress *CYP7A1* mRNA levels in human primary hepatocytes (Holt et al. 2003). *In vivo* administration of bile acids or an FXR

agonist (GW4064) in mice induces *Fgf15* expression in epithelial cells of the ileum and both FGF15 and FGF19 can completely suppress *Cyp7a1* expression in liver (Inagaki et al. 2005). FGF15/19 fails to repress *Cyp7a1* in *Fgfr4*^{-/-} mice demonstrating the specificity of FGF15's action.

Further evidence for the requirement of FGF15/19 in maintaining proper bile acid homeostasis has come from analysis of various animal models harboring deletions on the FGF15 signaling axis. *Fgfr4*^{-/-}, *Klb*^{-/-} (i.e., β -Klotho-null), and *Fgf15*^{-/-} mice all have increased levels of *Cyp7a1* expression as well as an elevated bile acid pool size (Yu et al. 2000; Inagaki et al. 2005; Ito et al. 2005). Moreover, administration of GW4064 or the endogenous FXR agonist, cholic acid, fails to repress *Cyp7a1* in *Fgfr4*^{-/-} or *Fgf15*^{-/-} mice. In addition, GW4064 was shown to repress *Cyp7a1* in liver-specific *Fxr*^{-/-} mice; however, this effect was completely abolished in ileum-specific *Fxr*^{-/-} mice (Kim et al. 2007). These findings confirmed that FXR-mediated negative feedback regulation is dependent on entero-hepatic signaling mediated by FGF15/19.

Results complementary to the above mouse studies have come from clinical studies. In humans, serum FGF19 levels peak after a postprandial rise in serum bile acid levels and this peak is followed by a declining phase of bile acid synthesis (Lundasen et al. 2006). In addition, patients with primary bile acid malabsorption syndrome have reduced FGF19 production by the ileum, which is associated with increased bile acid synthesis and bile acid diarrhea (Walters et al. 2009). Moreover, inflammatory bowel disease patients with resected distal ileum exhibit dysregulated bile acid metabolism with reduced serum FGF19 and elevated serum bile acid levels (Lenicek et al. 2011).

Although there has been considerable progress in the field of bile acid regulation, the exact mechanism of *Cyp7a1* repression remains elusive. In addition to the FGF15/19 signaling pathway, it has been shown that orphan nuclear receptor small heterodimer partner (SHP) is required for repression of *Cyp7a1*, since administration of FXR agonist or FGF15/19 fails to repress *Cyp7a1* transcription in *Shp*-deficient mice (Kerr et al. 2002; Wang et al. 2002; Inagaki et al. 2005). However, the mechanism by which the FGF15/19-FGFR4- β -Klotho signaling pathway intersects with the SHP repression pathway to mediate repression *Cyp7a1* transcription remains the focus of current research.

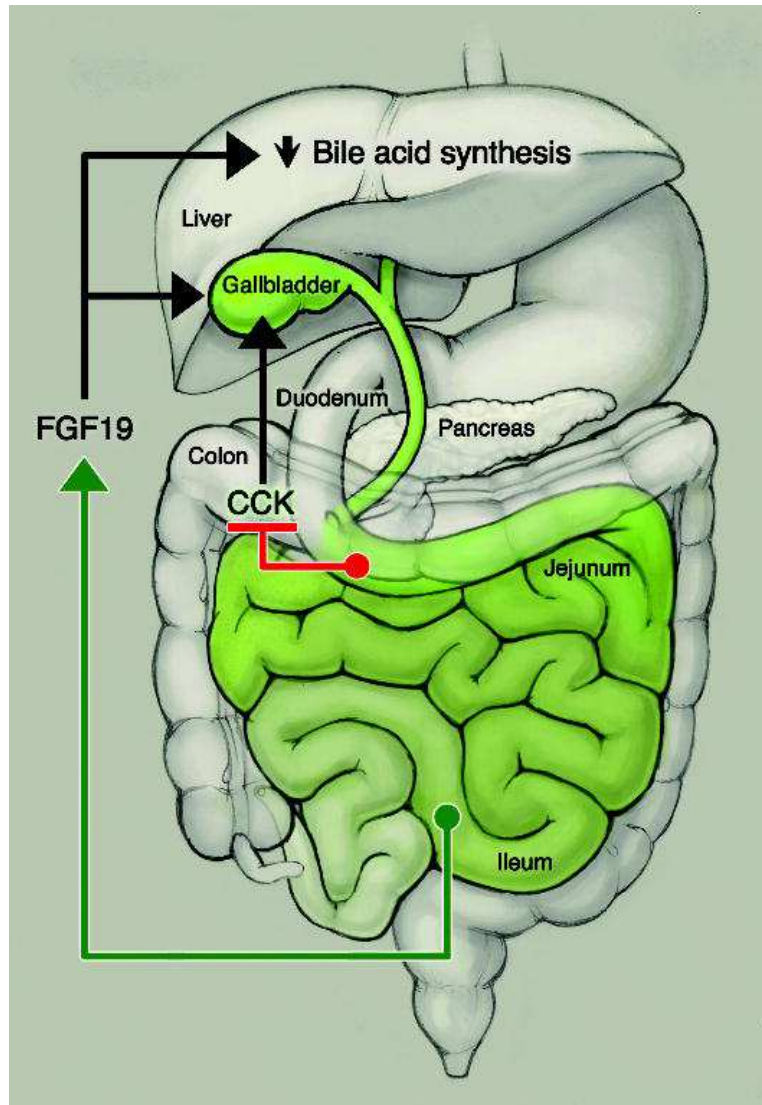


Figure 1.4 Regulation of bile acid metabolism by CCK and FGF19. Cholecystokinin (CCK) stimulates contraction of the gallbladder and release of bile acids into the intestine. As detergents, bile acids facilitate solubilization and absorption of lipids in the intestine. In addition, bile acids also act as messenger molecules. They inhibit CCK secretion from the duodenum in a negative feedback loop to block further gallbladder contraction. In the ileum, bile acids bind to and activate FXR and induce FGF19 expression. In contrast to CCK, FGF19 stimulates gallbladder relaxation and filling. Around 95% of bile acids released into the intestine are re-absorbed and recycled back to liver. By inducing gallbladder relaxation, FGF19 facilitates this recycling process. In addition, FGF19 suppresses bile acid synthesis in liver during this bile acid peak time in the portal circulation.

A second role for FGF15/19 in bile acid regulation has been described in gallbladder. *Fgf15*^{-/-} mice have virtually empty gallbladders and restoring back FGF15 to these mice restores the gallbladder back to its normal volume, implicating an essential role for FGF15/19 in gallbladder filling (Choi et al. 2006). Cholecystokinin (CCK), another intestine-derived postprandial hormone, is a well-known inducer of gallbladder emptying. FGF15/19 administration was shown to oppose the action of CCK directly by relaxing gallbladder smooth muscle and inducing gallbladder filling in CCK-treated mice (Choi et al. 2006). These findings defined the hormonal basis for gallbladder filling and suggested that bile acids traversing the intestine act as a reset switch for postprandial gallbladder emptying first by repressing CCK secretion in the duodenum, and secondly by inducing gallbladder filling by activating FGF19 expression in the ileum (Fig. 1.4).

1.3.2 FGF19 Improves Glucose Metabolism in Diabetic Mice

Effects of FGF19 on glucose metabolism were first described in FGF19 transgenic mice. These animals displayed increased metabolic rate, decreased adiposity, reduced liver triglycerides, increased fatty acid oxidation, reduced serum glucose and improved insulin sensitivity. Furthermore, FGF19 transgenic mice did not become obese or diabetic on a high fat diet (Tomlinson et al. 2002). FGF19 treatment of obese, diabetic mice led to similar improvements in metabolism. These striking effects of FGF19 on metabolic rate and glucose metabolism lead to the possibility that FGF19 might have therapeutic potential for the treatment of Type II diabetes. However, unfortunately, FGF19 transgenic mice were shown to develop liver tumors as they aged (Nicholes et al.

2002). Serum FGF19 levels in these mice are much higher than physiologic levels and are in a pharmacologic range. Currently, it is not known whether repeated FGF19 treatment can cause similar complications in humans. Repeated FGF19 treatment was shown to induce cell proliferation in liver but it did not induce tumors (Nicholes et al. 2002). Further studies need to be performed to understand the nature and cause of this adverse effect of FGF19. It is also possible that FGF19 variants which lack the mitogenic effect but retain the glucose lowering effects can be engineered (Wu et al. 2010; Wu et al. 2011).

CHAPTER 2

Nuclear Receptors HNF4 α and LRH-1 Are Essential Regulators of *Cyp7a1* Transcription

2.1 INTRODUCTION

Bile acids are natural detergents that facilitate solubilization and absorption of lipid molecules in the intestine. Due to their toxic nature, metabolism of bile acids is tightly regulated. Bile acid nuclear receptor FXR plays a central role in this regulation. Bile acids produced in liver bind to and activate FXR which up-regulates expression of bile acid conjugation enzymes and transporters to induce bile acid storage in the gallbladder. After each meal, bile acids are released into the intestine for their role as biologic detergents and around 95% of them are reabsorbed by the intestine where they again activate FXR, which then up-regulates expression of bile acid binding and transporter proteins to facilitate transfer of bile acids into the portal circulation (Lee et al. 2006a).

In the ileum, FXR also induces expression of Fibroblast Growth Factor 19 (FGF19; or FGF15 in rodents), which is an endocrine FGF and an important hormonal regulator of bile acid synthesis. First, FGF15/19 stimulates gallbladder relaxation to facilitate gallbladder filling by the bile acids being recycled back to liver. Secondly, FGF15/19 represses further bile acid synthesis in liver during this bile acid peak time in the portal circulation. FGF15/19 is crucial for both processes as *Fgf15*-deficient mice

display defects in gallbladder filling and repression of bile acid synthesis in response to FXR activation (Inagaki et al. 2005; Choi et al. 2006).

Negative feedback regulation of bile acid synthesis by the FXR-FGF15/19 axis is achieved via transcriptional repression of Cholesterol 7 α -hydroxylase (CYP7A1) that catalyzes the first and the rate limiting step in the major bile acid synthesis pathway in liver. Repression of *Cyp7a1* expression by FXR or FGF15/19 requires Small Heterodimer Partner (SHP), which is an atypical nuclear receptor that lacks a DNA binding domain (Kerr et al. 2002; Wang et al. 2002; Inagaki et al. 2005). SHP has been considered to interact with the nuclear receptor Liver Receptor Homolog-1 (LRH-1) for binding to the *Cyp7a1* promoter (Goodwin et al. 2000; Lu et al. 2000). However, *Lrh-1*-deficient mice did not display severe defects in negative feedback regulation of *Cyp7a1* (Lee et al. 2008). Here, I tested roles of LRH-1 and Hepatocyte Nuclear Factor 4 α (HNF4 α), another nuclear receptor implicated in bile acid regulation (De Fabiani et al. 2001; Inoue et al. 2006b), for SHP binding to the *Cyp7a1* promoter and repression of *Cyp7a1* expression by FGF19. I show that both LRH-1 and HNF4 α are crucial transcriptional activators of the *Cyp7a1* promoter and are required for SHP binding and FGF19-dependent repression of *Cyp7a1*.

2.2 RESULTS

2.2.1 SHP Interacts with Both HNF4 α and LRH-1

It was previously shown that FGF15 overexpression fails to repress *Cyp7a1* transcription in *Shp*^{-/-} mice (Inagaki et al. 2005; Choi et al. 2006). Because recombinant

mouse FGF15 is unstable with variable bioactivity but shows strongly overlapping effects with human FGF19 (Potthoff et al. 2011), I used FGF19 protein in mouse studies. FGF19 treatment also failed to inhibit *Cyp7a1* transcription in *Shp*^{-/-} mice, demonstrating that SHP protein is crucial for *Cyp7a1* repression (Fig. 2.1A). SHP is an unusual nuclear receptor that does not bind to DNA but interacts with other nuclear receptors and acts as a co-repressor. The *Cyp7a1* promoter contains conserved putative DNA binding sites for two nuclear receptors; HNF4 α and LRH-1. Therefore, I tested interaction of SHP with these two proteins in cell culture. FLAG-HA tagged SHP co-immunoprecipitated FLAG-tagged HNF4 α and LRH-1 (Fig. 2.1B). Furthermore, SHP overexpression repressed HNF4 α or LRH-1-induced transcriptional activity in luciferase reporter assays, demonstrating functional interactions between these proteins (Fig. 2.1, C and D).

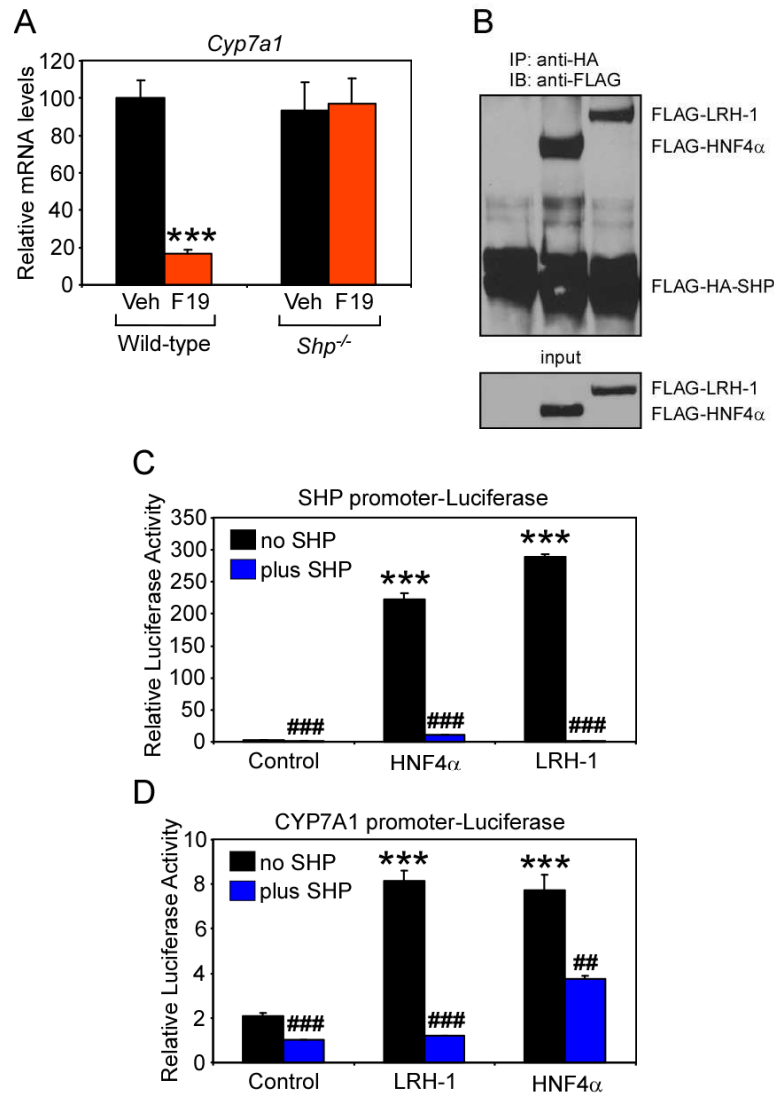


Figure 2.1 SHP interactions with HNF4 α and LRH-1. (A) Overnight-fasted mice (n = 6) were injected i.p. with vehicle or FGF19 protein (1mg/kg; 1 mg per kg body weight). Mice were sacrificed 6 hours after the injections and hepatic *Cyp7a1* mRNA levels were measured by RT-qPCR. (B) Tagged proteins were overexpressed in HEK293 cells and immunoprecipitated with HA antibody beads. (C) HEK293 cells were transfected with a luciferase reporter under the control of the human *SHP* promoter and with expression plasmids for indicated proteins (n = 4). (D) HepG2 cells were transfected with a luciferase reporter under the control of rat *Cyp7a1* promoter and with expression plasmids for indicated proteins (n = 4). Values are means \pm SEM. Statistics by two-tailed *t* test. (*) refer to differences between control and HNF4 α or LRH-1 groups. (#) refer to differences between no SHP and plus SHP groups. ****P*<0.0005, ##*P*<0.005, ###*P*<0.0005.

2.2.2 SHP, HNF4 α and LRH-1 Bind to the Same Location on the *Cyp7a1* Promoter

Next, I tested binding of SHP, HNF4 α and LRH-1 to the *Cyp7a1* promoter in mouse liver. Lacking a SHP antibody that detects endogenous SHP protein, I overexpressed FLAG-tagged SHP in liver via adenoviral expression. Chromatin immunoprecipitation (IP) experiments were performed with anti-FLAG beads. Specific FLAG-SHP binding was detected at around 150 nucleotides upstream of the transcription start site, where putative HNF4 α and LRH-1 binding sites are located. In fact, HNF4 α and LRH-1 binding on the *Cyp7a1* promoter was shown at the same location, implicating that SHP interacts with HNF4 α and LRH-1 *in vivo* as well (Fig. 2.2).

HNF4 α and LRH-1 binding sites on the *Cyp7a1* promoter partially overlap (Fig. 2.3A). Binding of HNF4 α and LRH-1 to the same location on the *Cyp7a1* promoter also implicated that they should occupy this location simultaneously. I tested this hypothesis by electrophoretic mobility shift assay (EMSA) and re-chromatin IP (re-ChIP) experiments. Incubation of HNF4 α protein with *Cyp7a1* promoter DNA probe led to a slower moving shift since HNF4 α binds to DNA as homodimers whereas LRH-1 binds as monomers. When both proteins were mixed, a third even slower moving shift appeared (Fig. 2.3B). The third shift disappeared if either HNF4 α or LRH-1 binding sites was mutated, ruling out the possibility that the third shift is due to a protein-protein interaction between the two proteins (Fig. 2.4). Based on this *in vitro* assay, HNF4 α and LRH-1 appear to bind simultaneously to the *Cyp7a1* promoter. Further confirmation of this simultaneous binding was obtained from re-ChIP. Liver chromatin was first immunoprecipitated with LRH-1 antibody, eluted and used in a second round of

chromatin IP with LRH-1 or HNF4 α antibodies. Comparable results from LRH-1 and HNF4 α re-ChIPs suggest that both proteins interact with *Cyp7a1* chromatin simultaneously (Fig. 2.3C).

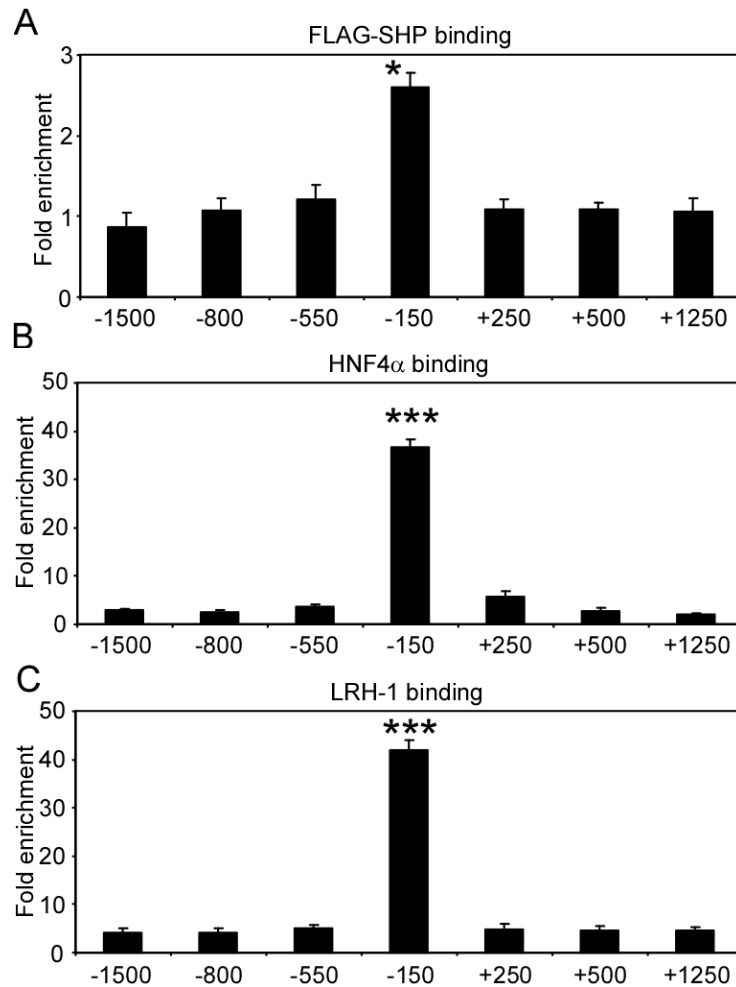


Figure 2.2 SHP, HNF4 α and LRH-1 binding to the *Cyp7a1* promoter. (A) FLAG-SHP was overexpressed in mouse liver via adenoviral expression. Chromatin IP was performed with FLAG antibody beads. Binding to different locations on the *Cyp7a1* promoter and proximal gene body was tested. (B and C) HNF4 α and LRH-1 antibodies were used for chromatin IP (n = 3). Values are means \pm SEM. Statistics by two-tailed *t* test. * P <0.05, *** P <0.0005.

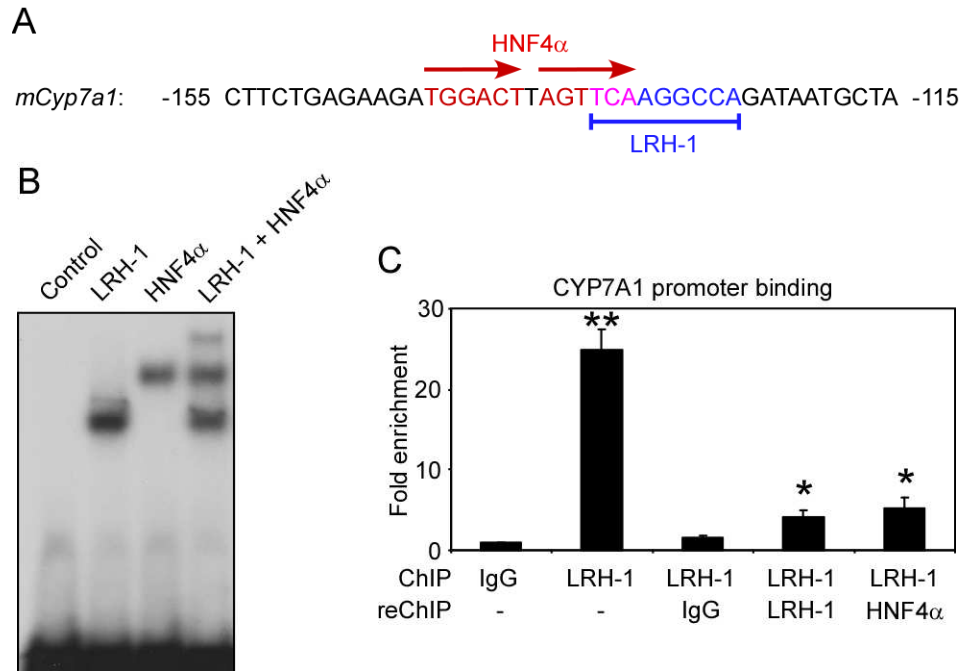


Figure 2.3 HNF4 α and LRH-1 co-occupy the *Cyp7a1* promoter. (A) Putative HNF4 α and LRH-1 binding sites on the *Cyp7a1* promoter are shown. (B) EMSA experiment was performed with *in vitro* translated proteins and a probe with the sequence shown in A. (C) LRH-1 bound chromatin was immunoprecipitated and used for a second round of chromatin IP with indicated antibodies (n = 3). Values are means \pm SEM. Statistics by two-tailed *t* test. * P <0.05, ** P <0.005 relative to IgG group.

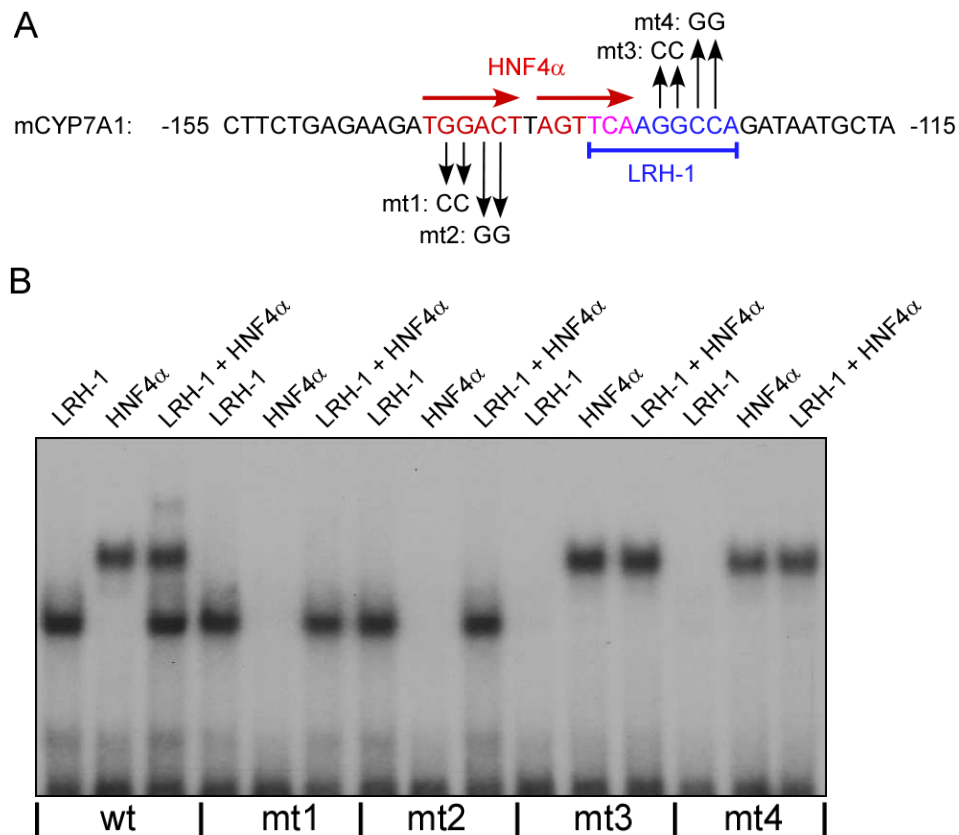


Figure 2.4 Mutagenesis of HNF4 α and LRH-1 binding sites on the *Cyp7a1* promoter. (A) Putative HNF4 α and LRH-1 binding sites on the *Cyp7a1* promoter were mutated as shown. (B) EMSA experiment was performed with *in vitro* translated proteins and indicated wild type or mutant probes.

2.2.3 SHP Interacts with Both HNF4 α and LRH-1 on the *Cyp7a1* Promoter

To demonstrate roles of HNF4 α and LRH-1 in SHP binding to the *Cyp7a1* promoter, I used conditional knockout models for *Hnf4a* and *Lrh-1*. Cre and/or FLAG-SHP were overexpressed in liver via adenoviral expression and FLAG-SHP binding was tested by chromatin IP.

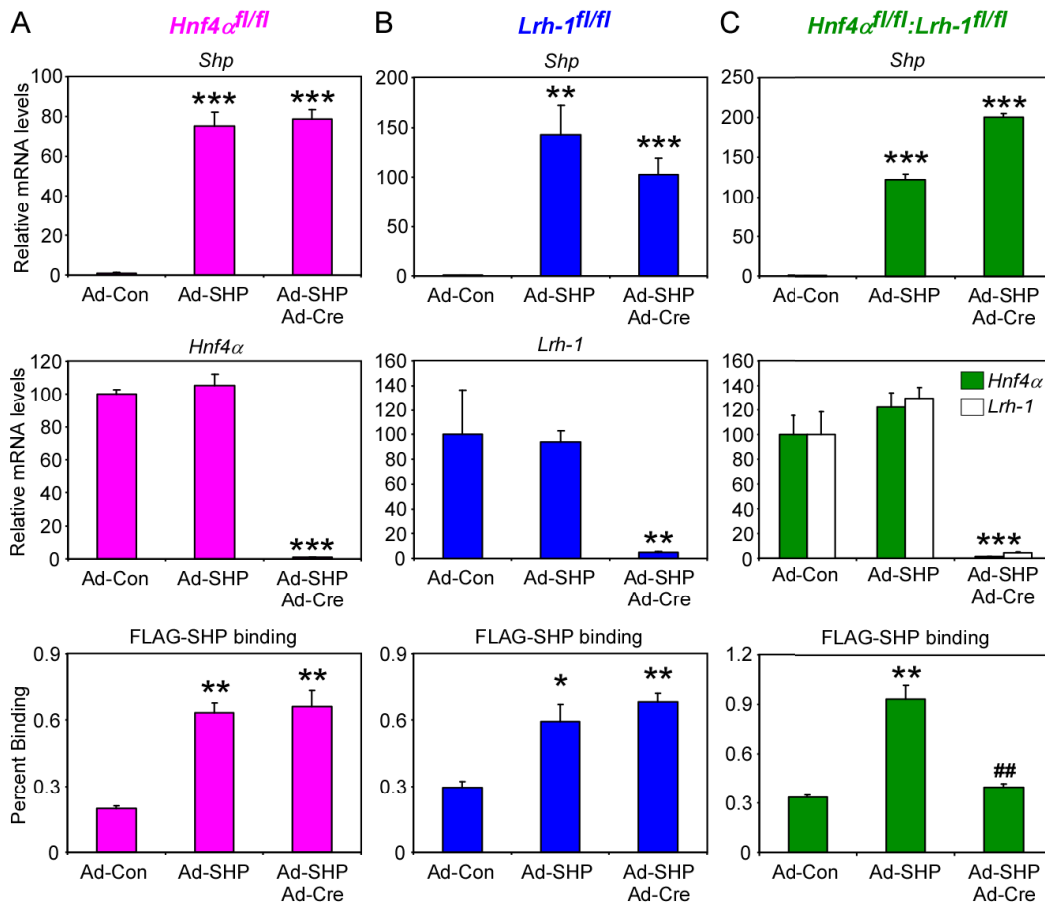


Figure 2.5 SHP requires HNF4 α or LRH-1 for binding to the *Cyp7a1* promoter. *Hnf4 α ^{fl/fl}* (A), *Lrh-1^{fl/fl}* (B) and *Hnf4 α ^{fl/fl}:Lrh-1^{fl/fl}* (C) mice (n = 3-6) were infected with control, Cre and/or FLAG-SHP adenoviruses. Hepatic *Shp*, *Hnf4 α* and *Lrh-1* mRNA levels were tested by RT-qPCR. FLAG-SHP binding to the *Cyp7a1* promoter was tested by chromatin IP (n = 3). Values are means \pm SEM. Statistics by two-tailed *t* test. (*) refer to differences compared to Ad-Con group. (#) refer to differences between Ad-SHP and Ad-SHP/Ad-Cre groups. **P*<0.05, ***P*<0.005, ****P*<0.0005, ##*P*<0.005.

While knockout of hepatic *Hnf4 α* in *Hnf4 α ^{fl/fl}* mice or knockout of hepatic *Lrh-1* in *Lrh-1^{fl/fl}* mice did not change FLAG-SHP binding to the *Cyp7a1* promoter in liver, knockout of both genes in *Hnf4 α ^{fl/fl}:Lrh-1^{fl/fl}* mice completely blocked FLAG-SHP

binding (Fig. 2.5). These results show that SHP can utilize both HNF4 α and LRH-1 as its binding partners on the *Cyp7a1* promoter.

2.2.4 HNF4 α and LRH-1 Are Essential Regulators of the *Cyp7a1* Promoter *In Vivo*

I next examined FGF19-dependent repression of *Cyp7a1* transcription in the conditional knockout mice. In Albumin-Cre liver specific *Hnf4 α* -knockout mice, hepatic *Cyp7a1* basal mRNA levels were reduced, however, FGF19 treatment further reduced *Cyp7a1* expression (Fig. 2.6A). As described previously (Lee et al. 2008), *Lrh-1* deficiency in livers of Albumin-Cre mice did not significantly disturb *Cyp7a1* mRNA levels. Just like FXR agonist GW4064 treatment (Lee et al. 2008), FGF19 treatment also repressed *Cyp7a1* transcription in *Lrh-1* liver knockout mice (Fig. 2.6B).

To avoid any compensatory mechanisms that might occur after Albumin-Cre expression starts in embryonic liver, I acutely knocked out *Hnf4 α* and/or *Lrh-1* via adenoviral Cre expression in liver. Acute knockout of hepatic *Hnf4 α* in *Hnf4 α ^{fl/fl}* mice gave results similar to Albumin-Cre knockout; *Cyp7a1* basal mRNA levels were reduced and FGF19-induced *Cyp7a1* repression was intact (Fig. 2.6C). Surprisingly, acute knockout of hepatic *Lrh-1* in *Lrh-1^{fl/fl}* mice differed from the Albumin-Cre knockout of *Lrh-1*. When LRH-1 was knocked out acutely, *Cyp7a1* basal mRNA levels were significantly decreased. However, FGF19 treatment still further repressed *Cyp7a1* transcription (Fig. 2.6D). Finally, I knocked out both *Hnf4 α* and *Lrh-1* in livers of *Hnf4 α ^{fl/fl}·Lrh-1^{fl/fl}* mice. This time *Cyp7a1* basal mRNA levels were severely reduced and FGF19 treatment did not further repress *Cyp7a1* transcription (Fig. 2.6E). These results

demonstrate that both HNF4 α and LRH-1 are transcriptional activators of the *Cyp7a1* promoter with complementary effects. These results are also consistent with my previous finding that SHP interacts with both HNF4 α and LRH-1 and thus the presence of either protein is sufficient for FGF19-induced *Cyp7a1* repression.

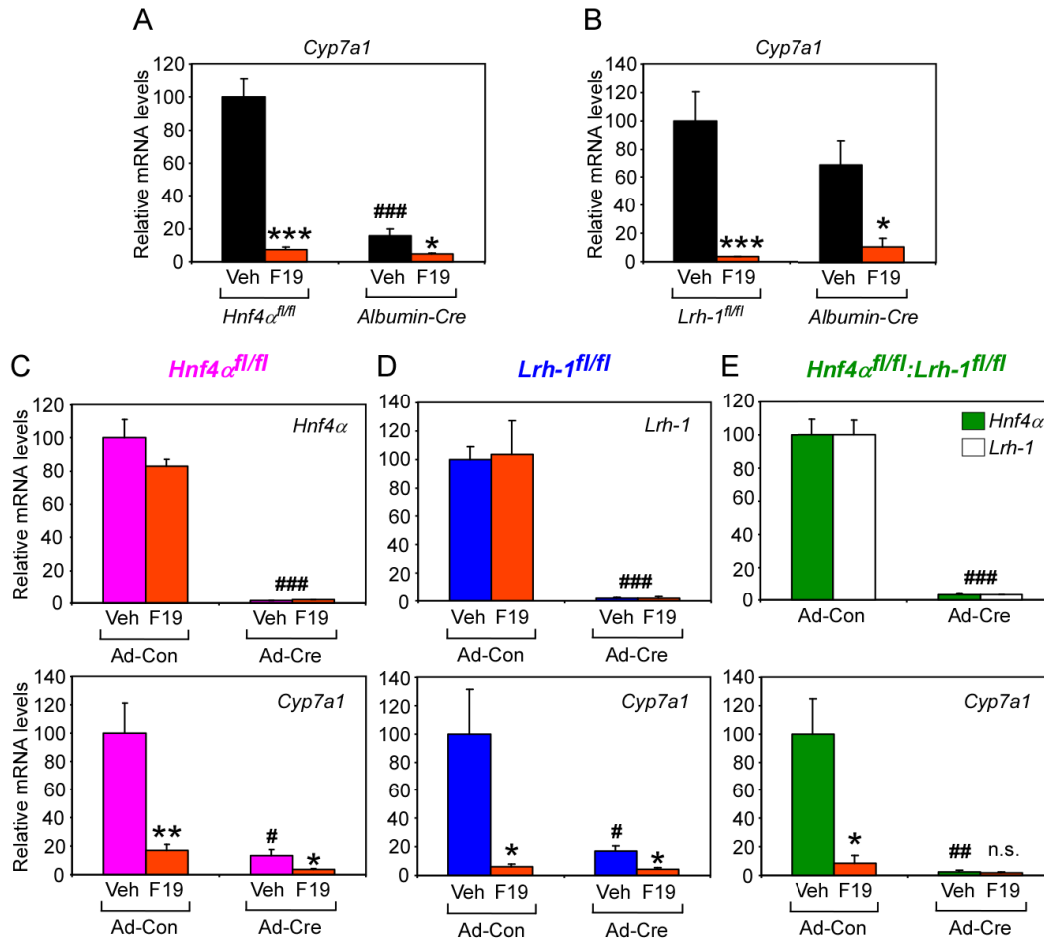


Figure 2.6 HNF4 α and LRH-1 maintain *Cyp7a1* expression and regulate FGF19-dependent repression. Overnight-fasted *Hnf4 α ^{fl/fl}* mice or their *Albumin-Cre* littermates (A) and *Lrh-1^{fl/fl}* mice or their *Albumin-Cre* littermates (B) were treated with vehicle or FGF19 (1mg/kg; i.p.) for 6 hours (n = 6). *Hnf4 α ^{fl/fl}* (C), *Lrh-1^{fl/fl}* (D), *Hnf4 α ^{fl/fl};Lrh-1^{fl/fl}* (E) mice were infected with control or Cre adenoviruses. Overnight-fasted mice (n = 4-6) were treated with vehicle or FGF19 (1mg/kg; i.p.) for 6 hours. Hepatic *Hnf4 α* , *Lrh-1* and *Cyp7a1* mRNA levels were tested by RT-qPCR. Values are means \pm SEM. Statistics by two-tailed *t* test. (*) refer to differences between Veh and F19 groups. (#) refer to

differences between two Veh groups. * $P < 0.05$, ** $P < 0.005$, *** $P < 0.0005$, # $P < 0.05$, ## $P < 0.005$, ### $P < 0.0005$. n.s. not significant.

2.2.5 FGF19 Does Not Regulate Nuclear Receptor Binding to the *Cyp7a1* Promoter

To test whether SHP binding to the *Cyp7a1* promoter is regulated by FGF19, FLAG-SHP protein was overexpressed in liver via adenoviral expression and SHP protein and mRNA levels were determined (Fig. 2.7, A and B). FGF19 treatment did not change nuclear FLAG-SHP protein levels, arguing against the previous suggested notion that FGF19 increases SHP protein stability by preventing degradation (Miao et al. 2009). SHP overexpression mildly decreased *Cyp7a1* expression while FGF19 treatment further repressed *Cyp7a1* levels, demonstrating that the FGF19-dependent repression mechanism is functional in this SHP-overexpression system. Surprisingly, FGF19 treatment did not change FLAG-SHP binding to the *Cyp7a1* promoter (Fig. 2.7, C and D). Similarly, FGF19 failed to alter neither HNF4 α /LRH-1 binding to the *Cyp7a1* promoter nor their nuclear protein levels (Fig. 2.8). These results indicate that FGF19 does not regulate SHP, HNF4 α and LRH-1 binding to the *Cyp7a1* promoter.

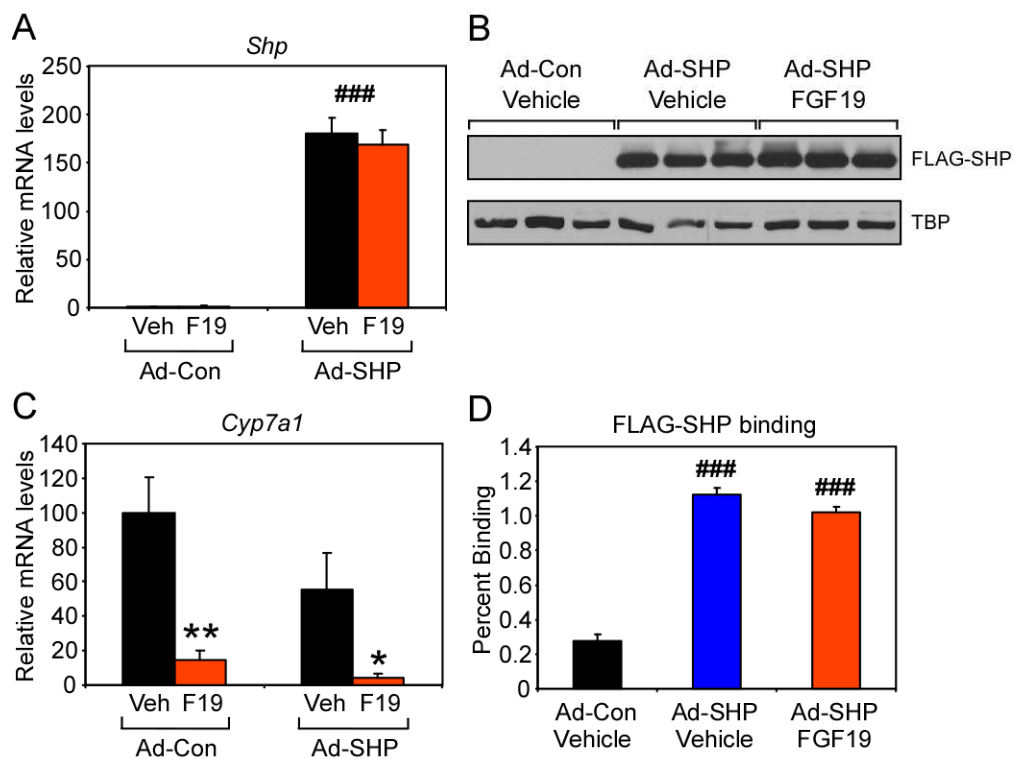


Figure 2.7 FGF19 does not change SHP binding to the *Cyp7a1* promoter. FLAG-SHP was overexpressed in mouse liver via adenoviral expression. Mice (n = 5-8) were treated with vehicle or FGF19 (1mg/kg; i.p.) for 6 hours. *Shp* mRNA levels (A), SHP protein levels (B), and *Cyp7a1* mRNA levels (C) are shown. FLAG-SHP binding to the *Cyp7a1* promoter was tested by chromatin IP (n = 3) (D). Values are means \pm SEM. Statistics by two-tailed *t* test. (*) refer to differences between Veh and F19 groups. (#) refer to differences relative to Ad-Con groups. * $P < 0.05$, ** $P < 0.005$, ### $P < 0.0005$.

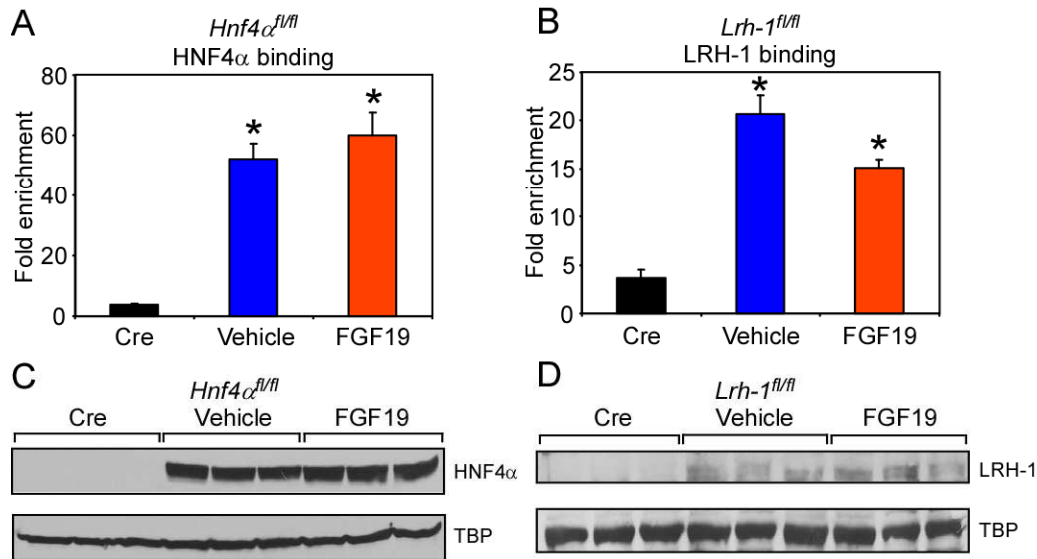


Figure 2.8 FGF19 does not change HNF4α and LRH-1 binding to the *Cyp7a1* promoter. HNF4α (A) and LRH-1 (B) binding to the *Cyp7a1* promoter was tested by chromatin IP on liver samples (n = 3) from the experiments shown in Fig. 2.6, A and B. Albumin-Cre samples were included to show the specificity of the antibodies. Nuclear HNF4α (C) and LRH-1 (D) protein levels are shown in triplicates. Values are means ± SEM. Statistics by two-tailed *t* test. **P*<0.05, relative to Cre groups.

2.2.6 FGF19 Causes Histone Deacetylation and Demethylation on the *Cyp7a1*

Promoter

To understand how the repressed state on the *Cyp7a1* promoter is achieved in response to FGF19, histone modifications on the promoter were examined. FGF19 treatment significantly reduced active transcription marks on the *Cyp7a1* promoter. Histone H3 acetylation was repressed by FGF19 in wild-type but not *Shp^{-/-}* mice (Fig. 2.9A). Knockout of *Hnf4α* or *Lrh-1* led to depletion of histone H3 acetylation, which is in agreement with decreased *Cyp7a1* mRNA levels. FGF19 treatment also further reduced acetylation in these knockout mice (Fig. 2.9, B and C).

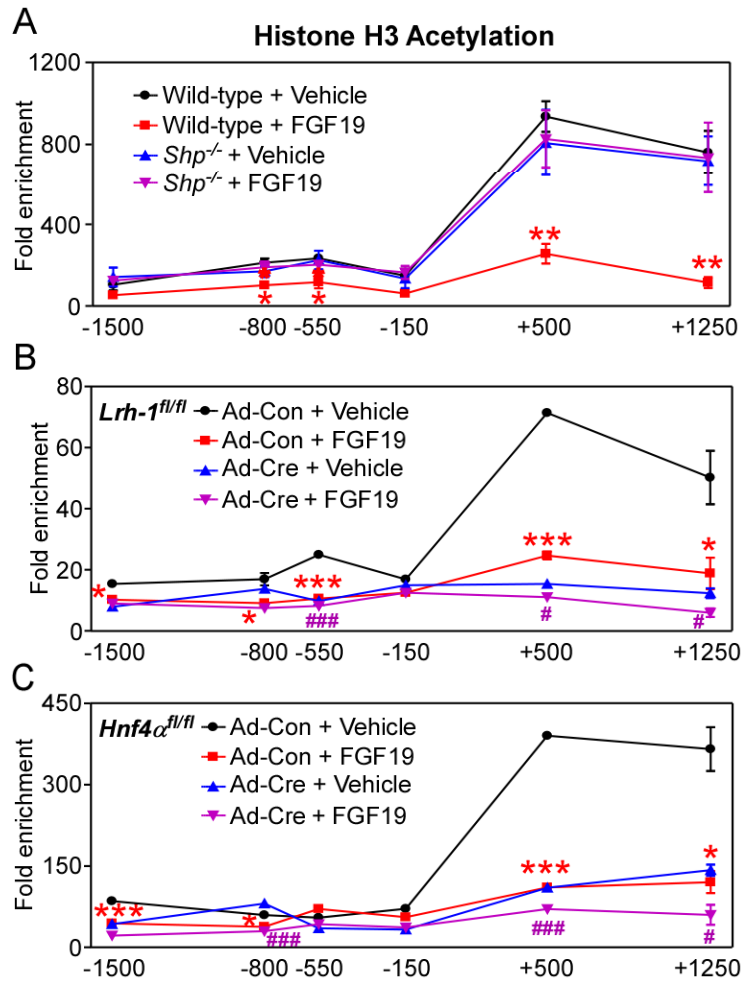


Figure 2.9 FGF19 reduces histone H3 acetylation on the *Cyp7a1* promoter. Histone H3 acetylation on the *Cyp7a1* promoter was tested by chromatin IP on liver samples ($n = 3$) from the experiments shown in Fig. 2.1A (A) or Fig. 2.6, C and D (B and C). Values are means \pm SEM. Statistics by two-tailed t test. (*) refer to differences between Wild-type or Ad-Con Vehicle and FGF19 groups. (#) refer to differences between Ad-Cre Vehicle and FGF19 groups. * $P < 0.05$, ** $P < 0.005$, *** $P < 0.0005$, # $P < 0.05$, ### $P < 0.0005$.

Similar results were obtained for two other active transcription marks; histone H4 acetylation (data not shown) and histone H3 lysine 4 trimethylation (Fig. 2.10). The decreases in active transcription marks completely correlate with

FGF19-induced repressed state in the *Cyp7a1* promoter. It appears that HNF4 α and LRH-1 maintain active transcriptional state in the promoter whereas SHP is absolutely required for repression.

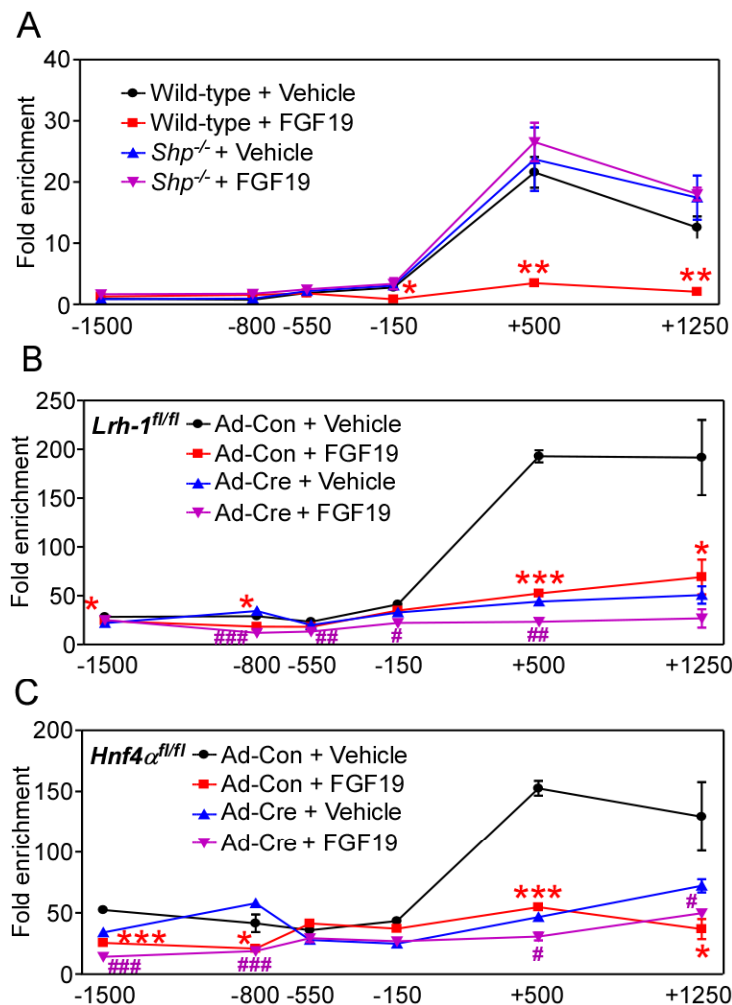


Figure 2.10 FGF19 reduces histone H3K4 trimethylation on the *Cyp7a1* promoter. Histone H3K4 trimethylation on the *Cyp7a1* promoter was tested by chromatin IP on liver samples (n = 3) from the experiments shown in Fig. 2.1A (A) or Fig. 2.6, C and D (B and C). Values are means \pm SEM. Statistics by two-tailed *t* test. (*) refer to differences between Wild-type or Ad-Con Vehicle and FGF19 groups. (#) refer to differences between Ad-Cre Vehicle and FGF19 groups. **P*<0.05, ***P*<0.005, ****P*<0.0005, #*P*<0.05, ##*P*<0.005, ###*P*<0.0005.

2.3 DISCUSSION

Here, I show that both HNF4 α and LRH-1 are essential regulators of *Cyp7a1* expression. HNF4 α and LRH-1 co-occupy the *Cyp7a1* promoter and maintain appropriate mRNA transcription from this promoter. They also interact with and recruit SHP to the *Cyp7a1* promoter. SHP is clearly required for the repression of *Cyp7a1* transcription by FGF19. Interestingly, FGF19 does not alter binding of any of these three nuclear receptors to the *Cyp7a1* promoter. Therefore, regulation of *Cyp7a1* promoter is not mediated by changes in promoter occupancy of these proteins. Instead, transcriptional co-regulators seem to be controlled as implicated by changes in histone acetylation and methylation in response to FGF19.

Unlike previous studies which did not describe altered *Cyp7a1* transcription in Albumin-Cre *Lrh-1* liver knockout mice (Mataki et al. 2007; Lee et al. 2008), we show that *Cyp7a1* mRNA levels are significantly reduced when *Lrh-1* is knocked out acutely. It is possible that Albumin-Cre driven loss of *Lrh-1* during liver development induces compensatory mechanisms that maintain *Cyp7a1* transcription and that are not gained acutely.

Reduced *Cyp7a1* transcription in response to loss of *Hnf4a* or *Lrh-1* well correlates with reduced active transcription histone marks on the promoter. FGF19 also down-regulates these histone modifications in a SHP-dependent manner. I have observed the most dramatic changes in histone H3 and H4 acetylation as well as histone H3K4 trimethylation. However, I do not rule out the possibility that other histone modifications or chromatin remodeling mechanisms might contribute too. I also observed that inhibition

of any single modification process (e.g. inhibition of histone deacetylases by trichostatin A) fails to block *Cyp7a1* repression by FGF19 (data not shown). At this level of regulation, there seems to be many chromatin regulatory pathways involved and there is inevitable redundancy.

The key to understand *Cyp7a1* regulation by FGF19 probably lies in upstream regulatory pathways involved. The Ras/MEK/ERK pathway is activated by FGF19 and has been shown to mediate some of FGF19's effects in liver (Kurosu et al. 2007; Lin et al. 2007; Kir et al. 2011). However, our preliminary results (discussed in the next section) suggest that FGF19-dependent activation of the ERK pathway is neither required nor sufficient to mediate *Cyp7a1* repression. I also want to note that previously described observations on FGF19-induced increases in SHP stability and SHP binding to the *Cyp7a1* promoter are not reproducible in our hands (Miao et al. 2009). I have found that FGF19 does not change binding of nuclear receptors HNF4 α , LRH-1 and SHP to this promoter. These findings, in fact, resemble ligand-dependent regulation of most nuclear receptors, where ligand binding does not change nuclear receptor occupancy on the DNA but rather alters interactions with co-regulators. Although FGF19 is not a ligand for any of these nuclear receptors, its action seems to mimic ligand-dependent regulation. Thus, it will be intriguing to ask whether FGF19 controls abundance of potential physiologic ligands of any of these nuclear receptors, especially SHP.

According to our current understanding of *Cyp7a1* regulation, SHP acts as a co-repressor of both HNF4 α and LRH-1. However, as a small protein, SHP lacks any enzymatic repressor activity. Therefore, it should function as a crucial adaptor protein between HNF4 α /LRH-1 and other transcriptional regulator that alter chromatin structure

on the *Cyp7a1* promoter. However, the exact nature and mechanism of how SHP-dependent repression of *Cyp7a1* is triggered by FGF19 remains elusive.

Understanding FGF19-dependent bile acid repression pathway represents therapeutic potential for the treatment of chronic diarrhea syndromes, such as bile acid malabsorption syndrome and inflammatory bowel diseases, where impaired bile acid absorption in the intestine leads to diarrhea. Repression of bile acid synthesis might help reducing the complications. In fact, reduced FGF19 function has been associated with some of these diseases (Walters et al. 2009; Lenicek et al. 2011). FGF19, itself, can be considered as therapeutic tool. However, there are concerns for the potential of FGF19 as a chronic drug since FGF19 transgenic mice were shown to form liver tumors (Nicholes et al. 2002). It is of great interest if any FGF19 pathway components can be targeted to induce *Cyp7a1* repression.

2.4 SUMMARY

Fibroblast Growth Factor (FGF) 19 is a postprandial enterokine up-regulated by bile acid receptor FXR upon bile acid uptake into the ileum. FGF19 inhibits bile acid synthesis in liver through transcriptional repression of Cholesterol 7 α -hydroxylase (CYP7A1) via a mechanism involving nuclear receptor SHP. Here, I show that nuclear receptors HNF4 α and LRH-1 enable SHP binding to the *Cyp7a1* promoter and therefore are important for negative feedback regulation of *Cyp7a1*. HNF4 α and LRH-1 are also crucial transcriptional activators of the *Cyp7a1* promoter. Loss of either protein in liver leads to reduced *Cyp7a1* expression. HNF4 α and LRH-1 maintain active transcription

histone marks on the *Cyp7a1* promoter whereas FGF19 down-regulates these marks in a SHP-dependent way.

CHAPTER 3

The MEK-ERK Pathway Is Integral for Regulation of Bile Acid Synthesis But Not Crucial for Regulation by FGF19

3.1 INTRODUCTION

FGF15/19 is a crucial hormonal factor that is required to maintain proper bile acid homeostasis as evidenced by elevated bile acid pool size and *Cyp7a1* expression levels seen in various animal models harboring deletions on the FGF15/19 signaling axis. e.g., *Fgfr4*^{-/-}, *Klb*^{-/-} (i.e., β -Klotho-null), and *Fgf15*^{-/-} mice (Yu et al. 2000; Inagaki et al. 2005; Ito et al. 2005). Administration of FXR agonist GW4064 fails to repress *Cyp7a1* in *Fgfr4*^{-/-} or *Fgf15*^{-/-} mice demonstrating the requirement of this pathway for FXR-dependent regulation of bile acid synthesis (Inagaki et al. 2005).

On its own, FGF19 fails to activate its preferred receptor FGFR4 due to its reduced affinity towards heparin that promotes the interaction between FGFs and their receptors. As the obligatory co-receptor, β -Klotho enables FGF19 binding to FGFR4 and permits FGF19-FGFR4 signaling (Kurosu et al. 2007; Lin et al. 2007). FGFR4 is a receptor tyrosine kinase that activates intracellular signaling pathways. To fully understand how FGF19 binding to FGFR4/ β -Klotho on the plasma membrane leads to transcriptional repression of *Cyp7a1* in the nucleus, it is imperative to know signaling pathways that are induced by FGFR4 in response to FGF19 binding and are required for *Cyp7a1* regulation. Here, I investigated activation of kinase signaling pathways by FGF19 and tested their requirement for *Cyp7a1* repression.

3.2 RESULTS

3.2.1 MEK Inhibition Has Profound Effects on *SHP* and *CYP7A1* mRNA Levels

I used kinase inhibitors in HepG2 cell culture to test roles of various signaling pathways in regulation of human *CYP7A1* gene expression and observed dramatic effects of MEK inhibitors. The Ras/MEK/ERK pathway is known to be activated by many growth factors and particularly by FGFs. MEK kinase inhibitors block MEK-dependent ERK phosphorylation which induces ERK kinase activity. PD-0325901 treatment of HepG2 cells completely blocked ERK phosphorylation in a dose-dependent manner and severely reduced *SHP* mRNA levels with an accompanying increase in *CYP7A1* expression (Fig. 3.1). Similar results were obtained with another MEK inhibitor, U0126 (Fig. 3.2). Among the other kinase inhibitors tested, only PD98059, also a MEK inhibitor, displayed similar effects (Fig. 3.3). These MEK inhibitors were also tested on other hepatic cell lines and similar effects on *SHP* and *CYP7A1* mRNA levels were observed (data not shown).

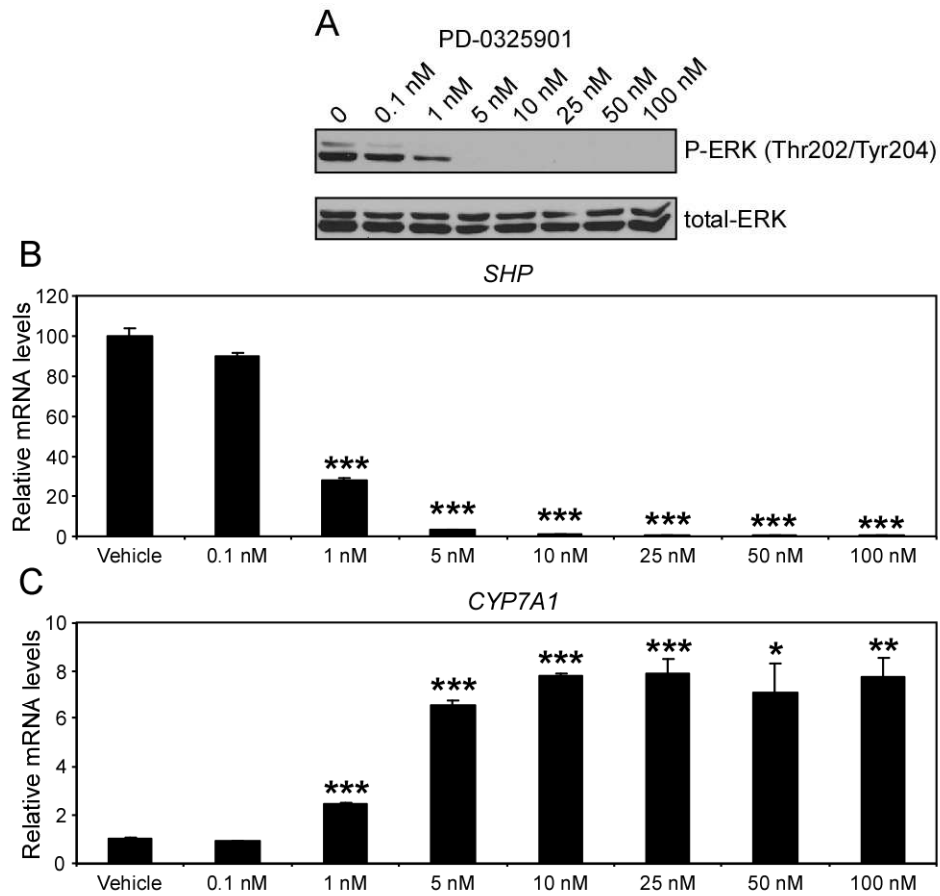


Figure 3.1 PD-0325901 treatment of HepG2 cells. Cells were treated with indicated concentrations of PD-0325901 for 6 hours. (A) ERK phosphorylation was determined by Western blotting. (B and C) *SHP* and *CYP7A1* mRNA levels were tested by RT-qPCR ($n = 3$). Values are means \pm SEM. Statistics by two-tailed t test. * $P < 0.05$, ** $P < 0.005$, *** $P < 0.0005$ relative to the Vehicle group.

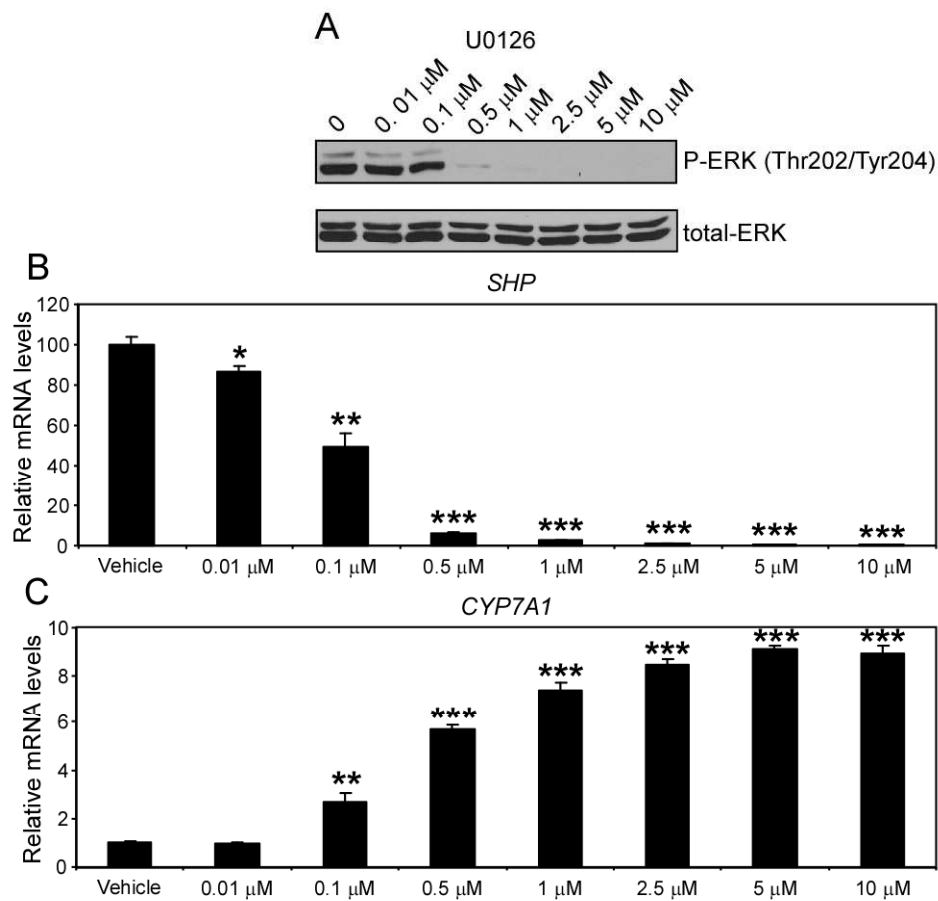


Figure 3.2 U0126 treatment of HepG2 cells. Cells were treated with indicated concentrations of U0125 for 6 hours. (A) ERK phosphorylation was determined by Western blotting. (B and C) *SHP* and *CYP7A1* mRNA levels were tested by RT-qPCR (n = 3). Values are means \pm SEM. Statistics by two-tailed *t* test. * P <0.05, ** P <0.005, *** P <0.0005 relative to the Vehicle group.

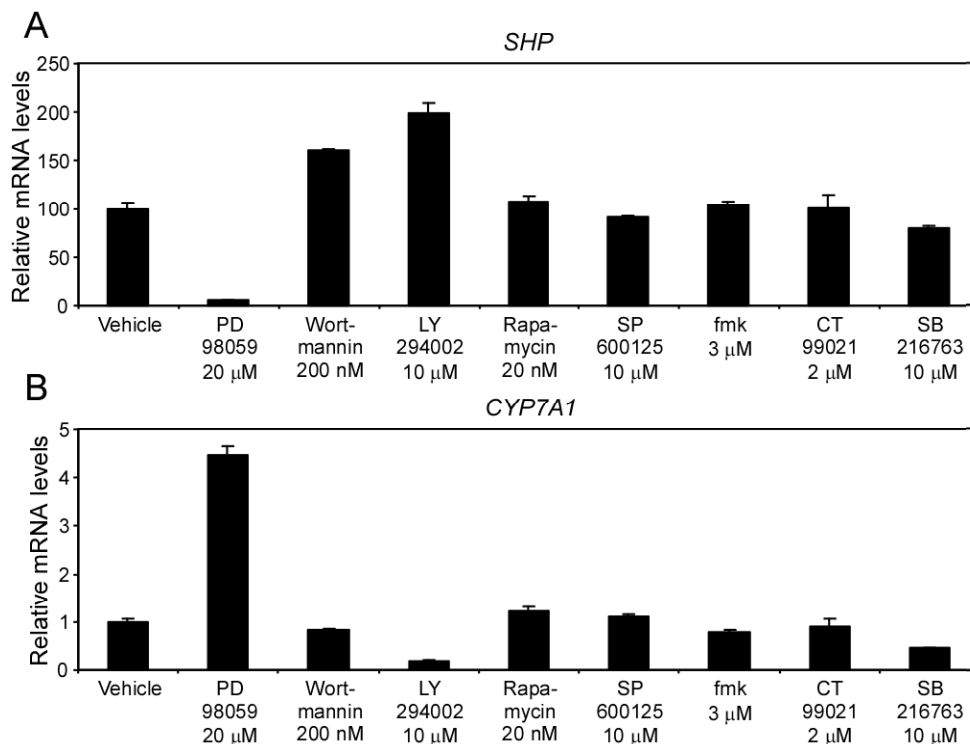


Figure 3.3 Treatment of HepG2 cells with various kinase inhibitors. Cells were treated with various kinase inhibitors at indicated concentrations for 6 hours. *SHP* (A) and *CYP7A1* (B) mRNA levels were tested by RT-qPCR (n = 3). Values are means \pm SEM.

To obtain more physiologic evidence and to rule out the possibility that the effects seen in cultured cells are due to some artifacts arising from culture conditions, I investigated MEK inhibition in mouse liver. PD-0325901 is a very potent MEK inhibitor that is in clinical trials for cancer treatment and is orally administrable (Brown et al. 2007; Barrett et al. 2008). Mice were gavaged with increasing amounts of this compound and ERK phosphorylation in liver was tested. PD-0325901 blocked ERK activation in a dose-dependent manner without causing any toxic symptoms (Fig. 3.4A). Inhibition of ERK activation severely reduced *Shp* mRNA levels with a concomitant increase in

Cyp7a1 transcription (Fig. 3.4, B and C). Since SHP is considered as the repressor of the *Cyp7a1* promoter, the negative correlation between *Shp* and *Cyp7a1* expression levels implicates a causal relationship in which decreased *Shp* expression leads to the increase in *Cyp7a1* mRNA levels. However, MEK inhibitor-dependent increase in *Cyp7a1* expression was also present in *Shp*^{-/-} mice, suggesting that the effects of the MEK/ERK pathway on *Shp* and *Cyp7a1* transcription levels are independent (Fig. 3.4D).

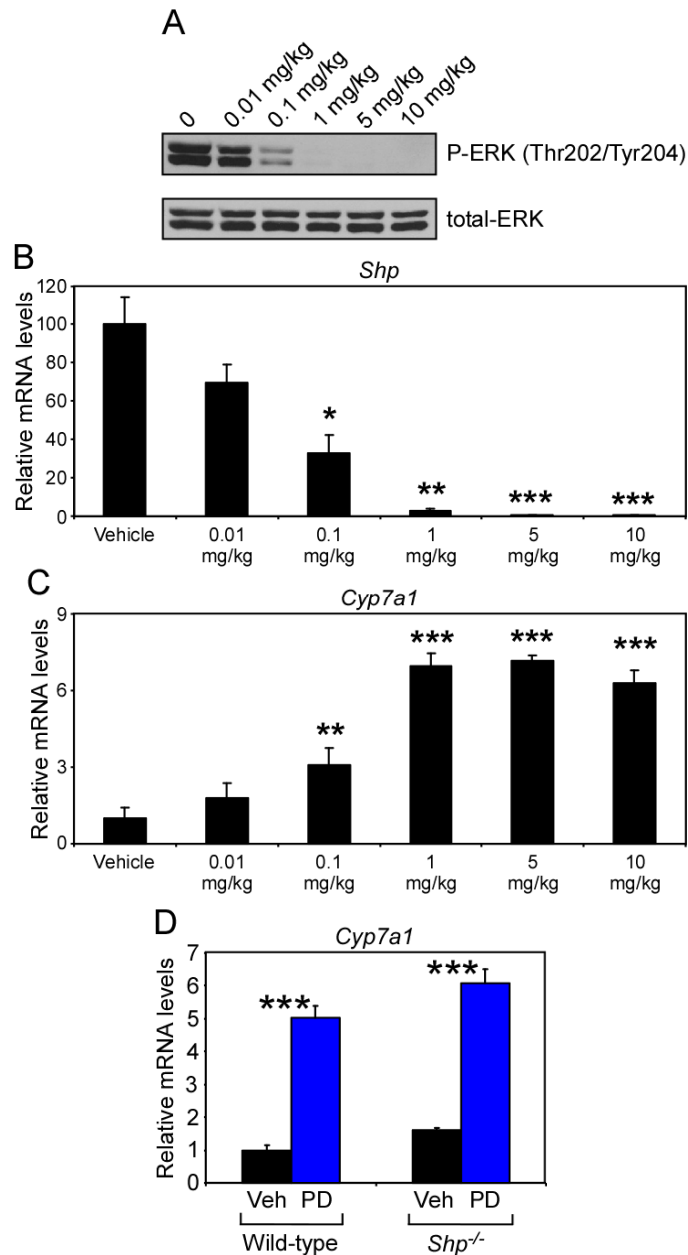


Figure 3.4 Dose response analysis of PD-0325901 treatment in mice. Overnight-fasted mice ($n = 4$) were treated with indicated amounts of PD-0325901 by oral gavage and sacrificed 3 hours later. (A) ERK phosphorylation was determined by Western blotting. (B and C) *Shp* and *Cyp7a1* mRNA levels were tested by RT-qPCR. (D) Wild-type and *Shp*^{-/-} mice ($n = 4$) were treated similarly and *Cyp7a1* mRNA levels were compared. Values are means \pm SEM. Statistics by two-tailed t test. * $P < 0.05$, ** $P < 0.005$, *** $P < 0.0005$ relative to Vehicle groups.

3.2.2 MEK Inhibition Disrupts *Shp* and *Cyp7a1* Promoter Activity

MEK inhibition changes *Shp* and *Cyp7a1* expression levels very quickly. In a time course experiment, dramatic effects were observed as early as 1 hour of treatment (Fig. 3.5). To understand the mechanism behind these changes, I investigated *Shp* and *Cyp7a1* promoter activity 1 hour after drug treatment. On the *Shp* promoter, MEK inhibition reduced histone H3 acetylation and RNA polymerase II binding, suggesting reduced transcriptional activity at this promoter. Furthermore, LRH-1 and HNF4 α occupancy on the *Shp* promoter was decreased, which might explain the reduced transcriptional activity (Fig. 3.6). On the contrary, MEK inhibition increased histone H3 acetylation and RNA polymerase binding to the *Cyp7a1* promoter, suggesting elevated transcriptional activity at this promoter. However, LRH-1 and HNF4 α binding to the *Cyp7a1* promoter were unchanged (Fig. 3.7).

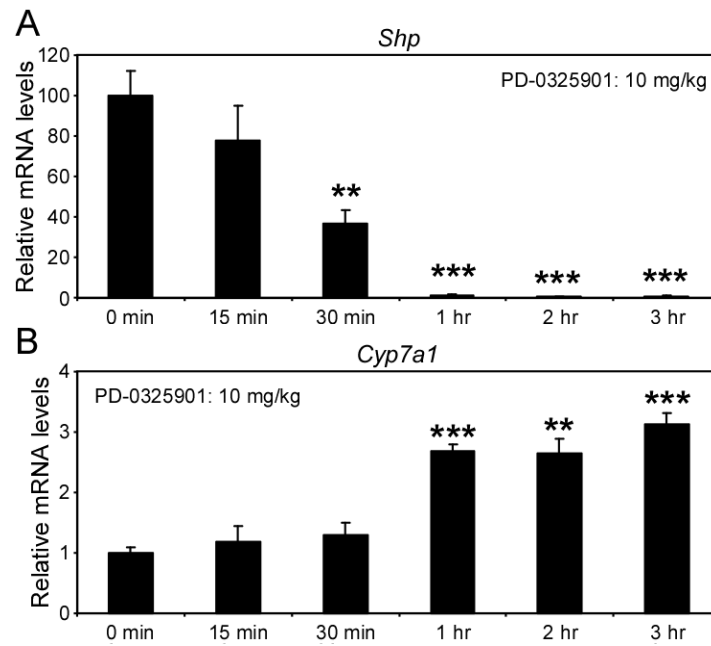


Figure 3.5 Time course analysis of PD-0325901 treatment in mice. Overnight-fasted mice ($n = 4$) were treated with 10 mg/kg PD-0325901 by oral gavage and sacrificed after indicated durations. *Shp* (A) and *Cyp7a1* (B) mRNA levels were tested by RT-qPCR. Values are means \pm SEM. Statistics by two-tailed t test. ** $P < 0.005$, *** $P < 0.0005$ relative to the 0 min group.

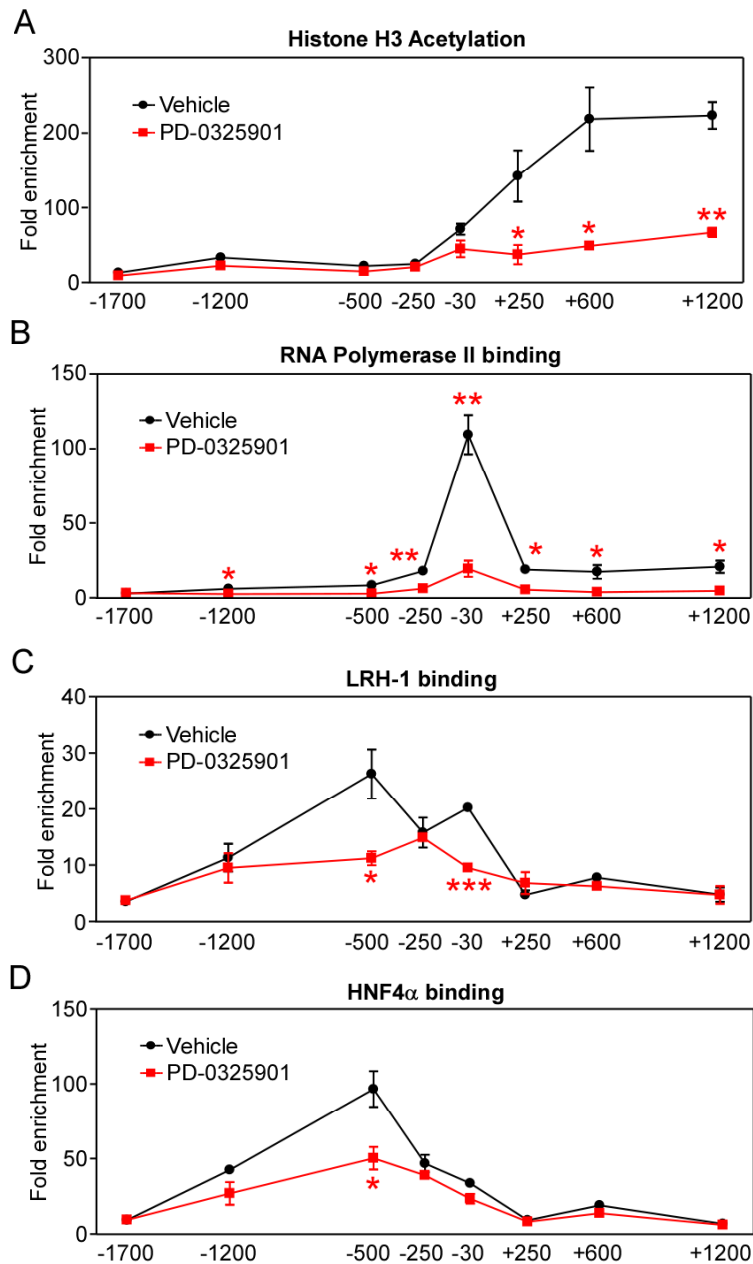


Figure 3.6 Effects of PD-0325901 on the *Shp* promoter activity. Overnight-fasted mice were treated with 10 mg/kg PD-0325901 by oral gavage and sacrificed 1 hour later. Histone H3 acetylation (A) and RNA Polymerase II (B), LRH-1 (C) and HNF4 α (D) binding on the *Shp* promoter were measured by chromatin IP (n = 3). LRH-1 has three binding sites on the *Shp* promoter. Two of them are close to the -500 location and another one is near the TATA box at the -30 location. Values are means \pm SEM. Statistics by two-tailed *t* test. * P <0.05, ** P <0.005, *** P <0.0005.

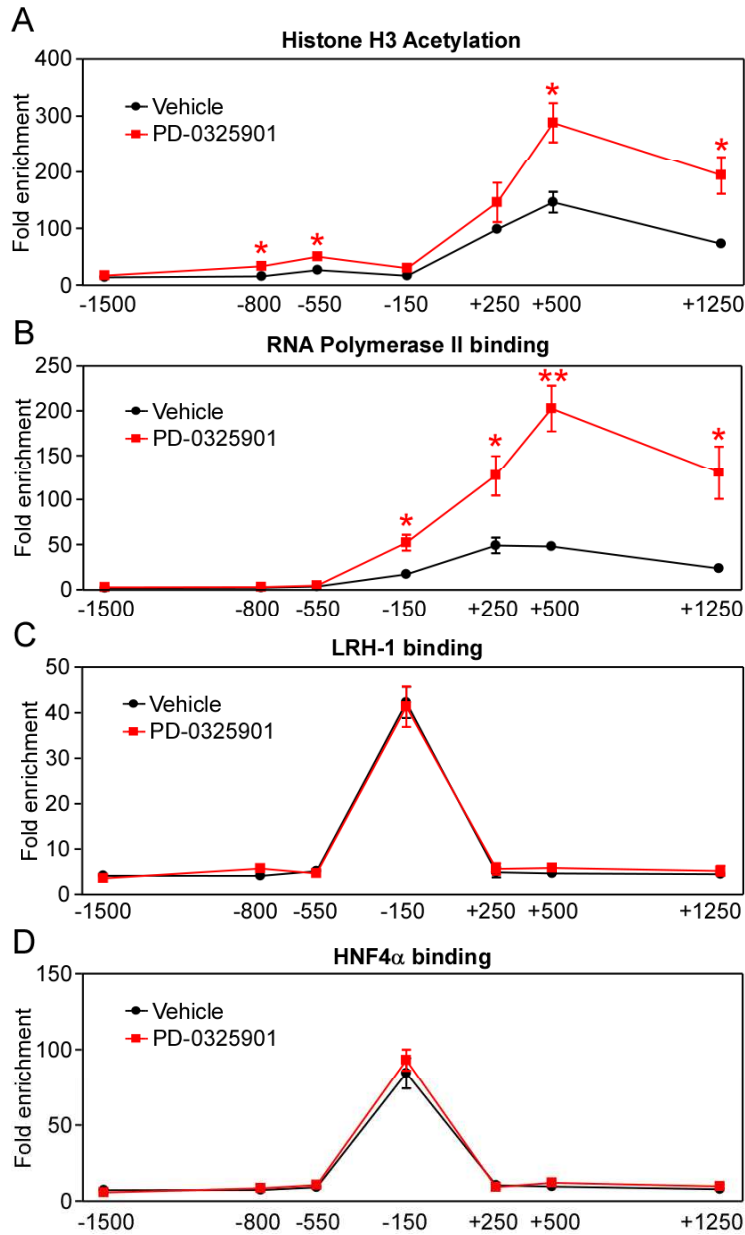


Figure 3.7 Effects of PD-0325901 on the *Cyp7a1* promoter activity. Overnight-fasted mice were treated with 10 mg/kg PD-0325901 by oral gavage and sacrificed 1 hour later. Histone H3 acetylation (A) and RNA Polymerase II (B), LRH-1 (C) and HNF4 α (D) binding on the *Cyp7a1* promoter were measured by chromatin IP (n = 3). Values are means \pm SEM. Statistics by two-tailed *t* test. * $P < 0.05$, ** $P < 0.005$.

3.2.3 HNF4 α and LRH-1 Are Important for Regulation of *Shp* Transcription

MEK inhibitor-induced loss of HNF4 α and LRH-1 from the *Shp* promoter suggests that the MEK/ERK pathway regulates binding of these proteins to the promoter. To determine roles of HNF4 α and LRH-1 in repression of *Shp* by MEK inhibition, *Hnf4 α* or *Lrh-1* Albumin-Cre liver specific knockout mice were treated with PD-0325901. As described previously (Lee et al. 2008), LRH-1 is an important activator of the *Shp* promoter and its deletion causes suppression of *Shp* expression (Fig. 3.8A). Thus, MEK inhibition-induced loss of LRH-1 from the *Shp* promoter must contribute to the reduced transcriptional activity at this promoter. Interestingly, in response to MEK inhibition, *Shp* expression was still further reduced in *Lrh-1* liver knockout mice, possibly due to loss of HNF4 α from the promoter (Fig. 3.8A). *Hnf4 α* depletion in liver slightly reduced basal *Shp* mRNA levels. However, MEK inhibition further suppressed *Shp* transcription in *Hnf4 α* liver knockout mice, possibly by down-regulating LRH-1 binding to the promoter (Fig. 3.8B). Consistent with unchanged HNF4 α and LRH-1 binding to the *Cyp7a1* promoter, MEK inhibitor-dependent increase in *Cyp7a1* expression was intact in both knockout models (Fig. 3.8, C and D). Based on these results, I propose that *Shp* repression by MEK inhibition is caused by loss of HNF4 α and LRH-1 from the *Shp* promoter and thus the MEK/ERK pathway must regulate HNF4 α and LRH-1 binding to this promoter. These effects seem to be promoter specific as MEK inhibition did not change HNF4 α and LRH-1 binding to the *Cyp7a1* promoter and thus, the mechanism for the elevated *Cyp7a1* expression must be different.

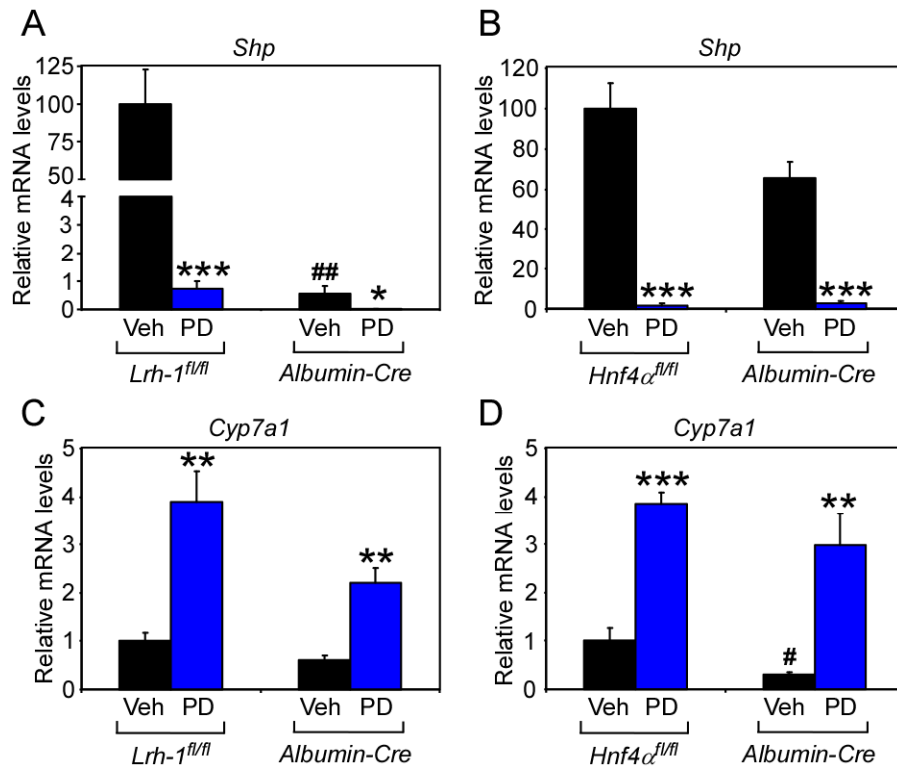


Figure 3.8 PD-0325901 treatment of HNF4 α or LRH-1 liver specific knockout mice. Overnight-fasted mice ($n = 5$) were treated with 10 mg/kg PD-0325901 by oral gavage and sacrificed 3 hours later. *Shp* (A and B) and *Cyp7a1* (C and D) mRNA levels were determined by RT-qPCR. Values are means \pm SEM. Statistics by two-tailed t test. (*) refer to differences between Veh and PD groups. (#) refer to differences between Veh groups. * $P < 0.05$, ** $P < 0.005$, *** $P < 0.0005$, # $P < 0.05$, ## $P < 0.005$.

3.2.4 The MEK/ERK Pathway Is Dispensable for Regulation of *Shp* and *Cyp7a1* by FGF19

The profound effects of MEK inhibition on *Shp* and *Cyp7a1* expression urged me to ask if the MEK/ERK pathway is involved in FGF19-dependent regulation of *Shp* and *Cyp7a1* transcription. In contrast to MEK inhibition, FGF19 treatment slightly increases *Shp* mRNA levels and potently represses *Cyp7a1* expression. In fact, FGF19 activated the

MEK/ERK pathway as shown by increased ERK phosphorylation in response to FGF19 (Fig. 3.9A). Thus, it is possible that FGF19's effects on *Shp* and *Cyp7a1* might be mediated by the MEK/ERK pathway. To test this hypothesis, mice were treated with PD-0325901 and/or FGF19. While the PD compound entirely blocked FGF19-induced ERK phosphorylation, it failed to completely inhibit *Cyp7a1* repression by FGF19 (Fig. 3.9). In this experiment, FGF19-induced *Cyp7a1* repression was suboptimal as the treatment duration was 3 hours instead of 6 hours in which much better *Cyp7a1* repression results are observed. The reason why I preferred a 3-hour-treatment was because MEK inhibitor treatment failed to block FGF19-induced ERK phosphorylation at later time points probably due to quick clearance of the drug from the circulation (Brown et al. 2007).

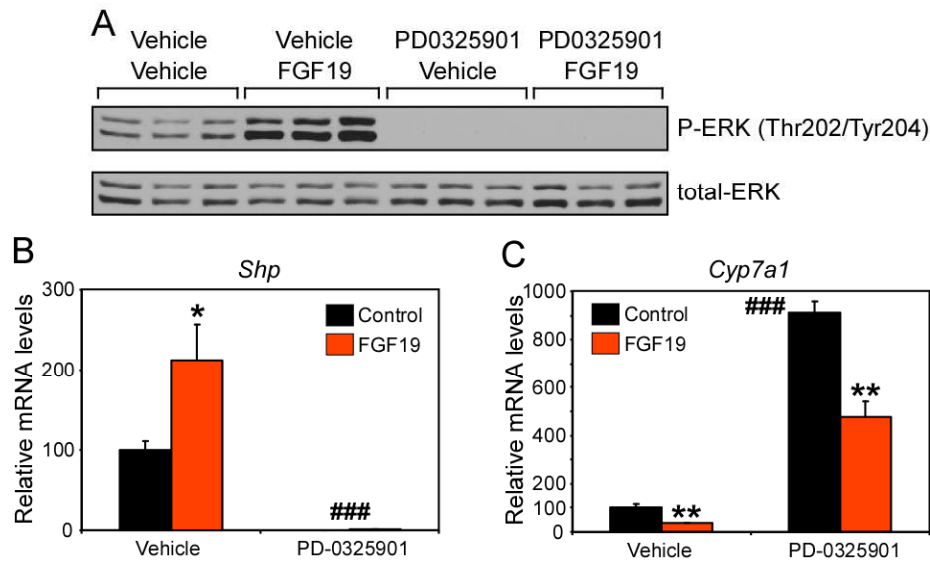


Figure 3.9 FGF19 and PD-0325901 co-treatment in mice. Overnight-fasted mice ($n = 5$) were treated with 100 mg/kg PD-0325901 by oral gavage and/or FGF19 (1mg/kg; i.p.) and sacrificed 3 hours later. (A) ERK phosphorylation was determined by Western blotting. (B and C) *Shp* and *Cyp7a1* mRNA levels were tested by RT-qPCR. Values are means \pm SEM. Statistics by two-tailed t test. (*) refer to differences between Control and FGF19 groups. (#) refer to differences between Vehicle and PD-0325901 groups. * $P < 0.05$, ** $P < 0.005$, ### $P < 0.0005$.

To study the combination of MEK inhibition and FGF19 treatment in a more steady system, I isolated mouse primary hepatocytes to recapitulate the above results. Here, MEK inhibitors U0126 and PD-0325901 blocked ERK phosphorylation for extended periods of time. Interestingly, FGF19 completely failed to induce ERK phosphorylation in primary hepatocytes (Fig. 3.10A). MEK inhibition led to a relatively less dramatic decrease in *Shp* mRNA levels but markedly induced *Cyp7a1* expression. In the presence of either MEK inhibitors, FGF19 rescued *Shp* mRNA levels and repressed *Cyp7a1* transcription without changing ERK phosphorylation (Fig. 3.10, B and C). These findings unequivocally demonstrate that FGF19 does not require the MEK/ERK pathway to elicit its effects on *Shp* and *Cyp7a1* transcription.

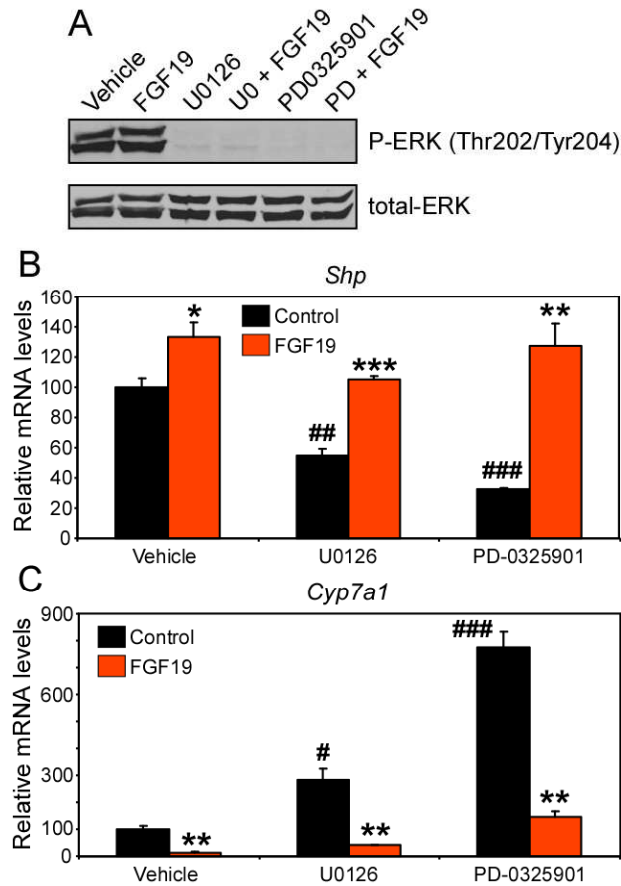


Figure 3.10 FGF19 and PD-0325901 co-treatment in mouse primary hepatocytes. Cells were treated with 2.5 μ M U0126 or 25 nM PD-0325901 and 250 ng/ml FGF19 for 6 hours. (A) ERK phosphorylation was determined by Western blotting. (B and C) *Shp* and *Cyp7a1* mRNA levels were tested by RT-qPCR (n = 3). Values are means \pm SEM. Statistics by two-tailed *t* test. (*) refer to differences between Control and FGF19 groups. (#) refer to differences compared to the Vehicle group. * P <0.05, ** P <0.005, *** P <0.0005, ## P <0.05, ### P <0.005, #### P <0.0005.

3.2.5 FGF19-dependent ERK Activation Is Not Sufficient for *Cyp7a1* Repression

FGF19 receptors FGFR4 and β -Klotho (*Klb*) are required for *Cyp7a1* regulation by FGF19 (Inagaki et al. 2005; Ito et al. 2005). In *Fgfr4*^{-/-} or *Klb*^{-/-} mice, FGF19-induced *Cyp7a1* repression was impaired (Fig. 3.11, A and B). However, interestingly, FGF19 induced ERK phosphorylation in *Fgfr4*^{-/-} but not *Klb*^{-/-} mice (Fig. 3.11, C and D). This is probably because other FGFRs are also expressed in liver and in the presence of β -Klotho, they substitute for FGFR4 to activate the ERK pathway; however, they are unable to mediate *Cyp7a1* repression. These findings implicate that there should be something unique about FGFR4 that enables proper *Cyp7a1* regulation in an ERK-independent fashion. FGFR4 might activate a unique signaling pathway that other FGFRs are unable to regulate. Thus, I looked for signaling pathways differentially regulated by FGF19 in wild-type and *Fgfr4*^{-/-} mice. In a candidate-based approach, I failed to identify any signaling pathways uniquely activated by FGFR4. FGF19 stimulated phosphorylation of RSK, JNK, Stat1, Stat3, GSK3 α/β in both wild-type and *Fgfr4*^{-/-} mice (data not shown). Therefore, phosphorylation of these proteins is not sufficient for *Cyp7a1* repression as well. A proteomics-based, unbiased approach would likely to resolve the identity of the exact signaling process required for *Cyp7a1* repression by FGF19.

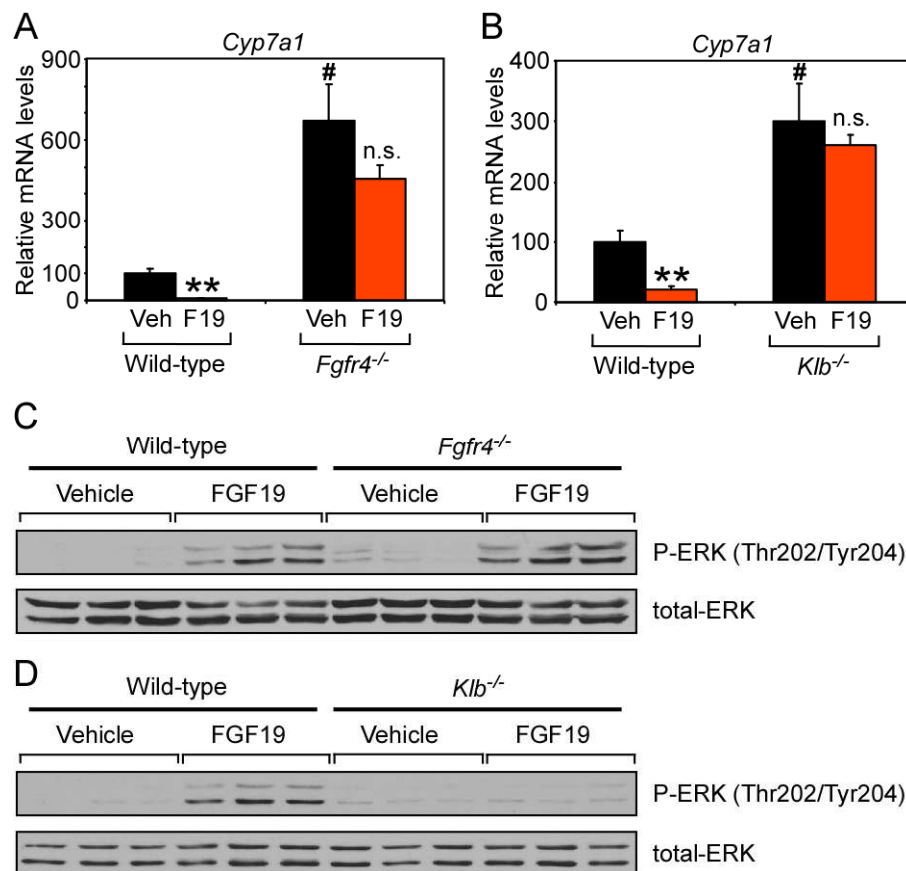


Figure 3.11 FGF19 signaling is intact in *Fgfr4*^{-/-} mice but *Cyp7a1* repression is impaired. (A and B) Overnight-fasted mice (n = 4-5) were treated with vehicle or FGF19 (1mg/kg; i.p.) and sacrificed 6 hours later. *Cyp7a1* mRNA levels were determined by RT-qPCR. (C and D) Overnight-fasted mice were treated with vehicle or FGF19 (1mg/kg; i.p.) and sacrificed 1 hour later. Total and phospho protein levels were determined by Western blotting with indicated antibodies. The results are shown in triplicates. *Klb*^{-/-} mice were generated by Xunshan Ding. Values are means \pm SEM. Statistics by two-tailed *t* test. (*) refer to differences between Veh and F19 groups. (#) refer to differences between Veh groups. ***P*<0.005, #*P*<0.05, n.s. not significant.

3.3 DISCUSSION

I have shown that the MEK/ERK pathway is an integral regulator of bile acid metabolism. ERK activity is required to maintain normal transcription of *Shp*. Furthermore, independent from its role in *Shp* transcription, ERK activity down-regulates *Cyp7a1* expression. In response to MEK inhibition, nuclear receptors HNF4 α and LRH-1 dissociate from the *Shp* promoter without changing their binding to the *Cyp7a1* promoter. Thus, the MEK/ERK pathway enables HNF4 α and LRH-1 binding specifically to the *Shp* promoter, however, the regulation of HNF4 α and LRH-1 by the MEK/ERK pathway must be promoter-specific. Direct phosphorylation of these proteins by ERK is a possibility but both HNF4 α and LRH-1 lack conserved MAP kinase substrate motifs PXpS/pTP. These proteins contain pS/pTP sites which can be phosphorylated by ERK *in vitro*; however, the physiologic relevance of these phosphorylations requires needs further investigation (Lee et al. 2006b and data not shown).

Although the MEK/ERK pathway is involved in regulation of both *Shp* and *Cyp7a1* transcription, it is not crucial for FGF19-dependent regulation of these genes. FGF19 induces *Shp* transcription and represses *Cyp7a1* transcription in the absence of ERK activation. Furthermore, FGF19 is unable to efficiently repress *Cyp7a1* in livers of *Fgfr4*^{-/-} mice, but is still able to induce ERK phosphorylation probably via other FGFRs. Therefore, FGFR4 must have a unique function that is not shared by other FGFRs and is required for *Cyp7a1* regulation. It is possible that there exists a signaling pathway that is solely activated by FGFR4. In fact, there has been evidence for such signaling mechanisms. FGFR4 was shown to associate with and induce phosphorylation of

uncharacterized substrates that were not regulated by FGFR1 (Vainikka et al. 1994; Vainikka et al. 1996).

In a recent study, it was shown that FGFR4 is required for regulation of bile acid metabolism by FGF19 but not for regulation of glucose metabolism (Wu et al. 2011). In agreement with these findings, I have found that FGF19 activated signaling pathways that regulate glucose metabolism in *Fgfr4*^{-/-} mice (data not shown). FGF19-induced *Cyp7a1* repression is largely impaired in *Fgfr4*^{-/-} mice; however, it is possible to observe a small degree of *Cyp7a1* repression (Wu et al. 2011). Since the MEK/ERK pathway is activated by FGF19 in these knockout mice, it might be true that this pathway contributes to *Cyp7a1* regulation by FGF19 but it is clearly a minor player. I believe that the major regulatory signaling mechanism awaits discovery.

3.4 SUMMARY

The MEK/ERK pathway is an integral regulator of bile acid metabolism. ERK activity is necessary to maintain hepatic *Shp* and *Cyp7a1* transcription at their physiologic levels. Inhibition of this pathway causes loss of *Shp* transcription by disrupting HNF4 α and LRH-1 binding to the *Shp* promoter. Independent from the effects on *Shp*, MEK/ERK inhibition increases transcription from the *Cyp7a1* promoter without changing HNF4 α and LRH-1 binding. Unexpectedly, the MEK/ERK pathway is not crucial for FGF19-dependent repression of bile acid synthesis as FGF19 represses *Cyp7a1* transcription in the absence of ERK activation. Although this pathway is activated by FGF19 in livers of *Fgfr4*-deficient mice probably via other FGFRs, *Cyp7a1*

repression is largely impaired. Thus, I propose that a signaling mechanism uniquely regulated by FGFR4 must be responsible for FGF19-dependent repression of bile acid synthesis.

CHAPTER 4

FGF19 Regulates Hepatic Protein and Glycogen Synthesis

4.1 INTRODUCTION

Several pharmacologic studies in hyperglycemic, obese animal models have shown that FGF19 can improve metabolic rate and reduce weight gain. FGF19 treatment lowers serum glucose, triglyceride and cholesterol levels as well as hepatic triglyceride and cholesterol levels (Tomlinson 2002; Fu et al. 2004). However, the mechanism by which FGF19 leads to these improved metabolic changes has remained unclear. While investigating FGF19-dependent regulation of bile acid metabolism, I also studied FGF19's other effects on liver metabolism in an effort to shed light on potential roles of FGF19 on glucose metabolism.

4.2 RESULTS

4.2.1 FGF19 Induces Phosphorylation of Translation Machinery Components

To elucidate effects of FGF19 on metabolism, I investigated FGF19-induced signaling in liver in normoglycemic wild-type animals. FGF19 increased phosphorylation of liver ERK1 and ERK2 of overnight-fasted mice. In contrast, insulin, but not FGF19, induced phosphorylation of the protein kinase Akt, demonstrating that FGF19 and insulin likely work through independent kinase signaling pathways (Fig. 4.1). However, both

FGF19 and insulin stimulated the phosphorylation of the eukaryotic initiation factors eIF4B on Ser⁴²² and eIF4E on Ser²⁰⁹ in liver (Fig. 4.1). These proteins are components of the eIF4F complex that mediates binding of mRNA to the ribosome and their phosphorylation promotes the initiation of translation (Gingras et al. 1999). Treatment of animals with insulin or FGF19 also produced similar increases in phosphorylation of Ser²³⁵ and Ser²³⁶ of ribosomal protein S6 (rpS6) (Fig. 4.1). Phosphorylation of rpS6 enhances global protein synthesis (Fumagalli et al. 2000).

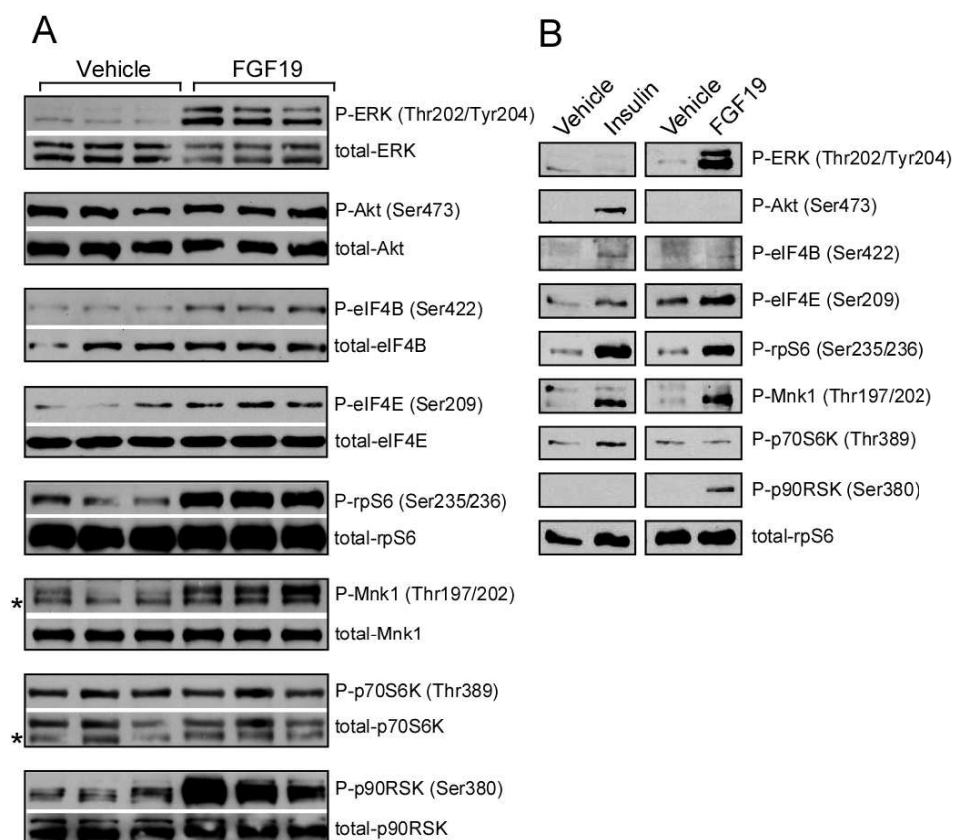


Figure 4.1 Stimulation by FGF19 of the signaling pathways that regulate protein synthesis in liver. (A) Overnight-fasted mice were injected i.v. with vehicle or 1 mg/kg FGF19 protein. The animals were sacrificed 1 hour after the injection. Liver homogenates were separated by SDS-PAGE and proteins were identified by Western blotting with the indicated antibodies. The results are shown in triplicates. * represents non-specific band.

(B) Overnight-fasted mice were injected i.p. with PBS or 1 U/kg insulin or i.v. with vehicle or 1 mg/kg FGF19. Animals in the insulin treatment group were sacrificed 15 minutes after the injection whereas those in the FGF19 treatment group were sacrificed 1 hour after the injection. Protein samples were prepared from livers. Western blotting was performed with the indicated antibodies.

4.2.2 FGF19 Activates the Ras/ERK/RSK Signaling Pathway

I investigated the kinases that might mediate phosphorylation of eIF4 or rpS6 in response to FGF19. Ser²⁰⁹ of eIF4E is a target for the protein kinase Mnk1, which can be activated by phosphorylation at Thr¹⁹⁷ and Thr²⁰² by ERK (Ueda et al. 2004). FGF19 induced phosphorylation of Mnk1, implicating FGF19 as the upstream stimulus of a Ras/ERK/Mnk1 signaling cascade that activates eIF4E (Fig. 4.1). rpS6 and eIF4B are well-known targets of p70 ribosomal S6 kinase (p70S6K), which is activated by insulin. However, FGF19 treatment did not induce the phosphorylation of p70S6K or Akt, which is known to activate mammalian target of rapamycin (mTOR) to stimulate p70S6K (Fig. 4.1). Instead, FGF19 induced the phosphorylation of p90 ribosomal S6 kinase (p90RSK), which also is known to phosphorylate rpS6 and eIF4B (Shahbazian et al. 2006; Roux et al. 2007).

4.2.3 FGF19-dependent Phosphorylation of rpS6 and eIF4B Depends on ERK/RSK Activity

Because p90RSK is a downstream target of ERK, the above results indicate that FGF19 utilizes a Ras/ERK/p90RSK pathway to induce phosphorylation of rpS6 and

eIF4B. In human hepatocarcinoma HepG2 cells that express FGFR4 and β -Klotho, FGF19 treatment increased the phosphorylation of rpS6 and eIF4B in HepG2 (Fig. 4.2). However, this effect was not inhibited by wortmannin, a potent phosphoinositide 3-kinase (PI3K) inhibitor, or rapamycin, an mTOR inhibitor, suggesting that FGF19 does not act through the Akt/mTOR/S6K pathway. In contrast, the ERK pathway inhibitor U0126 and p90RSK inhibitor BI-D1870 (Sapkota et al. 2007) completely inhibited both basal and FGF19-dependent phosphorylation of rpS6 and eIF4B (Fig. 4.2), as well as ERK and p90RSK. In HepG2 cells, FGF19 treatment also failed to induce the phosphorylation of Akt or p70S6K (data not shown).

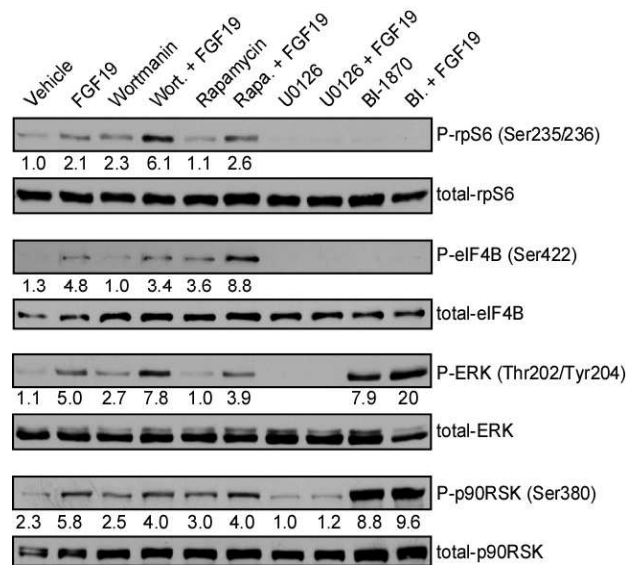


Figure 4.2 FGF19-induced signaling depends on ERK and RSK kinase activity. Overnight serum-starved HepG2 cells were starved for amino acids in HBSS media for 1 hour. DMSO, wortmannin (200 nM), rapamycin (20 nM), U0126 (10 μ M) or BI-D1870 (10 μ M) was added for a further 1 hour treatment. The cells were treated with vehicle or 250 ng/ml FGF19 and harvested after 30 minutes. Proteins were identified by Western blotting with the indicated antibodies. BI-D1870 treatment blocks the negative feedback effect of p90RSK on ERK, which results in increased basal phosphorylation of ERK and p90RSK. Numbers below blots represent fold change relative to the vehicle group.

4.2.4 FGF19 Promotes Protein Synthesis in Liver

The above findings link FGF19 to stimulation of protein synthesis in liver. Rate of protein synthesis in mouse liver was analyzed by using $^2\text{H}_2\text{O}$ labeling (Dufner et al. 2005; Rachdaoui et al. 2009). When injected into animals, $^2\text{H}_2\text{O}$ equilibrates with body water within 90 minutes and ^2H incorporates into amino acids. To determine the normal rate of protein synthesis after fasting and re-feeding, mice were fasted overnight and then re-fed or continually fasted for another 6 hours. In response to re-feeding, a 25% increase in the rate of global liver protein synthesis was observed (Fig. 4.3A) consistent with previous studies (Anderson et al. 2008). In comparison, injection of FGF19 significantly increased total protein synthesis by 18% (Fig. 4.3B). The de novo synthesis rate of albumin, the major protein product of liver, was increased 40% by FGF19 (Fig. 4.3C). Moreover, continuous treatment with FGF19 significantly increased plasma albumin levels by 10% (Fig. 4.3D). Thus FGF19 is a positive regulator of hepatic protein synthesis.

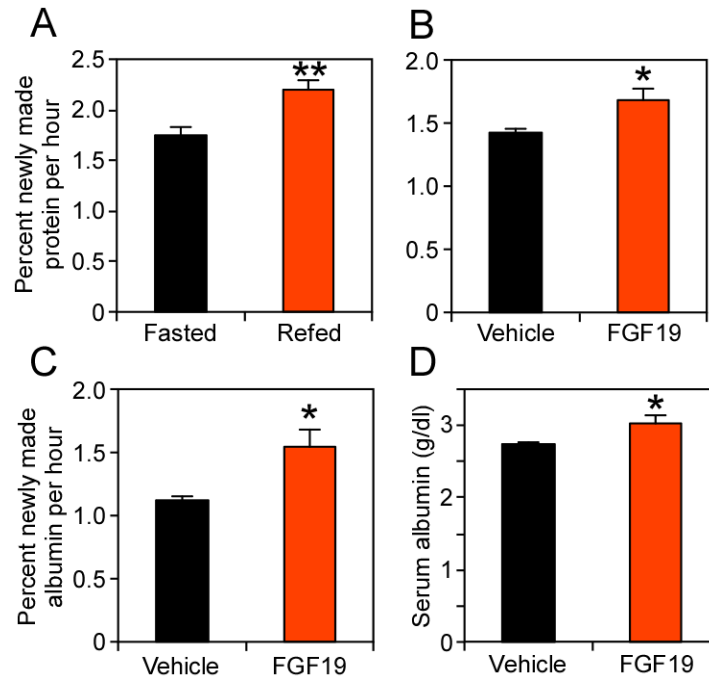


Figure 4.3 Increased rates of protein synthesis in mice liver after FGF19 treatment.

(A) Overnight-fasted mice received 0.5 ml $^2\text{H}_2\text{O}$ i.p. 90 minutes later, the animals were refed or kept fasted for 6 hours and sacrificed (n=10). Protein samples were hydrolyzed and ^2H labeling of alanine was determined via mass spectrometry. (B and C) Mice fed ad libitum received 0.5 ml $^2\text{H}_2\text{O}$. 90 minutes later (at 6 pm), vehicle or 1 mg/kg FGF19 was injected subcutaneously. The next morning (8 am), animals were injected again with the same dose, and 6 hours later sacrificed (n=10). Protein samples were hydrolyzed and ^2H labeling of alanine was determined via mass spectrometry. For albumin synthesis, ^2H incorporation into plasma albumin was measured in the same way. Protein synthesis measurements were done in collaboration with the Stephen Previs lab. (D) Over a 3-day-period, mice (n=6) received vehicle or 1 mg/kg FGF19 subcutaneously 3 times at 6 pm and once on the day of sacrifice at 8 am. 6 hours after the last injection, the livers were harvested. Plasma albumin levels were determined with a Vitros 250 instrument. Values are means \pm SEM. Statistics by two-tailed *t* test. **P*<0.05, ***P*<0.005.

4.2.5 FGF19 Inhibits GSK3 Kinases and Activates Glycogen Synthase

The effects FGF19 on protein synthesis prompted me to investigate glycogen synthesis, another target of insulin action. Glycogen synthesis in liver is negatively

regulated by glycogen synthase kinase (GSK) 3 α and GSK3 β , which phosphorylate and inhibit the enzyme glycogen synthase (GS). Phosphorylation also inactivates GSK3 kinases, which prevents inhibition of GS and thus increases glycogen synthesis (Cohen et al. 2001). In animals fasted overnight, FGF19 induced phosphorylation of both GSK3 α (Ser²¹) and GSK3 β (Ser⁹), which correlated with decreased phosphorylation of Ser⁶⁴¹ and Ser⁶⁴⁵ on GS and increased GS activity (Fig. 4.4).

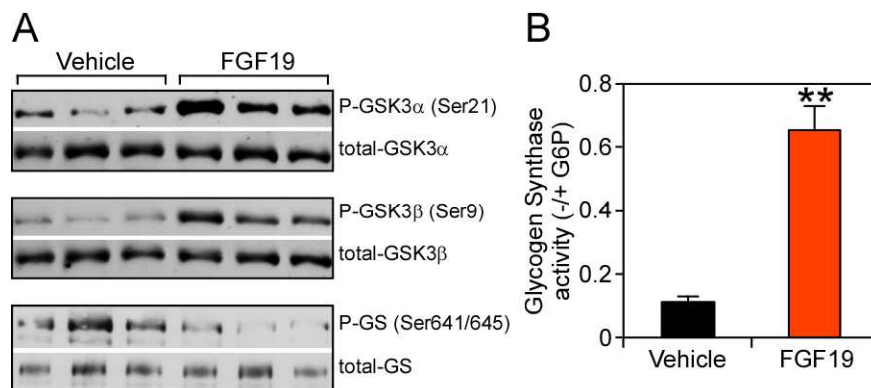


Figure 4.4 FGF19 inhibits GSK3 signaling to induce liver glycogen synthase in mice. (A) Overnight-fasted mice were treated i.v. with vehicle or 1 mg/kg FGF19 and sacrificed 10 minutes later. Liver homogenates were separated by SDS-PAGE and proteins identified by Western blotting with the indicated antibodies. Results represent triplicate experiments. (B) The ability of glycogen synthase in the homogenates of the same livers to incorporate radiolabeled UDP-glucose into glycogen in the absence and presence of glucose-6-phosphate was measured and the ratio shown as glycogen synthase activity (n=3). Values are means \pm SEM. Statistics by two-tailed *t* test. ***P*<0.005.

4.2.6 FGF19 Promotes Glycogen Synthesis in Liver

Concomitant to the above results, FGF19 treatment caused a 30% increase in liver glycogen content that led to a small but significant increase in liver weight in FGF19-treated mice compared to that of control animals (Fig. 4.5, A and B). FGF19 treatment had no effect on liver cholesterol or triglycerides (data not shown), nor did it

change plasma insulin or glucagon concentrations, strengthening the idea that it acts directly on liver (data not shown). I also analyzed the hepatic glycogen concentration in mice lacking *Fgf15* (the mouse ortholog of FGF19). Fed *Fgf15*-null mice had >50% less hepatic glycogen than did wild-type animals (Fig. 4.5C), demonstrating the physiologic requirement for FGF15 in maintaining normal glycogen metabolism. Moreover, *Fgf15*-null mice showed impaired glucose uptake from the circulation. FGF19 administration completely rescued this phenotype (Fig. 4.5D).

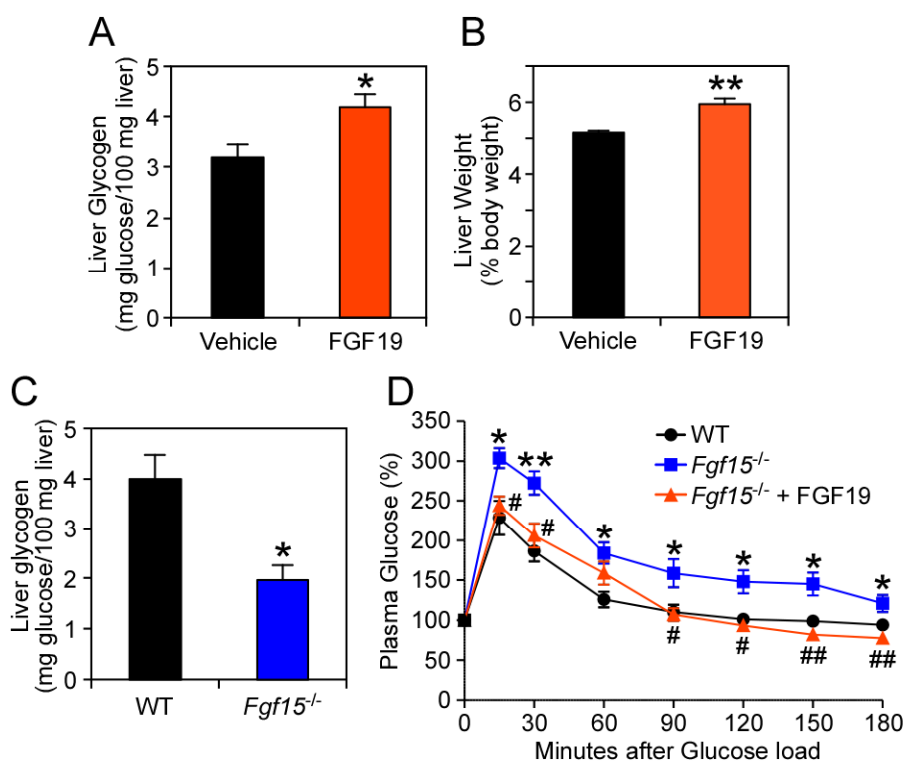


Figure 4.5 Liver glycogen synthesis is regulated by FGF15/19. (A and B) Mice fed ad libitum were injected subcutaneously with vehicle or 1 mg/kg FGF19 at 6 pm and the next morning at 8 am. 6 hours after the last injection, the animals were sacrificed, liver weight and glycogen content were determined (n=6). (C) Liver glycogen content was determined in wild-type and *Fgf15*^{-/-} mice fed ad libitum. (n=5) (D) Oral glucose tolerance test in wild-type and *Fgf15*^{-/-} mice. Values are means \pm SEM (n=6). Statistics by two-tailed *t* test. **P*<0.05, ***P*<0.005.

4.2.7 FGF19-dependent Phosphorylation of GSK3 and GS Depends on ERK/RSK Activity

Activity

Akt and p90RSK phosphorylate the same residues of GSK3 α/β (Sutherland et al. 1993; Stambolic et al. 1994; Cohen et al. 2001; Ding et al. 2005). To test whether p90RSK might mediate phosphorylation of GSK3 kinases for FGF19, I treated HepG2 cells with FGF19 and either the PI3-kinase or p90RSK inhibitor. FGF19-induced phosphorylation of GSK3 kinases in HepG2 cells was compromised in BI-D1870 treated cells, but not in wortmannin treated cells (Fig. 4.6). These data further support the idea that FGF19 acts through an insulin-independent Ras/ERK/p90RSK pathway to regulate glycogen synthesis.

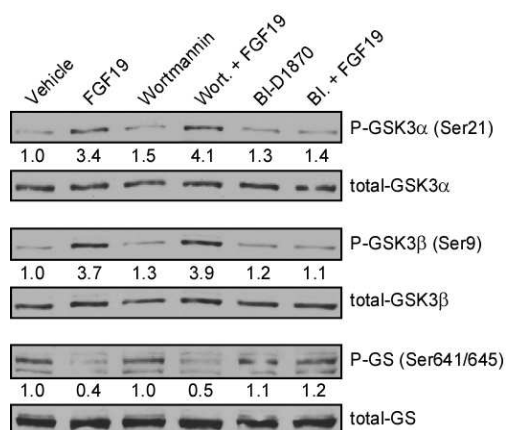


Figure 4.6 FGF19-induced signaling depends on RSK kinase activity. Overnight serum-starved HepG2 cells were pre-treated with DMSO, wortmannin (200 nM) or BI-D1870 (10 μ M) for 1 hour. The cells were lysed 30 minutes after vehicle or FGF19 (250 ng/ml) treatment. Proteins were identified by Western blotting with the indicated antibodies. Numbers below blots represent fold change relative to the vehicle group.

4.2.8 FGF19 Promotes Glycogen Synthesis in Diabetic Animals Lacking Insulin

To rule out the possibility that FGF19 promoted glycogen synthesis by modulating insulin activity, diabetic animals lacking insulin were used. Streptozotocin is a toxic chemical that particularly causes death of insulin-producing pancreatic beta cells. Streptozotocin (STZ)-treated mice are severely diabetic and have almost no detectable insulin in the blood (Fig. 4.7A). STZ treatment reduced liver glycogen content to 50% of that of control animals. Notably, FGF19 treatment restored hepatic glycogen amounts (Fig. 4.7A). Insulin-independent effects of FGF19 on the rate of net hepatic glycogen synthesis were also investigated in rats fasted overnight. A hyperglycemic clamp was used in combination with somatostatin to inhibit endogenous insulin and glucagon secretion. Under matched conditions of plasma glucose, insulin, and glucagon concentrations, FGF19 increased net hepatic glycogen synthesis by 70% compared to that in control rats (Fig. 4.7B). Thus FGF19 appears to act in parallel to and independent from insulin to promote liver glycogen synthesis.

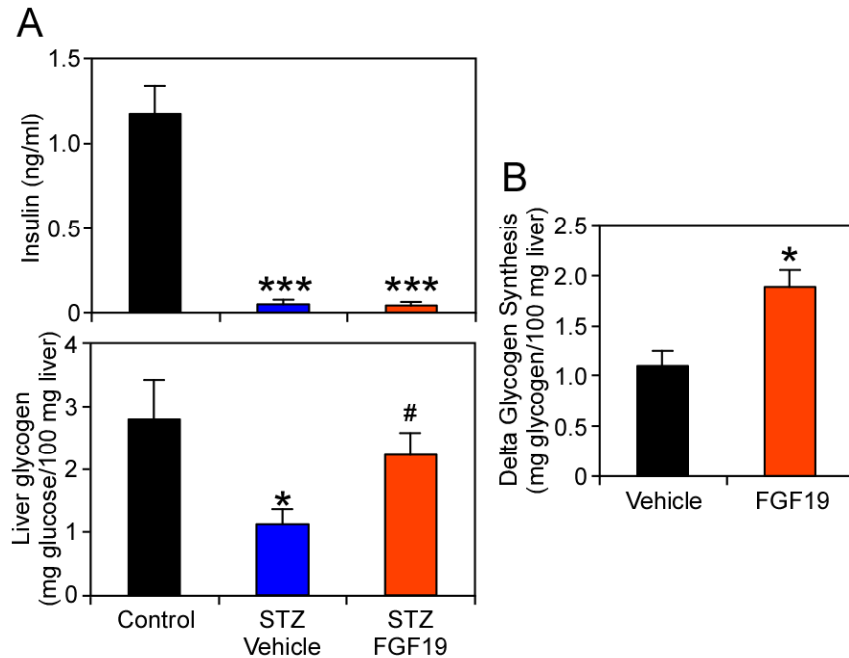


Figure 4.7 FGF19-induced glycogen synthesis is independent of insulin. (A) Mice were treated i.p. with STZ (175 mg/kg). 8 days later, diabetic animals were chosen and treated with vehicle or 1 mg/kg FGF19 i.p. at 6 pm for 7 consecutive days and sacrificed 6 hours after the last injection at 8 am (n=5-9). Liver glycogen content and plasma insulin levels were determined. *, $P < 0.05$ is between control and STZ-vehicle groups; #, $P < 0.05$ is between STZ-vehicle and STZ-FGF19 groups. (B) Three-hour-hyperglycemic clamp study was performed on overnight-fasted rats. Animals were continuously infused with insulin and somatostatin to maintain low levels of insulin and glucagon and variably infused with glucose to maintain hyperglycemia. Net glycogen synthesis was determined by assessing the glycogen content in the clamped animals subtracted by the glycogen content of unclamped animals that were euthanized after the same duration of fasting. This clamp experiment was done in collaboration with the Gerald Shulman lab. Values are means \pm SEM. Statistics by two-tailed t test. * $P < 0.05$, *** $P < 0.0005$.

4.3 DISCUSSION

4.3.1 FGF19 and Insulin Work in a Coordinated Temporal Fashion

Taken together, these studies suggest FGF19 functions in a bile acid-induced endocrine signaling pathway. Like insulin, pharmacologic administration of FGF19 can induce protein and glycogen synthesis in liver, whereas loss of the physiologic hormone in *Fgf15*^{-/-} mice results in glucose intolerance and reduced hepatic glycogen. However, whereas insulin reaches its maximum serum concentration within 1 hour of a meal in humans, peak FGF19 levels are achieved ~3 hours after a meal (Lundasen et al. 2006) just before glycogen accumulation peaks in the liver (Taylor et al. 1996; Krssak et al. 2004). Thus, I propose insulin and FGF19 work in a coordinated temporal fashion to facilitate the proper postprandial storage of nutrients. Of the anabolic enterokines (e.g., the incretins, GLP-1 and GIP), FGF19 is unusual in that it mimics insulin action rather than stimulating its release.

4.3.2 FGF19 and Insulin Activate Different Signaling Pathways and Have Both Overlapping and Separate Effects on Liver Metabolism

The different signaling pathways used by FGF19 and insulin permit overlapping but distinct biological effects for the two hormones (Fig. 4.8). For example, unlike insulin, FGF19 did not increase hepatic triglycerides or induce SREBP-1c-dependent lipogenic gene expression (data not shown), which requires the PI3K/Akt/mTOR

signaling pathway (Porstmann et al. 2008; Li et al. 2010). Indeed, FGF19 appears to be unique in its ability to differentially govern glycogen synthesis and lipogenesis. The requirement of FGF15/19 to maintain normal glycogen levels in fed mice and its ability to use the alternative Ras/ERK/p90RSK pathway may explain the puzzling observation that liver-specific loss of insulin signaling in IRS1-IRS2 null mice does not fully block glycogen storage in response to feeding (Dong et al. 2006; Kubota et al. 2008). Our findings may also help explain the glucose- and insulin-lowering actions of FGF19 in diabetic rodents (Tomlinson et al. 2002; Fu et al. 2004). Thus, pharmacologically targeting the FGF19 pathway might be an attractive alternative to using insulin to increase glycogen storage without affecting lipogenesis.

Recently, another insulin-like effect of FGF19 on liver metabolism was described (Potthoff et al. 2011). In these studies, administration of FGF19 reduced hepatic gluconeogenesis by repressing expression of the transcription co-factor PGC1 α , and the PGC1 α target genes, glucose-6-phosphatase (G6pase) and phosphoenolpyruvate carboxykinase (Pepck). Insulin represses gluconeogenic genes by promoting Akt-dependent phosphorylation and subsequent degradation of FOXO1, a transcription factor involved in fasting-mediated induction of gluconeogenic gene expression. Unlike insulin, FGF19 was shown to regulate gluconeogenic gene expression via inhibition of cAMP regulatory element binding protein (CREB) phosphorylation and CREB binding to the *Pgc1 α* promoter (Potthoff et al. 2011).

After a meal, endogenous glucose production falls as exogenous glucose appears in the circulation. Gluconeogenesis approximately accounts for half of endogenous glucose production and rate of gluconeogenesis stays low up to ~4 hours after a meal

(Woerle et al. 2003). Again, when the timing of postprandial insulin and FGF19 levels are considered, the delayed repression of gluconeogenesis implicates a coordinated temporal response in which insulin and FGF19 work to repress hepatic gluconeogenesis.

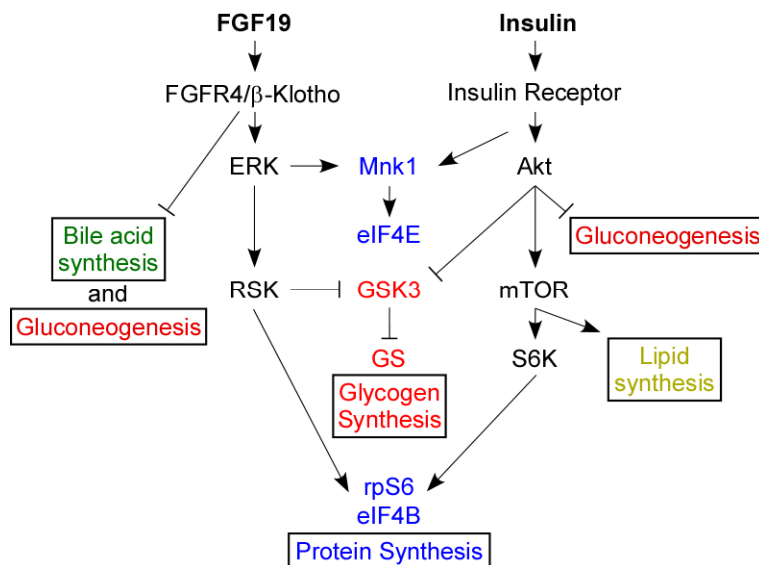


Figure 4.8. Insulin and FGF19 act through different signaling pathways to coordinate overlapping but distinct postprandial responses in liver.

FGF19 functions as a postprandial hormone to govern hepatic protein synthesis, glycogen synthesis and gluconeogenesis, making it remarkably similar to insulin in many ways. However, unlike insulin, FGF19 does not stimulate lipogenesis. In fact, FGF19 has been shown to reduce hepatic triglycerides and cholesterol through an unknown mechanism (Tomlinson et al. 2002; Fu et al. 2004). Another major difference is the regulation of bile acid homeostasis, which is a hallmark role of FGF19 in liver metabolism. In contrast, insulin is not considered as a primary regulator of bile acid biology (Fig. 4.8 and Table 4.1).

Table 4.1 Metabolic effects of FGF19 and insulin in liver.

	FGF19	Insulin
Bile acid synthesis	↓	—
Protein synthesis	↑	↑
Glycogen synthesis	↑	↑
Gluconeogenesis	↓	↓
Lipogenesis	—	↑
Triglycerides	↓	↑
Cholesterol	↓	—

To gain more insights into how FGF19 might be regulating gluconeogenesis and hepatic lipid metabolism, I asked whether any other signaling pathways are regulated by FGF19. As discussed so far, FGF19 induced the phosphorylation of ERK in liver but not in muscle and failed to induce the phosphorylation of Akt that is very potently activated by insulin. Unexpectedly, I discovered that FGF19 stimulated phosphorylation of STAT1 and STAT3 transcription factors in liver (Fig. 4.9). The STAT family of transcription factors is involved in a variety of biological processes. Phosphorylation of these proteins is known to induce their dimerization, nuclear localization and transcriptional activation (Darnell 1997).

While STATs 2, 4 and 6 exclusively regulate inflammation and interferon response, STATs 1, 3 and 5 can be activated by receptor tyrosine kinases and are involved in various physiologic regulations. For instance, growth hormone activates STAT5, whereas STAT3 is an integral component of Leptin-dependent regulation of satiety (Darnell 1997). Interestingly, STAT3 has also been described as a negative regulator of hepatic gluconeogenesis and is activated postprandially through an unclear mechanism (Inoue et al. 2004; Inoue et al. 2006a). Thus, it will be interesting to test

whether FGF19-dependent STAT3 and perhaps STAT1 activation has any roles in regulation of liver metabolism by FGF19.

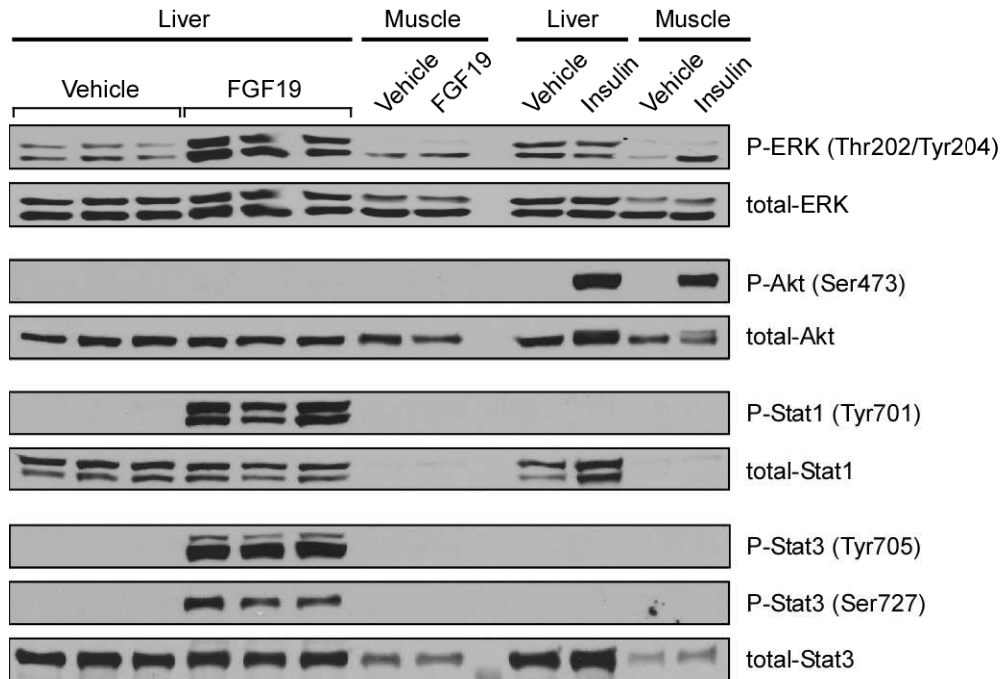


Figure 4.9 FGF19 activates STAT1 and STAT3 in liver. This experiment is the same as the one in Fig. 4.1B. Phospho and total protein levels were detected by indicated antibodies.

4.3.3 FGF19 as a Therapeutic Agent in the Treatment of Diabetes

The overlapping but distinct functions of FGF19 versus insulin raise the possibility of using FGF19 as a therapeutic agent in the treatment of both Type I and Type II diabetes. The non-lipogenic, triglyceride/cholesterol lowering and insulin sensitivity increasing effects of FGF19 make this notion even more appealing. Nevertheless, there are concerns for the potential of FGF19 as a chronic therapeutic.

Transgenic mice that continually overexpress FGF19 eventually form liver tumors (Nicholes et al. 2002) and FGF19 has been implicated as an associated factor with hepatocellular carcinoma (Ho et al. 2009). However, whether exogenous administration of FGF19 can cause similar effects is not clear. There is also the possibility of separating mitogenic and metabolic effects of FGF19 by generating synthetic FGF19 variants that does not stimulate cell proliferation (Wu et al. 2010; Wu et al. 2011). A closely related member of the FGF19 subfamily, FGF21, has also been shown to have profound effects on metabolism. FGF21 reduces plasma glucose, triglyceride and insulin parameters and improves insulin sensitivity in diabetic animal models. Unlike FGF19, FGF21 does not show significant mitogenic effects and thus may have a greater therapeutic promise (Kharitononkov et al. 2005). Thus, engineering of easily administrable, modified peptide variants of these hormones has the potential to define the future of metabolic syndrome treatment.

4.4 SUMMARY

FGF19 stimulates hepatic protein and glycogen synthesis, but does not induce lipogenesis. The effects of FGF19 are independent of the activity of either insulin or the protein kinase Akt, and instead are mediated through a mitogen-activated protein kinase signaling pathway that activates components of the protein translation machinery and stimulates glycogen synthase activity. Mice lacking FGF15 (the mouse FGF19 ortholog) fail to properly regulate blood glucose and fail to maintain normal postprandial amounts of liver glycogen. FGF19 treatment restored the loss of glycogen in diabetic animals

lacking insulin. Thus, FGF19 activates a physiologically important, insulin-independent endocrine pathway that regulates hepatic protein and glycogen metabolism.

CHAPTER 5

Materials and Methods

5.1 Cell Culture and Reagents

HEK293 and HepG2 cells were maintained in DMEM (Invitrogen) and MEM (Sigma), respectively. The media also contained 10% FBS and $1 \times$ penicillin/streptomycin. In experiments where cells were starved of amino acids, they were plated on collagen-coated plates to prevent detachment. Transfection experiments were performed by using LipofectamineTM 2000 (Invitrogen) on HEK293 cells and Fugene® HD (Roche) on HepG2 cells according to manufacturer's instructions. p650-*rCyp7a1* and p569-h*SHP* promoter-luciferase reporters were described before (Lu et al. 2000). Luciferase data were normalized to an internal β -galactosidase control.

All antibodies used in Western blotting were purchased from Cell Signaling, except phospho-Ser³⁸⁰-p90RSK, HNF4 α and LRH-1 (Perseus proteomics), total GSK3 α/β and phospho-GS Ser⁶⁴¹/Ser⁶⁴⁵ (Invitrogen) and TBP (Santa Cruz). HA and FLAG antibody beads as well as FLAG antibody were purchased from Sigma. Wortmannin, rapamycin and U0126 were purchased from Cell Signaling. BI-D1870 was purchased from the University of Dundee, Division of Signal Transduction Therapy. PD-0325901 was purchased from Selleck Chemicals. Recombinant FGF19 was prepared as described (Inagaki et al. 2005).

5.2 Mouse Animal Experiments

All animal experiments were approved by the Institutional Animal Care and Research Advisory Committee of the University of Texas Southwestern Medical Center and Yale University. Unless otherwise noted, mice were 6-8 weeks old, wild-type pure C57BL6 and were housed in a pathogen-free and a temperature-controlled environment with 12-hour light/dark cycles (6 am-6 pm) and fed standard irradiated rodent chow. All conditional and germ-line knockout mice and their matched wild-type controls were maintained in the C57BL6/129 mixed strain background (except for *Shp*^{-/-} which is pure C57BL6) and used at 8-12 weeks of age. *Hnf4*^{fl/fl} (Hayhurst et al. 2001), *Lrh-1*^{fl/fl} (Lee et al. 2008), *Shp*^{-/-} (Kerr et al. 2002), *Ffgr4*^{-/-} (Weinstein et al. 1998) and *Ffg15*^{-/-} (Wright et al. 2004) mice were described before. *Klb*^{-/-} mice were generated by mating *Klb*^{fl/fl} mice with Meox-Cre mice (Xunshan Ding, unpublished data). Since the use of recombinant FGF15 is limited by its decreased stability and bioactivity, the human ortholog, FGF19, was used for these studies. FGF19 protein was administered in a buffer (i.e., vehicle) containing PBS and up to 4% glycerol. Details of each experiment are described in figure legends. Vena cava and tail blood were collected and transferred into EDTA-dipotassium tubes (Sarstedt) and centrifuged at 3,000 rpm at 4 °C for 30 minutes and total plasma albumin levels were measured using a Vitros 250 automated analyzer.

Adenoviruses were prepared as described before (Inagaki et al. 2005). Mice were infected with adenovirus by injection into the jugular vein. Each mouse received 1×10^{10} particles/g body weight FLAG-SHP adenovirus and/or 3×10^{10} particles/g body weight Cre adenovirus in 0.15 ml of saline. Mice were killed 3-5 days after injection.

PD-0325901 compound was prepared as a suspension in aqueous 0.5% hydroxypropyl methylcellulose and 0.2% Tween 80 and administered by oral gavage.

For oral glucose tolerance tests, overnight-fasted mice were injected i.p. with vehicle or 1 mg/kg FGF19. Five minutes later, mice were gavaged with 2 g glucose/kg body weight. Tail blood was taken at t = 0, 15, 30, 60, 90, 120 and 180 minutes and plasma glucose levels were measured and expressed as % basal (t=0) level.

Plasma glucose and glucagon, and insulin levels were measured with kits from Wako and Crystal Chem Inc. respectively. Hepatic cholesterol and triglyceride concentrations were measured using kits from Roche as previously described (Kalaany et al. 2005) except that Triton X-100 was used in place of Triton X-114.

5.3 RT-qPCR

RNA was extracted from frozen liver samples using RNA-STAT60™ (Isotex diagnostics), DNase treated, and reverse transcribed using random hexamers. Resulting cDNA was analyzed by RT-qPCR. Briefly, 25 ng of cDNA and 150 nmol of each primer were mixed with SYBR® GreenER™ PCR Master Mix (Invitrogen). Reactions were performed in triplicates in 384-well format using an ABI PRISM® 7900HT instrument (Applied Biosystems). Relative mRNA levels were calculated using the comparative CT method normalized to cyclophilin. The following primers were designed using Primer Express® Software (Applied Biosystems): *CYP7A1*: 5'-catgctgttgctatggcttattct-3', 5'-acagcccaggtatggaattaatc3'; *SHP*: 5'-cctgcctgaaaggacat-3', 5'-ctgcaggtgcccaatgtg-3'; *Cyp7a1*: 5'-agcaactaaacaacctgccagtacta-3'; 5'-gtccgatattcaaggatgca-3'; *Shp*: 5'-

cgatcctcttcaaccagatg-3', 5'-agggtccaagacttcacaca-3'; *Hnf4 α* (for knockout detection): 5'-agcctgcctccatcaac-3', 5'-ccagagatgggagagtgatc-3'; *Lrh-1* (for knockout detection): 5'-gaactgtccaaaacaaaaagg-3' 5'-ctccagcttcatccaac-3.

5.4 Chromatin Immunoprecipitation

Frozen and crushed liver samples were crosslinked with 1% formaldehyde for 15 minutes in PBS at room temperature. Crosslinking was stopped by addition of glycine. After two washes with PBS, samples were homogenized with glass homogenizers in a hypotonic buffer containing 10 mM HEPES (pH 7.9), 1.5 mM MgCl₂, 10 mM KCl, 0.2% NP40, 0.15 mM spermine, 0.5 mM spermidine, 1 mM EDTA, 1 mM DTT, 5% sucrose and protease inhibitors. The homogenate was laid on a cushion buffer containing 10 mM Tris-HCl (pH 7.5), 15 mM NaCl, 60 mM KCl, 0.15 mM spermine, 0.5 mM spermidine, 1 mM EDTA, 10% sucrose and spun down to obtain nuclear pellets. The pellet was washed once with PBS and lysed in SDS lysis buffer containing 0.5% SDS, 0.5% Triton X-100, 5 mM EDTA, 33 mM Tris (pH 8.1), 84 mM NaCl and then sonicated. After centrifugation, the supernatant (chromatin) was aliquoted and used for immunoprecipitations performed with the Millipore chromatin IP kit by following manufacturer's protocols. Antibodies for the following proteins were purchased from indicated suppliers: HNF4 α and LRH-1 (Persues Proteomics), Histone H3K4 trimethyl and RNA Polymerase II-CTD (Abcam) and Acety histone H3 (Millipore). The PCR purification kit from Qiagen was used to purify final DNA products.

For re-ChIP experiments, the above protocol was used. In the first round of ChIP, antibody-bound chromatin on protein A beads was eluted with an elution buffer containing 1% SDS, 0.1 M NaHCO₃ and 5 mM DTT and diluted 10 times with dilution buffer and used in the second round of chromatin IP by again following the Millipore protocol.

For FLAG-SHP chromatin IP experiments, a dual crosslinking protocol was followed as SHP protein loosely interacts with chromatin. Liver samples were first crosslinked with 2 mM di(N-succinimidyl) glutarate (Sigma) in PBS at room temperature for 45 minutes. After two washes with PBS, the samples were crosslinked with formaldehyde and processed as described above. FLAG antibody-conjugated beads were purchased from Sigma.

The following primer sets were designed using Primer Express® Software (Applied Biosystems) for qPCR analysis of chromatin IP products: *Cyp7a1*: +1250: 5'-gttgaggatcaaaggaagggtt-3', 5'-actggaggtgtggctcaatg-3'; +500: 5'-tgcagtcactctgggtttctg-3', 5'-aaactcaggctctgtgctctca-3'; +250: 5'-ccttcattgattacacagcatgaaa-3', 5'-ccagtggatgaatgtgaatgctca-3'; -150: 5'-gcttatcgactattgcagctctct-3', 5'-ctggccttgaactaagtccatct-3'; -550: 5'-tgagtgtgggaggtttctatt-3', 5'-aagccacaggtgcttcatg-3'; -800: 5'-gggccattggtcaatcttc-3', 5'-ctggtatacaacttccaactttactc-3'; -1500: 5'-ctctggcctagtgtcactctacct-3', 5'-gccaaagcgaccctctca-3'. *Shp*: +1200: 5'-tcatagctttgaggaagacaagaga-3', 5'-gggactgctactgctatgtgaca-3'; +600: 5'-aagggcacgatcctcttca-3', 5'-gaccaccatccaggagtgtct-3'; +250: 5'-ccttggatgtcctagccaaga-3', 5'-gccgccgctgatcct-3'; -30: 5'-ttctggagtcaaggtgtttgg-3', 5'-actgtgagtgtattatccttcatg-3'; -250: 5'-accttggcctgtgctaca-3', 5'-tcggatgactcaagtcataaac-3'; -500: 5'-

gccccaggtaggcaaa-3', 5'-catgaccagcctggaagt-3'; -1250: 5'-gacaagctgacagtcacacactaga-3', 5'-gcctggcacctggtta-3'; -1700: 5'-gcaaaaagcatcatccttct-3', 5'-tcagtgggctgcttga-3'.

5.5 Electrophoretic Mobility Shift Assay (EMSA)

HNF4 α and LRH-1 were in vitro translated with the TNT Quick Coupled Transcription/Translation System (Promega). Double-stranded oligonucleotides with GCTA overhangs were generated and labeled with ^{32}P -CTP by end filling. Binding reactions were performed in a total volume of 20 μl containing 75 mM KCl, 20 mM HEPES (pH 7.4), 2 mM DTT, 7.5% glycerol, 0.1% NP-40, 2 μg of poly[d(I-C)] (Sigma), 40 pmol of a nonspecific single-stranded oligonucleotide (to remove nonspecific binding), and 1 μl of each in vitro translation protein lysates. Later, 40 fmol of ^{32}P -labeled probe was added and further incubated at room temperature for 20 minutes. Samples were then analyzed on 5% polyacrylamide gels run in 0.25 x TBE and were visualized by autoradiography.

5.6 Nuclear Lysate Preparation

Frozen and crushed liver samples were homogenized by using glass homogenizers in a hypotonic buffer containing 20 mM Tris (pH 7.4), 2 mM MgCl_2 , 0.25 M Sucrose, 10 mM EDTA, 10 mM EGTA, 1 mM DTT and protease inhibitors. After centrifugation, the precipitated nuclear pellet was washed once with homogenization buffer and incubated with hypertonic Buffer C containing 20 mM HEPES (pH 7.9), 2.5%

glycerol, 0.42 M NaCl, 1.5 mM MgCl₂, 1 mM EDTA, 1 mM EGTA and protease inhibitors for 45 minutes at 4°C with agitation. After centrifugation at 70000 rpm for 20 minutes, the supernatant was used as the nuclear extract.

5.7 Western Blotting

Frozen and crushed liver samples were homogenized in liver lysis buffer containing 10 mM Tris-HCl (pH 7.5), 150 mM NaCl, 0.5% NP40, 10% glycerol, 5 mM EDTA, 50 mM NaF, 10 mM β-glycerol phosphate, 1 mM Na₃VO₄, 1 mM PMSF and complete protease inhibitor cocktail. The homogenates were centrifuged at 13,000 rpm for 10 minutes and the supernatants were used as whole cell lysates. Cultured cells were lysed in cell lysis buffer containing 20 mM Tris-HCl (pH 7.5), 150 mM NaCl, 1% Triton X-100, 5 mM EDTA, 50 mM NaF, 10 mM β-glycerol phosphate, 1 mM Na₃VO₄, 1 mM PMSF and complete protease inhibitor cocktail. Protein concentrations were determined by Bio-Rad Bradford assay and 30 μg of proteins were used in each SDS-PAGE run. Nitrocellulose membrane was used for blotting. Primary antibody incubation was performed in TBS containing 0.05% Tween and 5% BSA. For secondary antibody incubation, TBS-T containing 5% milk was used. For visualization of the results, either SuperSignal West Pico or ECL Western blotting substrates from Pierce were used. Quantification of the blots was performed by using ImageJ software. For each sample, the integrated density of phospho-antibody band was divided by that of total antibody band and the values were normalized relative to the vehicle group.

5.8 Mouse Primary Hepatocyte Isolation

By inserting a catheter into the portal vein and maintaining continuous flow using a peristaltic pump, liver was perfused and digested with liver perfusion buffer and liver digestion medium from Invitrogen (30 ml each per mouse). Liver was cut out from the mouse and washed once with DMEM low glucose (Invitrogen) and transferred into 10 ml of digestion medium. The liver surface was peeled off and cells were shed off and filtered through a 100 μm cell strainer. Viable cells were counted by the trypan blue exclusion test and plated into collagen-coated plates in an attachment medium containing William's E medium (Invitrogen) 5% charcoal stripped FBS, 10 nM insulin, 10 nM Dexamethasone and 1 \times penicillin/streptomycin. 2 hours later, attached cells were washed with PBS and then maintained in an experiment medium containing DMEM high glucose (Invitrogen), 100 nM Dexamethasone, 100 nM T3, 1 \times insulin-Transferrin-Selenium (Invitrogen) and 1 \times penicillin/streptomycin. Inhibitor and FGF19 treatment was done 48 hours post hepatocyte isolation.

5.9 ^2H -Labeling of Protein-bound Alanine

The fractional rates of protein synthesis in liver and plasma albumin were determined from the incorporation of [^2H]alanine using a precursor:product relationship (Previs et al. 2004; Anderson et al. 2008). Briefly, liver samples were homogenized in trichloroacetic acid (TCA, 0.1 g of tissue in 1 ml of 10% TCA, w/v) and centrifuged for 10 min at 4,000 rpm. The protein pellet was washed twice with 5% TCA and then

hydrolyzed for 20 h in 1 ml of 6N HCl at 100°C. To determine rates of plasma albumin synthesis, ~ 200 µl of plasma was treated with 1 ml of 10% TCA (Debro et al. 1956). The protein pellet was washed twice with 5% TCA, albumin was then extracted from the pellet into 100% ethanol. Following the evaporation of ethanol, samples were hydrolyzed in 1 ml of 6N HCl at 100°C. An aliquot of a hydrolyzed protein sample was evaporated to dryness. The samples were then reacted to form the “methyl-8” derivative of alanine, made by mixing acetonitrile, methanol and “Methyl-8” reagent (Pierce, Rockford, IL; 1:2:3, v:v:v) and heating the sample at 75°C for 30 min (Thenot et al. 1972). The sample was transferred to a GC-MS vial and analyzed using an Agilent 5973N-MSD equipped with an Agilent 6890 GC system. A DB17-MS capillary column (30 m x 0.25 mm x 0.25 µm) was used in all assays. The initial temperature program was set at 90°C and hold for 5 min, increased by 5°C per min to 130°C, increased by 40°C per min to 240°C and hold for 5 min, with a helium flow of 1 ml per min. Alanine elutes at ~ 12 min. The mass spectrometer was operated in the electron impact mode. Selective ion monitoring of m/z 99 and 100 (total ²H-labeling of alanine) was performed using a dwell time of 10 ms per ion.

5.10 Protein Synthesis Rate Calculations

The rate of protein synthesis was calculated using the equation: ²H-labeling protein-derived alanine (%) / [²H-labeling body water (%) x 3.7 x time (h)], where the factor 3.7 represents an incomplete exchange of ²H between body water and alanine, i.e. 3.7 of the 4 carbon-bound hydrogens of alanine exchange with water (Previs et al. 2004;

Anderson et al. 2008). This equation assumes that the ^2H -labeling in body water equilibrates with free alanine more rapidly than alanine is incorporated into newly made protein and that protein synthesis is linear over the study (Wolfe et al. 2004). In cases where the mice were exposed to tracer for ~6 h, we assumed a steady-state labeling of body water at a value equal to that measured at the end of the study. In cases where the mice were exposed to tracer for longer periods of time (e.g., overnight), we calculated the average water labeling determined using samples collected ~90 min post-injection and at the end of the study.

5.11 Glycogen Synthase Activity Assay

Frozen and crushed liver samples were homogenized in lysis buffer containing 50 mM Tris-HCl (pH 7.5), 1% Triton X-100, 5 mM EDTA, 0.27 M Sucrose, 50 mM NaF, 10 mM β -glycerol phosphate, and 1 mM Na_3VO_4 . The homogenates were centrifuged at 13,000 rpm for 10 min. Protein concentration was determined by Bio-Rad Bradford assay. 300 μg of protein was used in each reaction and diluted with the lysis buffer to 50 μl volume. A reaction buffer which contains all the ingredients in the lysis buffer and 17.8 mM UDP-glucose (Sigma), 13.4 mg/ml rabbit liver glycogen (Sigma) and 0.07 μCi of ^{14}C -UDP-glucose (Perkin Elmer) per reaction was prepared and split into two tubes one of which is supplemented with 10mM glucose-6-phosphate (G6P) (Sigma). For each sample, two reactions (– and + G6P) in duplicate were set by adding 50 μl of reaction buffer into the diluted protein lysate making a final volume of 100 μl . Each sample was incubated at 30°C for 20 min. After the incubation, the samples were spotted

onto Whatman Grade 3 circle filters and washed twice with 66% ethanol for 20 min at room temperature and once in acetone for 5 min. After drying, filters were put into scintillation vials with 10 ml of scintillation liquid and ^{14}C -glucose incorporation into glycogen was quantified. The glycogen synthase activity is defined as the activity measured in the absence of G6P divided by the activity measured in the presence of G6P.

5.12 Glycogen Content Determination

Liver samples were weighed and homogenized in 1 ml of 30% KOH and boiled for 15 min. After centrifugation at 3,000 rpm, 75 μl of homogenates were spotted on Whatman Grade 3 circle filters. Filters were washed once in 70% Ethanol at 4°C for 30 min and twice at room temperature for 15 min each. The filters were briefly rinsed with acetone. After drying, filters were placed in Fisher glass tubes and 1 ml of amyloglucosidase reaction mix which contains 2 mg of amyloglucosidase enzyme (Sigma) per 5 ml of 50 mM NaOAc was added. After incubation at 37°C for 90 min with periodic mixing, samples were used in Wako Autokit glucose assay to determine the glucose concentration. Glycogen content results were calculated as mg glucose over 100 mg liver.

5.13 Hyperglycemic-Basal Insulin Clamp Study

Harlan male Sprague-Dawley rats (350 g) underwent placement of chronic jugular vein and carotid artery catheters. After recovery from surgery (5-7 days), rats were fasted

overnight prior to experiments. Continuous infusions of insulin [1 mU/(kg-min)] and somatostatin [4 mcg/(kg-min)] were started at T=0 min. Animals were continuously infused with insulin and somatostatin to maintain low levels of insulin and glucagon and variably infused with glucose to maintain hyperglycemia. Animals were given either vehicle or FGF19. A second group of animals were not clamped and were kept fasted throughout the experiment. The FGF19 group received 540 µg/kg total recombinant FGF19 administered i.v. in two divided doses (at T=0 and 90 min). A variable infusion of 20% glucose enriched with 20% [U-¹³C] glucose was started at 5 min and adjusted to maintain a plasma glucose concentration of ~250 mg/dL for a total of 180 min. Under these conditions, glycogen phosphorylase activity is inhibited. At 180 min, rats were euthanized with an i.v. bolus of pentobarbital and livers were freeze-clamped *in situ* using brass plated tongs pre-cooled in liquid nitrogen. Liver samples were stored at -80°C until further analysis.

Net glycogen synthesis was determined by assessing the glycogen content in the clamped animals subtracted by the glycogen content of similar unclamped rats euthanized with the same duration of fasting, using methods previously described (McNulty et al. 1996). Incorporation of glucose_{M+6} into glycogen to determine the percent of glycogen synthesized by the direct pathway was assessed by GC/MS, as previously described (Samuel et al. 2004). Insulin and glucagon were assayed by R.I.A. (Bio-Rad).

5.14 Statistical Analysis

Values are expressed as mean ± SEM. Significant differences between two groups were evaluated using two-tailed, unpaired *t* test.

BIBLIOGRAPHY

- Anderson SR, Gilge DA, Steiber AL, Previs SF. 2008. Diet-induced obesity alters protein synthesis: tissue-specific effects in fasted versus fed mice. *Metabolism* **57**: 347-354.
- Barrett SD, Bridges AJ, Dudley DT, Saltiel AR, Fergus JH, Flamme CM, Delaney AM, Kaufman M, LePage S, Leopold WR, Przybranowski SA, Sebolt-Leopold J, Van Becelaere K, Doherty AM, Kennedy RM, Marston D, Howard WA, Jr., Smith Y, Warmus JS, Teclé H. 2008. The discovery of the benzhydroxamate MEK inhibitors CI-1040 and PD 0325901. *Bioorg Med Chem Lett* **18**: 6501-6504.
- Bavner A, Sanyal S, Gustafsson JA, Treuter E. 2005. Transcriptional corepression by SHP: molecular mechanisms and physiological consequences. *Trends Endocrinol Metab* **16**: 478-488.
- Beenken A, Mohammadi M. 2009. The FGF family: biology, pathophysiology and therapy. *Nat Rev Drug Discov* **8**: 235-253.
- Bolotin E, Schnabl J, Sladek FM. 2010. Hepatocyte Nuclear Factor 4. *Transcription Factor Encyclopedia*.
- Brown AP, Carlson TC, Loi CM, Graziano MJ. 2007. Pharmacodynamic and toxicokinetic evaluation of the novel MEK inhibitor, PD0325901, in the rat following oral and intravenous administration. *Cancer Chemother Pharmacol* **59**: 671-679.
- Choi M, Moschetta A, Bookout AL, Peng L, Umetani M, Holmstrom SR, Suino-Powell K, Xu HE, Richardson JA, Gerard RD, Mangelsdorf DJ, Kliewer SA. 2006. Identification of a hormonal basis for gallbladder filling. *Nat Med* **12**: 1253-1255.
- Cohen P, Frame S. 2001. The renaissance of GSK3. *Nat Rev Mol Cell Biol* **2**: 769-776.
- Darnell JE, Jr. 1997. STATs and gene regulation. *Science* **277**: 1630-1635.
- De Fabiani E, Mitro N, Anzulovich AC, Pinelli A, Galli G, Crestani M. 2001. The negative effects of bile acids and tumor necrosis factor-alpha on the transcription of cholesterol 7alpha-hydroxylase gene (CYP7A1) converge

to hepatic nuclear factor-4: a novel mechanism of feedback regulation of bile acid synthesis mediated by nuclear receptors. *J Biol Chem* **276**: 30708-30716.

Debro JR, Korner A. 1956. Solubility of albumin in alcohol after precipitation by trichloroacetic acid: a simplified procedure for separation of albumin. *Nature* **178**: 1067.

Ding Q, Xia W, Liu JC, Yang JY, Lee DF, Xia J, Bartholomeusz G, Li Y, Pan Y, Li Z, Bargou RC, Qin J, Lai CC, Tsai FJ, Tsai CH, Hung MC. 2005. Erk associates with and primes GSK-3beta for its inactivation resulting in upregulation of beta-catenin. *Mol Cell* **19**: 159-170.

Dong X, Park S, Lin X, Copps K, Yi X, White MF. 2006. Irs1 and Irs2 signaling is essential for hepatic glucose homeostasis and systemic growth. *J Clin Invest* **116**: 101-114.

Dufner DA, Bederman IR, Brunengraber DZ, Rachdaoui N, Ismail-Beigi F, Siegfried BA, Kimball SR, Previs SF. 2005. Using 2H2O to study the influence of feeding on protein synthesis: effect of isotope equilibration in vivo vs. in cell culture. *Am J Physiol Endocrinol Metab* **288**: E1277-1283.

Fayard E, Auwerx J, Schoonjans K. 2004. LRH-1: an orphan nuclear receptor involved in development, metabolism and steroidogenesis. *Trends Cell Biol* **14**: 250-260.

Forman BM. 2005. Are those phospholipids in your pocket? *Cell Metab* **1**: 153-155.

Fu L, John LM, Adams SH, Yu XX, Tomlinson E, Renz M, Williams PM, Soriano R, Corpuz R, Moffat B, Vandlen R, Simmons L, Foster J, Stephan JP, Tsai SP, Stewart TA. 2004. Fibroblast growth factor 19 increases metabolic rate and reverses dietary and leptin-deficient diabetes. *Endocrinology* **145**: 2594-2603.

Fumagalli S, Thomas G. 2000. in *Translational Control of Gene Expression* (eds. N Sonenberg, N Sonenberg, N Sonenberg, N Sonenberg, N Sonenberg, N Sonenberg), pp. 695-717. Cold Spring Harbor Laboratory Press, New York.

- Gingras AC, Raught B, Sonenberg N. 1999. eIF4 initiation factors: effectors of mRNA recruitment to ribosomes and regulators of translation. *Annu Rev Biochem* **68**: 913-963.
- Goodwin B, Jones SA, Price RR, Watson MA, McKee DD, Moore LB, Galardi C, Wilson JG, Lewis MC, Roth ME, Maloney PR, Willson TM, Kliewer SA. 2000. A regulatory cascade of the nuclear receptors FXR, SHP-1, and LRH-1 represses bile acid biosynthesis. *Mol Cell* **6**: 517-526.
- Hayhurst GP, Lee YH, Lambert G, Ward JM, Gonzalez FJ. 2001. Hepatocyte nuclear factor 4alpha (nuclear receptor 2A1) is essential for maintenance of hepatic gene expression and lipid homeostasis. *Mol Cell Biol* **21**: 1393-1403.
- Ho HK, Pok S, Streit S, Ruhe JE, Hart S, Lim KS, Loo HL, Aung MO, Lim SG, Ullrich A. 2009. Fibroblast growth factor receptor 4 regulates proliferation, anti-apoptosis and alpha-fetoprotein secretion during hepatocellular carcinoma progression and represents a potential target for therapeutic intervention. *J Hepatol* **50**: 118-127.
- Holt JA, Luo G, Billin AN, Bisi J, McNeill YY, Kozarsky KF, Donahee M, Wang DY, Mansfield TA, Kliewer SA, Goodwin B, Jones SA. 2003. Definition of a novel growth factor-dependent signal cascade for the suppression of bile acid biosynthesis. *Genes Dev* **17**: 1581-1591.
- Inagaki T, Choi M, Moschetta A, Peng L, Cummins CL, McDonald JG, Luo G, Jones SA, Goodwin B, Richardson JA, Gerard RD, Repa JJ, Mangelsdorf DJ, Kliewer SA. 2005. Fibroblast growth factor 15 functions as an enterohepatic signal to regulate bile acid homeostasis. *Cell Metab* **2**: 217-225.
- Inoue H, Ogawa W, Asakawa A, Okamoto Y, Nishizawa A, Matsumoto M, Teshigawara K, Matsuki Y, Watanabe E, Hiramatsu R, Notohara K, Katayose K, Okamura H, Kahn CR, Noda T, Takeda K, Akira S, Inui A, Kasuga M. 2006a. Role of hepatic STAT3 in brain-insulin action on hepatic glucose production. *Cell Metab* **3**: 267-275.
- Inoue H, Ogawa W, Ozaki M, Haga S, Matsumoto M, Furukawa K, Hashimoto N, Kido Y, Mori T, Sakaue H, Teshigawara K, Jin S, Iguchi H, Hiramatsu R, LeRoith D, Takeda K, Akira S, Kasuga M. 2004. Role of STAT-3 in regulation of hepatic gluconeogenic genes and carbohydrate metabolism in vivo. *Nat Med* **10**: 168-174.

- Inoue Y, Yu AM, Yim SH, Ma X, Krausz KW, Inoue J, Xiang CC, Brownstein MJ, Eggertsen G, Bjorkhem I, Gonzalez FJ. 2006b. Regulation of bile acid biosynthesis by hepatocyte nuclear factor 4alpha. *J Lipid Res* **47**: 215-227.
- Ito S, Fujimori T, Furuya A, Satoh J, Nabeshima Y. 2005. Impaired negative feedback suppression of bile acid synthesis in mice lacking betaKlotho. *J Clin Invest* **115**: 2202-2208.
- Kalaany NY, Gauthier KC, Zavacki AM, Mammen PP, Kitazume T, Peterson JA, Horton JD, Garry DJ, Bianco AC, Mangelsdorf DJ. 2005. LXRs regulate the balance between fat storage and oxidation. *Cell Metab* **1**: 231-244.
- Kerr TA, Saeki S, Schneider M, Schaefer K, Berdy S, Redder T, Shan B, Russell DW, Schwarz M. 2002. Loss of nuclear receptor SHP impairs but does not eliminate negative feedback regulation of bile acid synthesis. *Dev Cell* **2**: 713-720.
- Kharitonov A, Shiyanova TL, Koester A, Ford AM, Micanovic R, Galbreath EJ, Sandusky GE, Hammond LJ, Moyers JS, Owens RA, Gromada J, Brozinick JT, Hawkins ED, Wroblewski VJ, Li DS, Mehrbod F, Jaskunas SR, Shanafelt AB. 2005. FGF-21 as a novel metabolic regulator. *J Clin Invest* **115**: 1627-1635.
- Kim I, Ahn SH, Inagaki T, Choi M, Ito S, Guo GL, Kliewer SA, Gonzalez FJ. 2007. Differential regulation of bile acid homeostasis by the farnesoid X receptor in liver and intestine. *J Lipid Res* **48**: 2664-2672.
- Kir S, Beddow SA, Samuel VT, Miller P, Previs SF, Suino-Powell K, Xu HE, Shulman GI, Kliewer SA, Mangelsdorf DJ. 2011. FGF19 as a postprandial, insulin-independent activator of hepatic protein and glycogen synthesis. *Science* **331**: 1621-1624.
- Krssak M, Brehm A, Bernroider E, Anderwald C, Nowotny P, Dalla Man C, Cobelli C, Cline GW, Shulman GI, Waldhausl W, Roden M. 2004. Alterations in postprandial hepatic glycogen metabolism in type 2 diabetes. *Diabetes* **53**: 3048-3056.
- Kubota N, Kubota T, Itoh S, Kumagai H, Kozono H, Takamoto I, Mineyama T, Ogata H, Tokuyama K, Ohsugi M, Sasako T, Moroi M, Sugi K, Kakuta S, Iwakura Y, Noda T, Ohnishi S, Nagai R, Tobe K, Terauchi Y, Ueki K, Kadowaki T. 2008. Dynamic functional relay between insulin receptor

substrate 1 and 2 in hepatic insulin signaling during fasting and feeding. *Cell Metab* **8**: 49-64.

- Kurosu H, Choi M, Ogawa Y, Dickson AS, Goetz R, Eliseenkova AV, Mohammadi M, Rosenblatt KP, Kliewer SA, Kuro-o M. 2007. Tissue-specific expression of betaKlotho and fibroblast growth factor (FGF) receptor isoforms determines metabolic activity of FGF19 and FGF21. *J Biol Chem* **282**: 26687-26695.
- Lee FY, Lee H, Hubbert ML, Edwards PA, Zhang Y. 2006a. FXR, a multipurpose nuclear receptor. *Trends Biochem Sci* **31**: 572-580.
- Lee YK, Choi YH, Chua S, Park YJ, Moore DD. 2006b. Phosphorylation of the hinge domain of the nuclear hormone receptor LRH-1 stimulates transactivation. *J Biol Chem* **281**: 7850-7855.
- Lee YK, Schmidt DR, Cummins CL, Choi M, Peng L, Zhang Y, Goodwin B, Hammer RE, Mangelsdorf DJ, Kliewer SA. 2008. Liver receptor homolog-1 regulates bile acid homeostasis but is not essential for feedback regulation of bile acid synthesis. *Mol Endocrinol* **22**: 1345-1356.
- Lenicek M, Duricova D, Komarek V, Gabrysova B, Lukas M, Smerhovsky Z, Vitek L. 2011. Bile acid malabsorption in inflammatory bowel disease: Assessment by serum markers. *Inflamm Bowel Dis* **17**: 1322-1327.
- Li S, Brown MS, Goldstein JL. 2010. Bifurcation of insulin signaling pathway in rat liver: mTORC1 required for stimulation of lipogenesis, but not inhibition of gluconeogenesis. *Proc Natl Acad Sci U S A* **107**: 3441-3446.
- Lin BC, Wang M, Blackmore C, Desnoyers LR. 2007. Liver-specific activities of FGF19 require Klotho beta. *J Biol Chem* **282**: 27277-27284.
- Lu TT, Makishima M, Repa JJ, Schoonjans K, Kerr TA, Auwerx J, Mangelsdorf DJ. 2000. Molecular basis for feedback regulation of bile acid synthesis by nuclear receptors. *Mol Cell* **6**: 507-515.
- Lundasen T, Galman C, Angelin B, Rudling M. 2006. Circulating intestinal fibroblast growth factor 19 has a pronounced diurnal variation and modulates hepatic bile acid synthesis in man. *J Intern Med* **260**: 530-536.
- Mataki C, Magnier BC, Houten SM, Annicotte JS, Argmann C, Thomas C, Overmars H, Kulik W, Metzger D, Auwerx J, Schoonjans K. 2007.

- Compromised intestinal lipid absorption in mice with a liver-specific deficiency of liver receptor homolog 1. *Mol Cell Biol* **27**: 8330-8339.
- McNulty PH, Sinusas AJ, Shi CQ, Dione D, Young LH, Cline GC, Shulman GI. 1996. Glucose metabolism distal to a critical coronary stenosis in a canine model of low-flow myocardial ischemia. *J Clin Invest* **98**: 62-69.
- Miao J, Xiao Z, Kanamaluru D, Min G, Yau PM, Veenstra TD, Ellis E, Strom S, Suino-Powell K, Xu HE, Kemper JK. 2009. Bile acid signaling pathways increase stability of Small Heterodimer Partner (SHP) by inhibiting ubiquitin-proteasomal degradation. *Genes Dev* **23**: 986-996.
- Nicholes K, Guillet S, Tomlinson E, Hillan K, Wright B, Frantz GD, Pham TA, Dillard-Telm L, Tsai SP, Stephan JP, Stinson J, Stewart T, French DM. 2002. A mouse model of hepatocellular carcinoma: ectopic expression of fibroblast growth factor 19 in skeletal muscle of transgenic mice. *Am J Pathol* **160**: 2295-2307.
- Porstmann T, Santos CR, Griffiths B, Cully M, Wu M, Leever S, Griffiths JR, Chung YL, Schulze A. 2008. SREBP activity is regulated by mTORC1 and contributes to Akt-dependent cell growth. *Cell Metab* **8**: 224-236.
- Potthoff MJ, Boney-Montoya J, Choi M, He T, Sunny NE, Satapati S, Suino-Powell K, Xu HE, Gerard RD, Finck BN, Burgess SC, Mangelsdorf DJ, Kliewer SA. 2011. FGF15/19 regulates hepatic glucose metabolism by inhibiting the CREB-PGC-1alpha Pathway. *Cell Metab* **13**: 729-738.
- Previs SF, Fatica R, Chandramouli V, Alexander JC, Brunengraber H, Landau BR. 2004. Quantifying rates of protein synthesis in humans by use of 2H2O: application to patients with end-stage renal disease. *Am J Physiol Endocrinol Metab* **286**: E665-672.
- Rachdaoui N, Austin L, Kramer E, Previs MJ, Anderson VE, Kasumov T, Previs SF. 2009. Measuring proteome dynamics in vivo: as easy as adding water? *Mol Cell Proteomics* **8**: 2653-2663.
- Roux PP, Shahbazian D, Vu H, Holz MK, Cohen MS, Taunton J, Sonenberg N, Blenis J. 2007. RAS/ERK signaling promotes site-specific ribosomal protein S6 phosphorylation via RSK and stimulates cap-dependent translation. *J Biol Chem* **282**: 14056-14064.

- Samuel VT, Liu ZX, Qu X, Elder BD, Bilz S, Befroy D, Romanelli AJ, Shulman GI. 2004. Mechanism of hepatic insulin resistance in non-alcoholic fatty liver disease. *J Biol Chem* **279**: 32345-32353.
- Sapkota GP, Cummings L, Newell FS, Armstrong C, Bain J, Frodin M, Grauert M, Hoffmann M, Schnapp G, Steegmaier M, Cohen P, Alessi DR. 2007. BI-D1870 is a specific inhibitor of the p90 RSK (ribosomal S6 kinase) isoforms in vitro and in vivo. *Biochem J* **401**: 29-38.
- Shahbazian D, Roux PP, Mieulet V, Cohen MS, Raught B, Taunton J, Hershey JW, Blenis J, Pende M, Sonenberg N. 2006. The mTOR/PI3K and MAPK pathways converge on eIF4B to control its phosphorylation and activity. *EMBO J* **25**: 2781-2791.
- Sinal CJ, Tohkin M, Miyata M, Ward JM, Lambert G, Gonzalez FJ. 2000. Targeted disruption of the nuclear receptor FXR/BAR impairs bile acid and lipid homeostasis. *Cell* **102**: 731-744.
- Sonoda J, Pei L, Evans RM. 2008. Nuclear receptors: decoding metabolic disease. *FEBS Lett* **582**: 2-9.
- Stambolic V, Woodgett JR. 1994. Mitogen inactivation of glycogen synthase kinase-3 beta in intact cells via serine 9 phosphorylation. *Biochem J* **303** (Pt 3): 701-704.
- Sutherland C, Leighton IA, Cohen P. 1993. Inactivation of glycogen synthase kinase-3 beta by phosphorylation: new kinase connections in insulin and growth-factor signalling. *Biochem J* **296** (Pt 1): 15-19.
- Taylor R, Magnusson I, Rothman DL, Cline GW, Caumo A, Cobelli C, Shulman GI. 1996. Direct assessment of liver glycogen storage by ¹³C nuclear magnetic resonance spectroscopy and regulation of glucose homeostasis after a mixed meal in normal subjects. *J Clin Invest* **97**: 126-132.
- Thenot JP, Horning EC. 1972. Amino acid N-dimethylaminomethylene alkyl esters. New derivatives for gas chromatographic and gas chromatographic-mass spectrometric studies. *Analytical Letters* **5**: 519-529
- Tomlinson E, Fu L, John L, Hultgren B, Huang X, Renz M, Stephan JP, Tsai SP, Powell-Braxton L, French D, Stewart TA. 2002. Transgenic mice expressing human fibroblast growth factor-19 display increased metabolic rate and decreased adiposity. *Endocrinology* **143**: 1741-1747.

- Ueda T, Watanabe-Fukunaga R, Fukuyama H, Nagata S, Fukunaga R. 2004. Mnk2 and Mnk1 are essential for constitutive and inducible phosphorylation of eukaryotic initiation factor 4E but not for cell growth or development. *Mol Cell Biol* **24**: 6539-6549.
- Vainikka S, Joukov V, Klint P, Alitalo K. 1996. Association of a 85-kDa serine kinase with activated fibroblast growth factor receptor-4. *J Biol Chem* **271**: 1270-1273.
- Vainikka S, Joukov V, Wennstrom S, Bergman M, Pelicci PG, Alitalo K. 1994. Signal transduction by fibroblast growth factor receptor-4 (FGFR-4). Comparison with FGFR-1. *J Biol Chem* **269**: 18320-18326.
- Walters JR, Tasleem AM, Omer OS, Brydon WG, Dew T, le Roux CW. 2009. A new mechanism for bile acid diarrhea: defective feedback inhibition of bile acid biosynthesis. *Clin Gastroenterol Hepatol* **7**: 1189-1194.
- Wang L, Lee YK, Bundman D, Han Y, Thevananther S, Kim CS, Chua SS, Wei P, Heyman RA, Karin M, Moore DD. 2002. Redundant pathways for negative feedback regulation of bile acid production. *Dev Cell* **2**: 721-731.
- Weinstein M, Xu X, Ohyama K, Deng CX. 1998. FGFR-3 and FGFR-4 function cooperatively to direct alveogenesis in the murine lung. *Development* **125**: 3615-3623.
- Woerle HJ, Meyer C, Dostou JM, Gosmanov NR, Islam N, Popa E, Wittlin SD, Welle SL, Gerich JE. 2003. Pathways for glucose disposal after meal ingestion in humans. *Am J Physiol Endocrinol Metab* **284**: E716-725.
- Wolfe RR, Chinkes DL. 2004. *Isotope Tracers in Metabolic Research: Principles and Practice of Kinetic Analyses*. Wiley-Liss, New York.
- Wright TJ, Ladher R, McWhirter J, Murre C, Schoenwolf GC, Mansour SL. 2004. Mouse FGF15 is the ortholog of human and chick FGF19, but is not uniquely required for otic induction. *Dev Biol* **269**: 264-275.
- Wu AL, Coulter S, Liddle C, Wong A, Eastham-Anderson J, French DM, Peterson AS, Sonoda J. 2011. FGF19 regulates cell proliferation, glucose and bile acid metabolism via FGFR4-dependent and independent pathways. *PLoS One* **6**: e17868.
- Wu X, Ge H, Lemon B, Vonderfecht S, Baribault H, Weiszmann J, Gupte J, Gardner J, Lindberg R, Wang Z, Li Y. 2010. Separating mitogenic and

metabolic activities of fibroblast growth factor 19 (FGF19). *Proc Natl Acad Sci U S A* **107**: 14158-14163.

Yu C, Wang F, Kan M, Jin C, Jones RB, Weinstein M, Deng CX, McKeehan WL. 2000. Elevated cholesterol metabolism and bile acid synthesis in mice lacking membrane tyrosine kinase receptor FGFR4. *J Biol Chem* **275**: 15482-15489.